Improving the application of recombinant membrane proteins in *Pichia pastoris*

MASTER'S THESIS

zur Erlangung des akademischen Grades eines

Diplom-Ingenieurs

der Studienrichtung Biotechnologie

an der

Technischen Universität Graz

Peter A. Augustin

Betreuer: **Ass.Prof. Dipl.-Ing. Dr.techn. Harald Pichler**

Graz, 2011

Deutsche Fassung:
Beschluss der Curricula-Kommission für Bachelor-, Master- und Diplomstudien vom 10.11.2008
Genehmigung des Senates am 1.12.2008

EIDESSTATTLICHE ERKLÄRUNG

Ich erkläre an Eides statt, dass ich die vorliegende Arbeit selbstständig verfasst, andere als die angegebenen Quellen/Hilfsmittel nicht benutzt, und die den benutzten Quellen wörtlich und inhaltlich entnommene Stellen als solche kenntlich gemacht habe.

Graz, am …… ……..
(Unterschrift)

Englische Fassung:

STATUTORY DECLARATION

I declare that I have authored this thesis independently, that I have not used other than the declared sources / resources, and that I have explicitly marked all material which has been quoted either literally or by content from the used sources.

…… ……..
date (signature)

Acknowledgment

Above all, I would like to thank my parents, Evelyn and Peter, and my grandparents, Mamama and Opapa, for their upbringing, their unconditional help through the years, their patience and financial support. Then I thank my colleagues and friends inside and outside the lab and especially those who managed to be both, you know who I'm talking about. I love you folks. I also would like to thank Prof. Helmut Schwab and the ACIB for the opportunity to do this work at the Institute for Molecular Biotechnology. Last, I thank my Master's thesis supervisors Harald and Tamara for sparing their time whenever needed in calm as well as in stressful times.

Abstract

Membrane-attached cytochrome P450 enzymes play a key role in the synthesis of natural compounds and are important tools in the production of drugs. They catalyze various industrially relevant reactions, such as the functionalization of hydrophobic compounds. Membrane proteins possess special properties, making them more difficult to handle than soluble proteins. Narrow substrate specificity, low stability and activity in heterologous expression and the need for a complex cofactor regeneration system are the major drawbacks of cytochrome P450 mediated reactions so far.

In this work, several attempts have been carried out to improve the application of a cytochrome P450 enzyme system in *Pichia pastoris* whole cell conversions of a very hydrophobic substrate. The coexpression of heterologous and intrinsic *Pichia pastoris* enzymes improved the reaction yield. Moreover, a system for the regeneration of the cofactor NADPH in *Pichia pastoris* whole cell conversions was created. The improvements in substrate conversion were documented by whole cell assays.

Zusammenfassung

Membrangebundene Cytochrom P450 Enzyme finden breite Anwendung in der Synthese wichtiger Naturstoffe und sind Hilfsmittel zur Herstellung von Arzneimitteln. Sie führen viele industriell relevante Reaktionen, wie zum Beispiel die Funktionalisierung von hydrophoben Verbindungen, durch. Aufgrund ihrer speziellen Eigenschaften sind sie im Vergleich zu löslichen Enzymen schwieriger handzuhaben. Vor allem enge Substratspezifität, schlechte Stabilität und Aktivität bei heterologer Expression und der nötige Einsatz eines komplexen Systems zur Regenerierung von Cofaktoren sind Limitierungen in ihrer Anwendung.

Mit verschiedenen Strategien wurde versucht die Anwendbarkeit eines Cytochrom P450 Enzymsystems im Zusammenhang mit der Umsetzug eines höchst hydrophoben Substrats zu verbessern. Dabei wurde der Einfluss von co-exprimierten heterologen und intrinsischen *Pichia pastoris* Enzymen auf die Ausbeute einer Modellreaktion getestet. Weiters wurde an Systemen gearbeitet, mit dem Ziel, die Regenerierung des Cofaktors NADPH in *Pichia pastoris* zu verbessern. Die Veränderungen in den Umsetzungen wurden anhand von Zell-Assays ermittelt und diskutiert.

Table of contents

List of abbreviations

aa	Amino acids
ADH	Alcohol dehydrogenase
Amp	Ampicillin
AOX1	Alcohol oxidase I gene
BLAST	Basic Local Alignment Search Tool
Bs	*Bacillus subtilis*
CCM	Czech collection of microorganisms
CDW	Cell dry weight
cPCR	Colony PCR
CPR	Cytochrome P450 reductase
CYP450	Cytochrome P450 enzyme
ddH_2O	Water, double distilled
DMSO	Dimethyl sulfoxide
dNTPs	Deoxynucleotide triphosphates
DSMZ	Deutsche Sammlung von Mikroorganismen und Zellkulturen
DTT	Dithiothreitol
DWP	Deep well plate
ER	Endoplasmic reticulum
EtAc	Ethyl acetate
FAD	Flavin adenine dinucleotide
FMN	Flavin mononucleotide
fw	Forward
G418	Geneticin
G6PDH	Glucose-6-phosphate dehydrogenase
GC-FID	Gas chromatography-flame ionization detection
GDH	Glucose 1-dehydrogenase
gDNA	Genomic DNA
HPO	*Hyascyamus muticus* premnaspirodiene oxygenase
HRP	Horse raddish peroxidase
IgG	Immunoglobulin G
Kan	Kanamycin
kDa	Kilo Dalton
LB	Lysogeny broth medium
MCS	Multiple cloning site
MD	Minimal dextrose medium
MeOH	Methanol
NAD(H)	Nicotinamide adenine dinucleotide
NADP(H)	Nicotinamide adenine dinucleotide phosphate
NCBI	National Center for Biotechnology Information
o/n	Over night
Pp	*Pichia pastoris*
PPP	Pentose phosphate pathway
pPp	Plasmid for *Pichia pastoris*
rev	Reverse
RT	Room temperature
SDS	Sodium dodecyl sulfate
SDS-PAGE	Sodium dodecyl sulfate polyacrylamide gel electrophoresis
SN	Supernatant
Std	Standard
Sy	*Sphingobium yanoikuyae*
Syn	Synthetic
TCA	Trichloroacetic acid
TRAFO	Transformation
TV	Theoretical valencene
TW	Tamara Wriessnegger
YPD	Yeast peptone dextrose medium
Zeo	Zeocin™

I. Introduction

The delicious aroma of grapefruits is mainly based on a terpene compound a growing number of researchers are interested in, **nootkatone** [1]. Its characteristic grapefruit smell and taste together with its unique organoleptic characteristics turn it into a highly demanded product for fragrance, food, cosmetics and pharmaceutical industries [2]. Unluckily, only trace amounts of nootkatone can be found in citrus fruits and being most abundant in grapefruits at 5 mg /100 g fresh weight, simple extraction is not profitable [3]. Biocatalytic conversion of the structurally highly similar compound valencene, which is abundant in all citrus fruits and thus can be obtained cheaply and in high amounts, is the method of choice to produce nootkatone (Figure 1).

This work presents different approaches to improve the application of membrane bound cytochrome P450 enzymes in *Pichia pastoris* and uses the conversion of valencene to nootkatone as a model reaction for cytochrome P450 mediated monooxygenation.

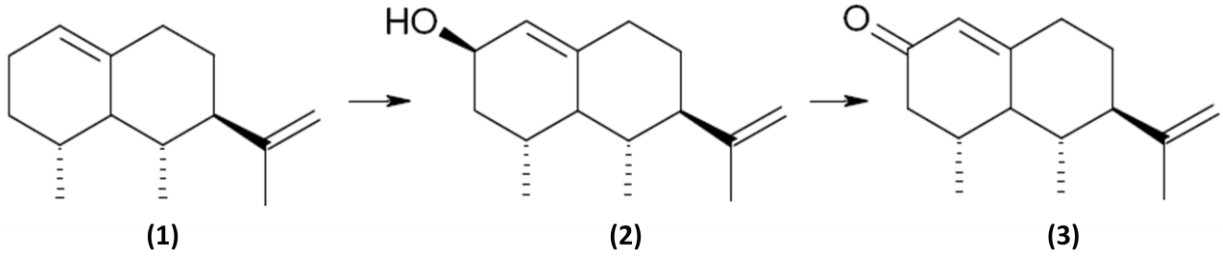

Figure 1: Model reaction: Oxidation of (+)-valencene (1) via *trans*-nootkatol (2) to (+)-nootkatone (3)

Pichia pastoris as expression host

Lately, the methylotropic yeast *Pichia pastoris* has emerged to be one of the most important hosts for heterologous protein expression and the most used yeast species for protein production [4]. The greatest advantages using *Pichia pastoris* include tightly regulated and efficient promoters and a strong tendency for respiratory growth, which greatly facilitates the culturing at high cell densities of >100 g/L cell dry weight. Moreover, the ability of manipulating *Pichia pastoris* at the molecular level with simple DNA transformation systems, i.e. stable integration of introduced DNA into the genome via homologous recombination, has made the yeast a model system for basic and applied studies [5]. The most successful system to express foreign proteins in *Pichia pastoris* is to make use of the alcohol oxidase I promoter (P_{AOX1}). P_{AOX1} is tightly regulated by a carbon source dependent repression/induction

mechanism [6]. The expression is fully repressed during growth of the yeast on glucose or glycerol and maximally induced during growth on methanol (MeOH). This mechanism comprises several benefits as easy induction of transcription by the addition of MeOH, obtaining good cell growth before the gene product is expressed and high level expression of proteins [7].

In this work, *Pichia pastoris* strain CBS7435*Δku70his4,* which derives from *Pichia* wild type strain CBS7435 (deposited in the **C**entraal**b**ureau voor **S**chimmelcultures) is used as starting point for all experiments. *Pp*CBS7435 has recently been classified as *Komagataella phaffii* and is the parental strain of the most used *Pichia* expression strains in industry [8]. In order to become more independent from patents including different existing *Pichia pastoris* expression strains, which makes the work with the yeast more complicated and expensive, the genome of strain CBS7435 has recently been sequenced and published by our institute [9]. The double knock-out strain *Pp*CBS7435*Δku70his4* was generated in house [10], is lacking a recombinase (*Ku70*) and thus the only possible way of integration into the strain is via homologous recombination [11]. Random integration of DNA is strongly reduced, which makes integration into *Pp*CBS7435*Δku70his4* genome more targeted and especially benefits the creation of knock-out strains. Furthermore, *HIS4* was knocked out resulting in a histidine auxotroph strain, which expanded the possibilities of strain manipulation, as only a very limited number of selectable markers were available for molecular genetic manipulation of *Pichia pastoris* [5]. Plasmids designed for integration via homologous integration in the disrupted *his4* locus harbor the *HIS4* wild-type allele that is used for selection of successful integration. Other plasmids used for integration in this work use homologous recombination at *AOX1* locus and introduce an antibiotic resistance for selection. In order not to disturb reading fluency in the work, strain *Pp*CBS7435*Δku70his4* will further on be referred to as WT or *Pp*CBS7435.

Cytochrome P450 enzymes

The stereo- and regioselective introduction of hydroxyl groups to non-activated C-H bonds is a nearly impossible task for synthetic organic chemists. In this context, monooxygenases, and in particular cytochrome P450 monooxygenases (CYP450), have long been in the focus of chemists and biochemists because of their extraordinary ability to catalyze this reaction with high stereoselectivity [12].

CYP450s, named for the absorption band at 450 nm of their carbon-monoxide-bound form, are a diverse group of heme-*b*-containing enzymes which catalyze a wide range of oxidative reactions and are found in all domains of life [13]. They play a fundamental role in biochemistry, pharmacology, and toxicology and have been the subject of intense research [14]. Substrates include natural compounds, such as

steroids, fatty acids, pheromones, leukotrienes and prostaglandins, or as in our case the sesquiterpene valencene. Although sequence conservation among CYP450 proteins of different families is often less than 20%, their mechanism of oxygen activation in the heme center of the enzyme is very conserved [15]. Ten classes of CYP450 systems have been classified depending on the topology of the protein components involved in the electron transfer to the CYP450 enzyme. Class II cytochromes P450 are the most common class in eukaryotes and are responsible for oxidative metabolism of endogenous compounds and involved in detoxification processes. In its simplest form, the monooxygenase system of class II enzymes is located in the endoplasmic reticulum (ER) of eukaryotes and contains two integral membrane proteins (Figure 2): The cytochrome P450 enzyme and the NADPH dependent cytochrome P450 reductase (CPR), containing a **f**lavin **a**denine **d**inucleotide (FAD) and **f**lavin **m**onon**u**cleotide (FMN) subunit, which transfers the required redox equivalents from NADPH to the cytochrome P450 enzyme. CYP450 and CPR are membrane proteins with a single N-terminal transmembrane domain leaving the main part of the protein including the active site facing the cytosol [16]. The process of monooxygenation requires the consecutive delivery of two electrons to the active site heme iron, mediated by interaction with the redox partner enzyme CPR. The CYP450 enzyme system studied in this work is a plant derived class II P450 enzyme system.

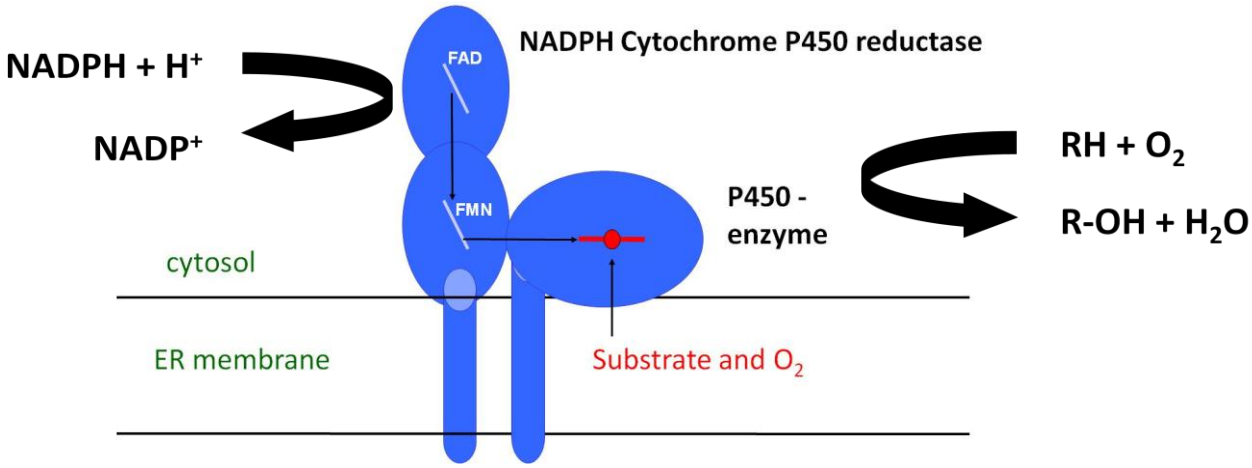

Figure 2: Scheme of a class II CYP450 enzyme complex

Model reaction: Valencene conversion to nootkatone

The direct conversion of the bulk fragrance valencene to nootkatone has been in the research focus of several groups lately [2]. The reaction consists of two consecutive reaction steps (Figure 3). The first is a monooxygenation to be performed by a cytochrome P450 enzyme, the second step is done by another enzyme. In whole cell conversions, most likely an alcohol dehydrogenase (ADH) of the host organism, e. g. *Pichia pastoris*, confers the respective activity [17].

Recently, the plant derived CYP450 ***H****yoscyamus muticus* **p**remnaspirodiene **o**xygenase (HPO) has been characterized, which catalyzes the oxidation of various sesquiterpenes, such as premnaspirodiene or valencene [18]. HPO, originating from the Egyptian henbane, monohydroxylates valencene to *trans*-nootkatol but fails to convert the monohydroxylated product to the ketone. This second reaction step has to be done by other proteins such as ADHs, which is further investigated in **Project 1** of my Master's thesis. Given the robust catalytic activity of HPO with valencene and low formation of unwanted side products in the oxygenation reaction, HPO is a good candidate to be studied for efficient valencene conversion.

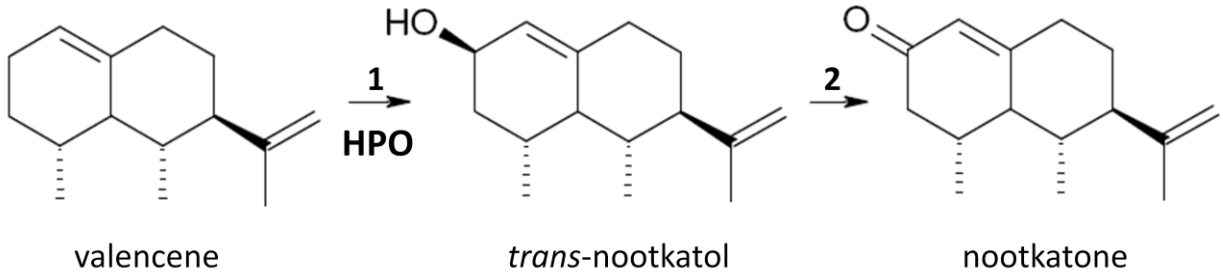

Figure 3: Conversion of valencene to nootkatone by HPO

In this work the cytochrome P450 enzyme HPO was used in combination with a CPR from *Arabidopsis thaliana* to form the class II cytochrome P450 complex in *Pichia pastoris* as host system. In contrast to the great diversity of CYP450 enzymes present in a single organism, there are often just a small number of reductases responsible for the catalysis of many different monooxygenation reactions. *Arabidopsis thaliana* for instance possesses more than 270 CYP450 enzymes [19], but only two isoforms of CPR proteins have been identified yet [20].

HPO and CPR used for the studies were codon-optimized by Tamara Wriessnegger and DSM for optimal expression in *Pichia pastoris.* The work I did was based on the knowledge and experience Tamara had

already got while working with these enzymes. The heterologously expressed enzymes were tested in whole cell in vivo conversion reactions.

Expression of membrane bound proteins in whole cell catalysis

The heterologous expression of membrane bound proteins in foreign hosts may entail several drawbacks such as relatively low expression levels and lack of stability and activity in the expression host [12]. As previously discussed, class II CYP450 catalysis always depends on membranes of the ER in the expression host. Many membrane proteins have specific lipid requirements, which can be involved in folding, stability and functionality of the protein and are unique for the organism the enzyme originally occurs in. The biotransformation in plant cells, where the respective CYP450 enzyme is originally derived, has the great drawbacks of costly culture conditions, slow growth and low product formation [2]. Therefore, the heterologous expression of the CYP450 enzyme is necessary to get reasonable yields with biotransformations of substances such as valencene [7]. Furthermore, all class II cytochrome P450 catalyzing complexes depend on an equimolar amount of the cofactor NADPH for each reaction cycle to ensure a sufficient transfer of electrons to the heme of the monooxygenase. For adequate cofactor regeneration, it is very often necessary to work with whole cell systems that are sufficiently able to regenerate the cofactors needed for the reaction. On the down side, whole cell systems lead to other effects such as limited substrate uptake/availability, toxicity of the substrate or product for the cell, product degradation by cell metabolism, formation of unwanted side products and the need for more complicated downstream processing. *Pichia pastoris* has been used before to successfully heterologously express plant membrane bound enzymes [21] or mammalian CYP450 enzymes [22] and was chosen as expression host because of the several advantages that have already been discussed above. The use of resting cells assays for the conversion of valencene to nootkatone circumvents several drawbacks mentioned. However, the availability of the substrate valencene for the cell, including the uptake of the compound into the cell, has to be regarded predominantly as a major drawback in this model system. As valencene is a very hydrophobic compound, cellular uptake and the reaction conditions for the assay are critical parameters.

Conversion of valencene in resting cells assays

Considering the problems discussed above, a resting cells valencene assay for *Pichia pastoris* was designed in order to document the valencene conversion in different strains generated during the work. The resting cells assay was performed in very high cell densities and in low volumes to achieve high

conversion rates and was established by Tamara Wriessnegger. The best vessel to perform the tests was determined to be robust glass tubes (Pyrex^{R}) and oxygen supply was ensured by extensive shaking. The highly volatile and hydrophobic substrate valencene was dissolved in DMSO containing a small amount of the detergent Triton^{R} X-100 in order to keep losses of substrate due to evaporation low during the preparation of substrate stocks and the reaction itself. As only a small amount of substrate/DMSO/Triton solution was added to the assay, leading to a final concentration of 2% DMSO and only 0.02% Triton^{R} X-100 in the assay, no detrimental effects on *Pichia pastoris* were expected by the compounds [23].

Outline for the Master's thesis

In this work, two projects were carried out to improve the application of membrane bound CYP450 enzymes in *Pichia pastoris* especially in reactions similar to the conversion of valencene to nootkatone. First, the direct improvement of valencene conversion by coexpression of different alcohol dehydrogenases was investigated and second, the applicability of a simple NADPH regeneration system in *Pichia pastoris* whole cell systems was investigated. The effects of the alterations on nootkatone yield and reaction performance were evaluated and discussed.

II. Results

Generation of HPO/CPR coexpressing *Pichia pastoris* strains

Outline

The successful monooxygenation of valencene in *Pichia pastoris* depends on the expression of two enzymes, HPO as the monooxygenase and CPR as its reductase. The best and easiest way to achieve good and balanced heterologous expression of both enzymes is to create a coexpression plasmid which comprises the expression cassettes of both genes on one plasmid (Figure 4). A coexpression plasmid has the advantages that both genes can be integrated at once into the expression host, only consuming one selection marker. The situation in *Pichia pastoris* is that dominant selectable markers, such as antibiotic resistances, are rather limited [5]. Only a handful of selection markers are available and tested in general. Even less are commonly used and established for selection. This limits the potential to integrate expression plasmids into *Pichia pastoris* in most cases to no more than two. Therefore, it was very important for my later work to preserve the available selection markers as far as possible. Additionally, using a coexpression plasmid has the advantage that both genes are likely to be expressed simultaneously and in great proximity to each other, which may enhance their potential to catalyze the desired reaction. Both genes were C-terminally tagged for immunological detection of the protein on Western blots, HPO with FLAG-tag and CPR with myc-tag.

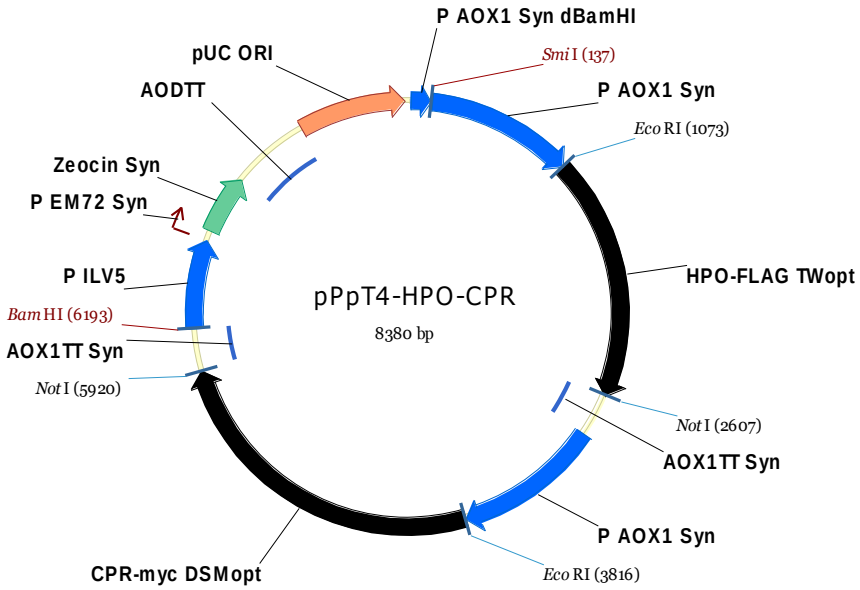

Figure 4: Coexpression plasmid pPpT4-HPO-CPR

Experimental

Generation of the coexpression plasmid pPpT4-HPO CPR and integration into PpCBS7435

The generation of the coexpression plasmid pPpT4-HPO-CPR (Figure 4) was facilitated by the work Tamara Wriessnegger had already done in this project. Tamara has designed several *Pichia pastoris* expression plasmids for codon-optimized HPO or CPR, like pPpHIS4-CPR and pPpT4-HPO (Figure 5). For my work, the codon-optimized HPO designed by Tamara Wriessnegger and the codon-optimized CPR designed by DSM were used.

The easiest way to create the pPpT4-HPO-CPR coexpression plasmid was to transfer the expression cassette for CPR from plasmid pPpHIS4-CPR to plasmid pPpT4-HPO, as the selection on Zeocin™-containing plates was preferred over histidine selection. The restriction sites of *Bgl*II and *Bam*HI are compatible and fragments of *Bgl*II and *Bam*HI sticky ends can be ligated under destruction of the restriction site (Figure 5).

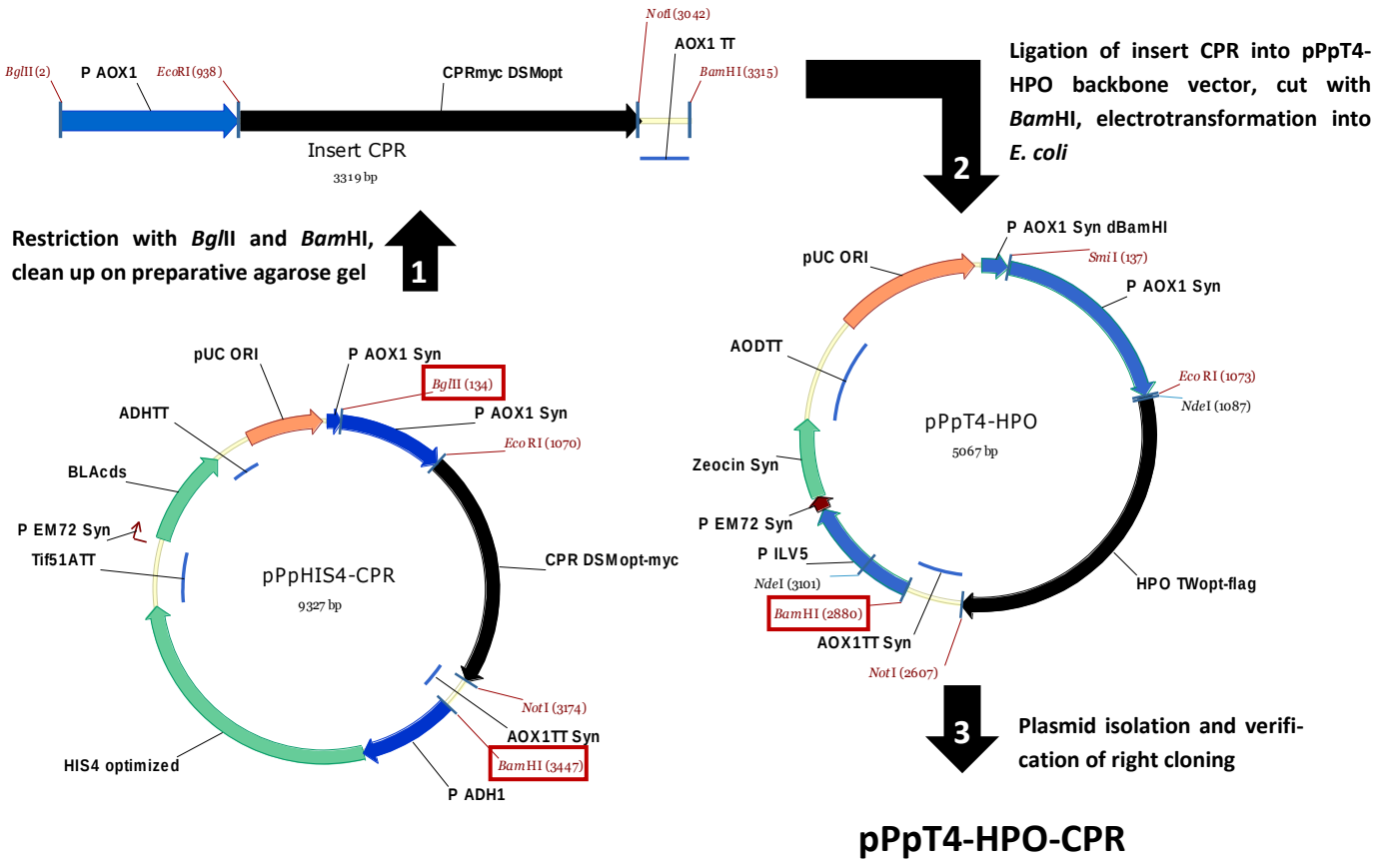

Figure 5: Creation of coexpression plasmid pPpT4-HPO-CPR (Figure 4)

In a first step, the expression cassette for CPR was cut out preparatively from pHIS4-CPR with *Bgl*II and *Bam*HI **(1)**. The fragment (insert) was isolated and cleaned up on a preparative agarose gel. The vector pPpT4-HPO (backbone) was linearized with *Bam*HI and cleaned up over a column. The concentrations of backbone and insert were determined photometrically for the ligation set up. The fragments were ligated and electrotransformed into *E. coli* TOP10F' electrocompetent cells **(2)**. Transformants were selected for on LB/Zeo^{100} plates and several colonies were streaked for plasmid isolation. After plasmid isolation, positive clones were identified with *Smi*I and *Bam*HI double digest and *Nde*I single digest (**3**, Table 1). As two of the three resulting bands upon *Nde*I cut nearly share the same size, they cannot be distinguished on analytical gel.

Table 1: Band quantities and sizes for restriction control cut

Restriction cut	Bands expected	Expected band sizes
*Smi*I & *Bam*HI	2	6 000 bp, 2 300 bp
*Nde*I	2 (3)	3 000 bp, 2 700 bp, 2 600 bp

Figure 6 shows the analytical gel of five different *E. coli* transformants tested. *Nde*I cut in both genes, HPO and CPR, and ensured that the insert was cloned into the plasmid in the right direction. *Smi*I and *Bam*HI double digest ensured that only one *Bam*HI restriction site was left and that *Smi*I restriction site for later linearization was present in the plasmid.

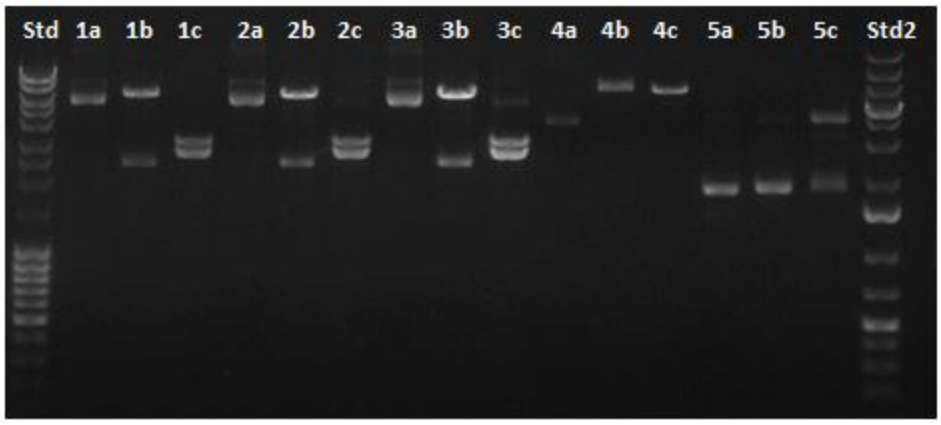

Figure 6: Control cut, double digest *Smi*I and *Bam*HI, pPpT4-HPO-CPR verification

Table 2: Lane description of Figure 6

Lane		Description	Bands	Estimated band sizes	Positive?
Std		MassRuler™ DNA ladder			
	a	Transformant 1 uncut	-	-	
1	b	Transformant 1 *Bam*HI & *Sma*I	2	6 000 bp, 2 300 bp	Yes
	c	Transformant 1 *Nde*I	2	2 700 bp, 3 000 bp	
	a	Transformant 2 uncut	-		
2	b	Transformant 2 *Bam*HI & *Sma*I	2	6 000 bp, 2 300 bp	Yes
	c	Transformant 2 *Nde*I	2	2 700 bp, 3 000 bp	
	a	Transformant 3 uncut	-		
3	b	Transformant 3 *Bam*HI & *Sma*I	2	6 000 bp, 2 300 bp	Yes
	c	Transformant 3 *Nde*I	2	2 700 bp, 3 000 bp	
	a	Transformant 4 uncut	-		
4	b	Transformant 4 *Bam*HI & *Sma*I	1	7 000 bp	No
	c	Transformant 4 *Nde*I	1	6 000 bp	
	a	Transformant 5 uncut	-		
5	b	Transformant 5 *Bam*HI & *Sma*I	1	1 800 bp	No
	c	Transformant 5 *Nde*I	2	2 000 bp	
Std2		GeneRuler™ 1kb Plus DNA ladder	-		

After verification of the pPpT4-HPO-CPR plasmid with restriction enzymes, the plasmids of transformants 2 and 3 were linearized with *Sma*I and integrated into *Pp*CBS7435 via double cross over at the *Pichia pastoris AOX1* locus. Transformants were selected for on YPD/Zeo^{100} plates and randomly chosen colonies were tested via Western blot according to their ability to express both proteins, HPO and CPR.

Western blot analysis

SDS-PAGE, Western blot and subsequent immunodetection of the proteins were done according to the protocol described in Materials and Methods. Approximately 20 µg of TCA-precipitated proteins were loaded onto SDS-gels (NuPAGE®-Novex, 4-12% Bis-Tris). After Western blot, the membranes were stained in Ponceau S solution to control the efficiency of protein transfer. Detection of HPO was done with mouse anti-FLAG primary antibody (1:1 000 dilution) and detection of CPR was carried out with rabbit anti-myc primary antibody (1:10 000 dilution). Secondary antibodies used were goat anti-mouse IgG-HRP (1:5 000) and goat anti-rabbit IgG-HRP (1:20 000).

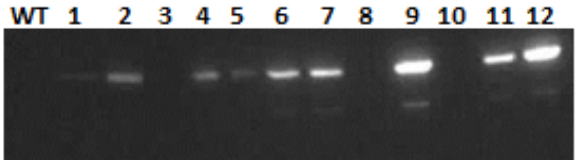

Figure 7: Western blot analysis of HPO expression in *Pichia pastoris* strains.

Table 3: Lane description of Figure 7

Lane	Description
WT	*Pp*CBS7435
1-12	Different transformants of pPpT4-HPO-CPR into *Pp*CBS7435

Figure 7 shows anti-HPO-FLAG Western blot of 12 transformants after integration of pPpT4-HPO-CPR into *Pp*CBS7435. Nine of them showed a band at the correct size of approximately 57 kDa. The slightly smaller band appearing at approximately 40 kDa might be unspecific antibody binding or degraded protein. Anti-myc detection of the transformants did not give any signal at all in chemoluminescence detection. Supposably, the anti-myc antibody used at that time was already too old. In addition, the dilution was too high for only low protein expression levels. To ensure that also the gene for CPR expression was indeed integrated into the genome of *Pp*CBS7435, a colony PCR (cPCR) with primers previously designed by Tamara Wriessnegger was performed. Also integration of HPO was controlled with cPCR. All primers used bind in the gene sequence or their expression cassette and a band corresponding to 1 000 bp is expected for both colony PCRs.

Colony PCR reaction mix, Maxima® Hot Start Green PCR Master Mix (2X)

HPO	
3 µL	Colony-SN
2 µL	**Prim_fw:** FwPpHPO_TW2
2 µL	**Prim_rev:** Rv_Pp_HIS4
25 µL	Maxima® Hot Start Green PCR Master Mix (2X)
18 µL	ddH_2O
50 µL	Total volume

CPR	
3 µL	Colony-SN
2 µL	**Prim_fw:** FwPpCPR_DSM3
2 µL	**Prim_rev:** Rv_Pp_HIS4
25 µL	Maxima® Hot Start Green PCR Master Mix (2X)
18 µL	ddH_2O
50 µL	Total volume

PCR cycling conditions: 95°C/4 min-(95°C/30 s-48°C/30 s-72°C/1 min 20 s) x 35 -72°C/7 min -4°C/∞

For cPCR, strains generated by Tamara Wriessnegger were used as positive controls. Positive control A+ represents strain TW 6+3t, comprising HPO and CPR integrated with two separate plasmids into *Pp*CBS7435. Strain TW 3F has only integrated HPO.

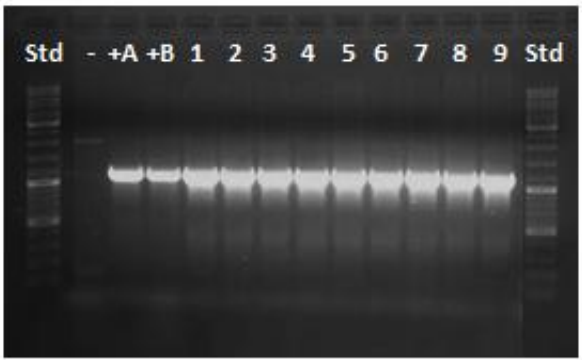

Figure 8: CPCR to verify HPO integration

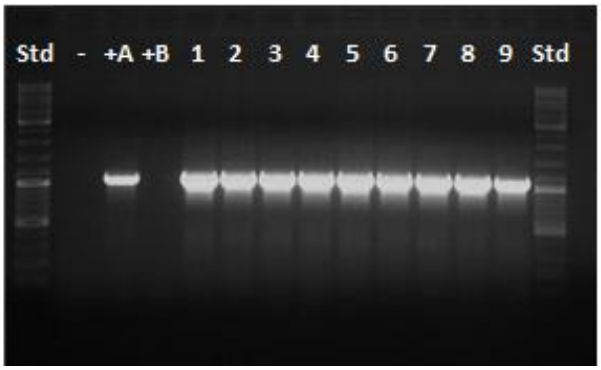

Figure 9: CPCR to verify CPR integration

Table 4: Lane description of Figure 8

Lane	Description	Visible bands
Std	GeneRuler™ DNA ladder mix	-
-	*Pp*CBS7435	-
+A	TW strain 6+3t	1 000 bp
+B	TW strain 3F	1 000 bp
1-9	Transformants upon pPpT4-HPO-CPR integration	1 000 bp

Table 5: Lane description of Figure 9

Lane	Description	Visible bands
Std	GeneRuler™ DNA ladder mix	-
-	*Pp*CBS7435	-
+A	TW strain 6+3t	1 000 bp
+B	TW strain 3F	-
1-9	Transformants upon pPpT4-HPO-CPR integration	1 000 bp

All nine strains tested positive for HPO expression by Western blot (Figure 7) showed also a strong band at 1 000 bp in colony PCR analytical gel (Figure 8). CPR gene integration into *Pp*CBS7435 was also verified by cPCR as all tested transformants showed a band at 1 000 bp.

Valencene resting cells assay

Western blot had proven that expression of HPO happened in several tested *Pichia pastoris* transformants and cPCR had shown that CPR was integrated into the genome. Five coexpression strains were tested in valencene resting cells assay to assess their potential of converting valencene into nootkatone.

Valencene resting cells assay was done following the standard protocol with valencene as substrate as described in Materials and Methods. Conversion of valencene to nootkatone was monitored for 24 h. Aliquots were withdrawn at 0 h and 24 h, extracted with ethyl acetate (EtAc) and analyzed with GC-FID. The amount of substrate and product was calculated accordingly in mg/g CDW and mg/L cell culture. A single measurement was performed. As positive control, strain TW 6+3t was used for comparison (Figure 10).

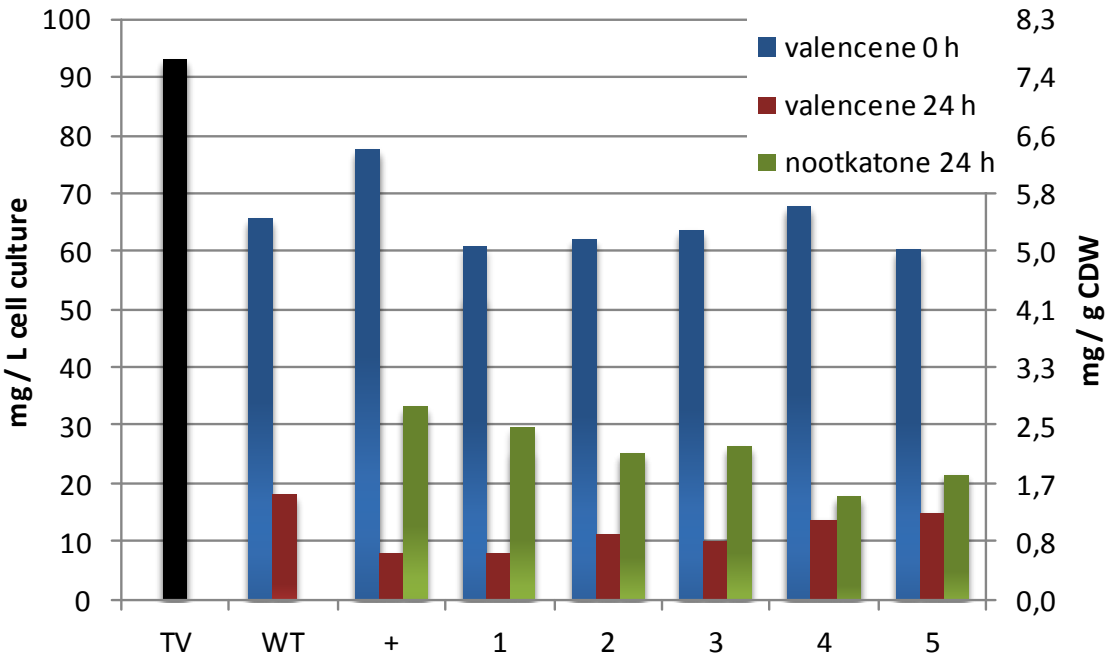

Figure 10: Valencene resting cells assay: pPpT4-HPO-CPR transformants

Table 6: Legend of Figure 10

	Description
TV	Amount of valencene theoretically added at 0 h
+	Positive control, strain TW 6+3t
1-5	Different transformants *Pp*CBS7435-pPpT4-HPO-CPR

Several strains containing the coexpression plasmid were able to convert valencene in different quantities in valencene resting cells assay. Strain 1 showed the best results and was chosen as the expression strain for further experiments. This strain is further on referred to as *Pp*HPO/CPR-**P**.

pPpHIS4-HPO/CPR

For different experiments, especially in **Project 2** of my thesis, dealing with the coexpression of glucose-1-dehydrogenase from *Bacillus subtilis* (*Bs*GDH) or glucose-6-phosphate dehydrogenase from *Pichia pastoris* (*Pp*G6PDH), it was necessary to use another coexpression strain generated by Tamara Wriessnegger. In this strain, the coexpression plasmid pPpHIS4-HPO-CPR (Figure 11) was integrated into the genome of *Pp*CBS7435*Δku70his4*.

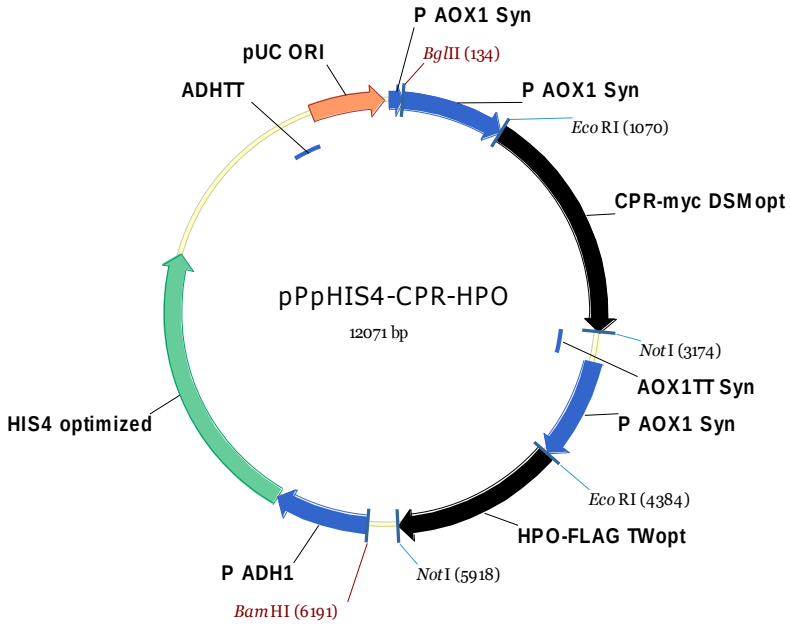

Figure 11: Coexpression plasmid pPpHIS4-CPR-HPO

Transformants were selected on MD^{-his} plates as the integration of pPpHIS4-CPR-HPO surmounts the histidine auxotrophy of *Pp*CBS7435. After transformation, several *Pichia* strains containing pPpHIS4-CPR-HPO were tested regarding their ability to convert valencene in resting cells assays by Tamara Wriessnegger. The best strain was chosen for later experiments and is referred to as *Pp*HPO/CPR-**T** in the subsequent work. Figure 12 compares expression strains *Pp*HPO/CPR-**P** and *Pp*HPO/CPR-**T** in a valencene resting cells assay.

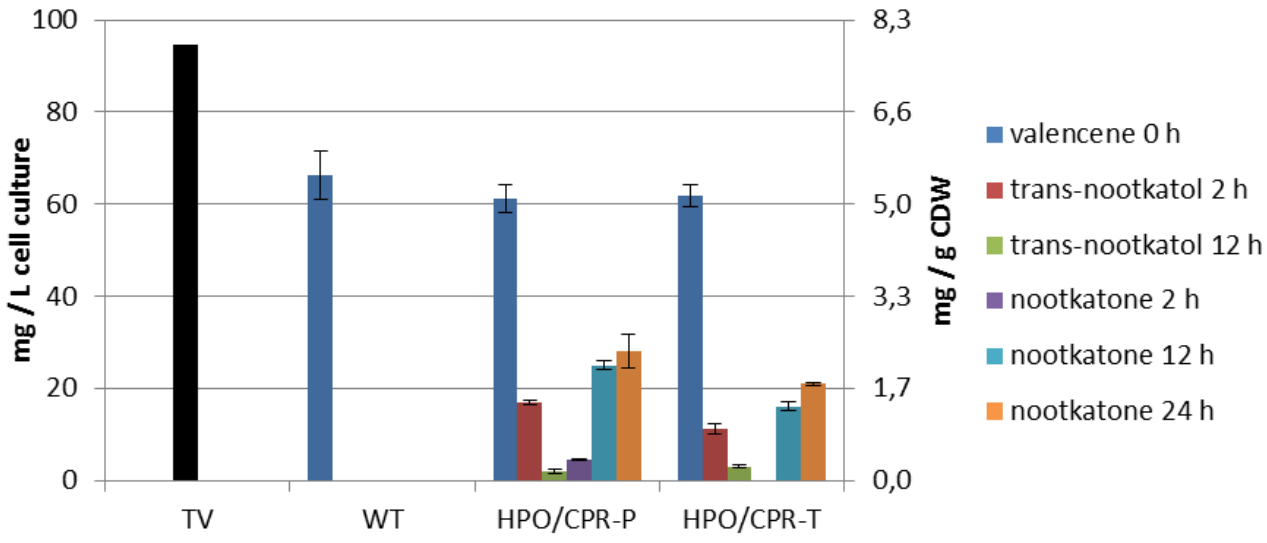

Figure 12: Valencene resting cells assay, *Pp*HPO/CPR-P and *Pp*HPO/CPR-T

Table 7: Legend of Figure 12

	Description
TV	Amount of valencene theoretically added at 0 h
WT	*Pp*CBS7435
HPO/CPR-**P**	WT-pPpT4-HPO-CPR
HPO/CPR-**T**	WT-pPpHIS4-CPR-HPO

Strain *Pp*HPO/CPR-**T** was performing slightly worse than *Pp*HPO/CPR-**P** in the assay. As the following experiments were predominantly supposed to show that nootkatone production could be improved with different techniques and consequential the final yield of nootkatone, this was of mediocre interest. The data obtained above serve as starting point for improvements.

Conclusion

The results of the valencene resting cells assay proved that it is possible to use the pPpT4 and the pPpHIS4 coexpression plasmids in order to integrate both genes simultaneously into *Pichia pastoris* genome and express both proteins functionally for valencene conversion. The strains *Pp*HPO/CPR-**P** and *Pp*HPO/CPR-**T** which had been chosen from several transformants tested have been used as basis for improvements in following experiments (Table 8). The aim was to prove that further alterations like the coexpression of different proteins are beneficial or unfavorable for valencene conversion, i.e. the performance of the CYP450 enzyme system.

Table 8: Use of HPO/CPR coexpression strains in the different experiments

	Project 1 *ADH-coexpression*	**Project 2** *NADPH-regeneration*
*Pp*HPO/CPR-**P**	Used for coexpression of three different ADHs	Used for coexpression of *Bs*GDH
*Pp*HPO/CPR-**T**	Not used	Used for coexpression of *Bs*GDH and *Pp*G6PDH

Project 1: Coexpression of different alcohol dehydrogenases to improve the conversion of nootkatol to nootkatone in *Pichia pastoris*

Outline

Alcohol dehydrogenases (ADHs, E.C. 1.1.1.1) are oxidoreductases that catalyze the reversible oxidation of alcohols to aldehydes or ketones with the concomitant reduction of NAD^+ or $NADP^+$ [24]. Figure 13 exemplarily shows the reversible oxidation of a secondary alcohol by an NAD(H) dependent ADH.

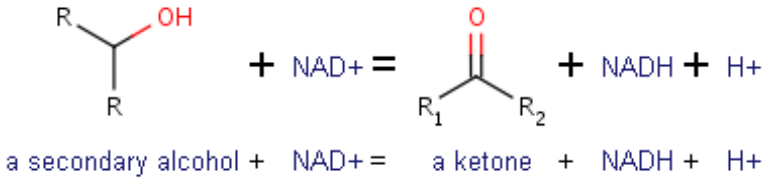

Figure 13: Reaction catalyzed by alcohol dehydrogenases [25]

The conversion of valencene in *Pichia pastoris* is a two step reaction mechanism (Figure 14) involving the monooxygenase HPO and the reductase CPR for the first step. The second step is most likely done by intrinsic *Pichia pastoris* ADHs that oxidize the intermediate product *trans*-nootkatol to nootkatone, which has been shown by previous experiments done by Tamara Wriessnegger.

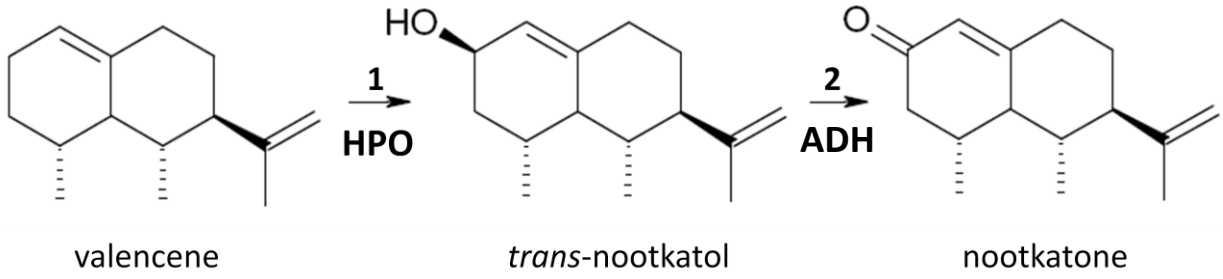

Figure 14: Two step reaction mechanism of valencene conversion

As these ADHs are uncharacterized, the question arose, whether the overexpression of certain intrinsic or foreign ADHs is beneficial for valencene conversion. The equilibrium of the reaction might be shifted and eventually more nootkatone may be produced in less time and overall valencene loss due to evaporation should be reduced. The requirements for these ADHs were, above all, a broad substrate tolerance and the ability of converting very bulky secondary alcohols, e.g. *trans*-nootkatol, to ketons. As ADHs in *Pichia pastoris* are not described in literature, a BLAST search was performed using the annotated and well characterized *ADH6* from *Saccharomyces cerevisiae* against the *Pichia pastoris*

GS115 genome, as the genome of CBS7435 has not been published at this time. ADHs in *Saccharomyces cerevisiae* are well reviewed [24] and *ADH6* was already characterized as a broad-specificity NADPH-dependet alcohol dehydrogenase. Due to the BLAST, two *Pichia pastoris* ADHs, one from chromosome 1 (ADH-C1) and one from chromosome 3 (ADH-C3), with sequence identities to *Sc*ADH6 of 43% or 37% were chosen. Both ADHs contain putative NAD(P) binding sites, but the cofactor dependency had not yet been determined experimentally. Furthermore, literature search resulted in further ADH candidates of direct interest for the experiments, such as the bacterial *Ras*ADH from *Ralstonia sp*. [26] or *Sy*ADH from *Sphingobium yanoikuyae* [27] achieving the requirements given. The latter was chosen for coexpression in *Pichia pastoris* because it has already been tested with bulky secondary alcohols similar to *trans*-nootkatol, such as 2-tetralol. Table 9 summarizes the most important information about the tested ADHs and their accession numbers in NCBI database.

Table 9: Enzymes used in ADH coexpression experiment

Enzyme	Acc. Number	Nucleotides	Amino acids	Size	C-terminal tag
ADH-C1	XP_002490014	1 074 bp	357 aa	39.4 kDa	FLAG
ADH-C3	XP_002492217	1 065 bp	354 aa	38.2 kDa	FLAG
ADH-SY	ACB78183	789 bp	262 aa	27.9 kDa	FLAG

ADH-C1, ADH-C3 and ADH-SY expressing HPO/CPR coexpression strains were generated and tested for protein expression in Western blots. The functional expression of the ADHs was assessed using a modified valencene resting cells assay with *cis*- and *trans*-nootkatol as substrates. Finally, strains expressing ADHs beside HPO and CPR were used in valencene resting cells assays to determine their potential of converting valencene and producing nootkatone.

Experimental

ADH-C1, ADH-C3 and ADH-SY expression constructs were created by cloning the desired ADH into a plasmid containing a KanMX6 (Kanamycin/Geneticin-G418 resistance) marker gene, Figure 15.

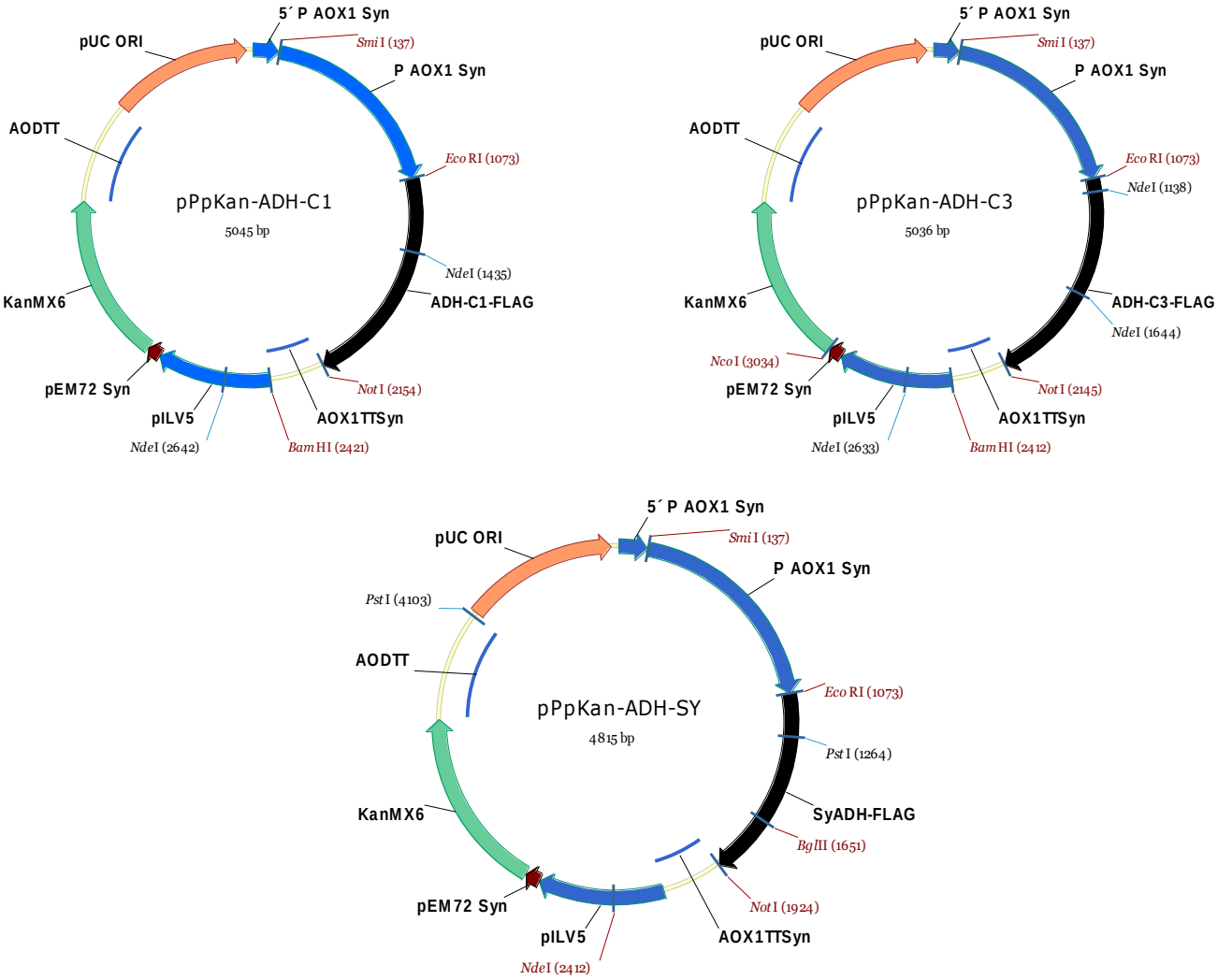

Figure 15: Plasmids for integration of ADH-FLAG genes into *P. pastoris* strains

The ADH genes were amplified by PCR from gDNA of *Pp*CBS7435 and cPCR from *Sphingobium yanoikuyae strain DSM 6900* and C-terminally FLAG-tagged using adequate primers.

PCR reaction mix, Phusion® High-Fidelity DNA Polymerase:

ADH-C1		ADH-C3		ADH-SY	
0.3 µL	gDNA* *Pp*CBS7435	0.3 µL	gDNA* *Pp*CBS7435	3 µL	Colony SN from *Sphingobium yanoikuyae*
3 µL	**Prim_fw:** FwADH-C1	3 µL	**Prim_fw:** FwADH-C3	3 µL	**Prim_fw:** Sy_ADH_fw
3 µL	**Prim_rev:** RvADH-C1	3 µL	**Prim_rev:** RvADH-C3	3 µL	**Prim_rev:** SyADHflag_rev
10 µL	5x Phusion® HF Buffer	10 µL	5x Phusion® HF Buffer	10 µL	5x Phusion® HF Buffer
5 µL	dNTPs (1 mM)	5 µL	dNTPs (1 mM)	5 µL	dNTPs (1 mM)
0.5 µL	Phusion® DNA Polymerase	0.5 µL	Phusion® DNA Polymerase	0.5 µL	Phusion® DNA Polymerase
28.2 µL	ddH_2O	28.2 µL	ddH_2O	25.5 µL	ddH_2O
50 µL	Total volume	50 µL	Total volume	50 µL	Total volume

`* gDNA was prepared by Tamara Wriessnegger

PCR cycling conditions:

ADH-C1: 98°C/30 s-(98°C/10 s-62°C/30 s-72°C/40 s) x35 -72°C/7 min -4°C/∞

ADH-C3: 98°C/30 s-(98°C/10 s-62°C/30 s-72°C/50 s) x35 -72°C/7 min -4°C/∞

ADH-SY: 98°C/1 min-(98°C/10 s-68°C/30 s-72°C/30 s) x35 -72°C/7 min -4°C/∞

After PCR, the amplified products were cleaned up on a preparative agarose gel. The PCR products (inserts), as well as vector pPpKan (backbone) were digested with *Eco*RI and *Not*I and again cleaned up on a preparative agarose gel. The concentrations and the right size of the constructs were determined with an analytical agarose gel. Table 10 shows the expected band sizes for the constructs (Figure 16).

Table 10: Band sizes for ADH-FLAG genes and pPpKan backbone vector

Construct	Expected band sizes
pPpKan	4 000 bp
ADH-SY-FLAG	900 bp
ADH-C1-FLAG	1 000 bp
ADH-C3-FLAG	1 000 bp

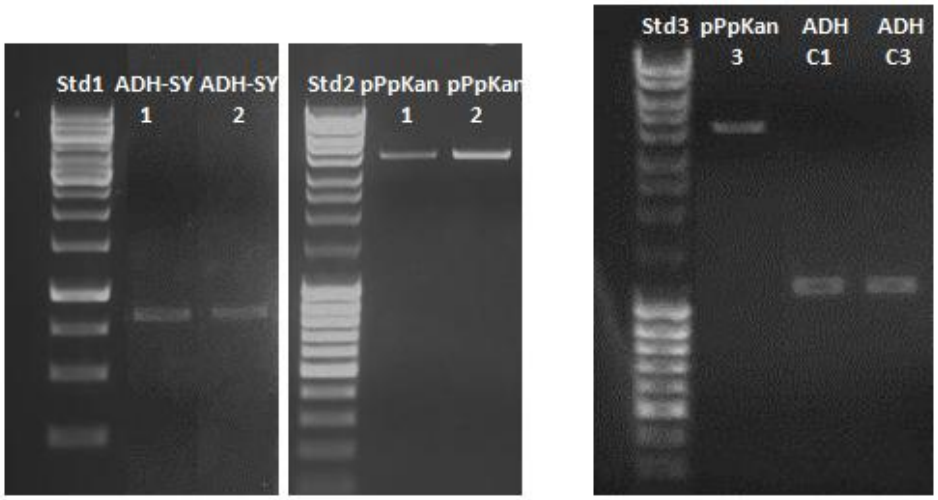

Figure 16: Analytical gels of ADH-C1, ADH-C3, ADH-SY and the backbone vector pPpKan

Table 11: Lane description of Figure 16

Lane	Description	Amount	Band	Concentration
Std1	GeneRuler™ 1kb DNA ladder	5 µL		
ADH-SY 1, 2	Insert for ligation, cut (*Eco*RI & *Not*I) and purified	1 µL	800 bp	5 ng/µL
Std2	MassRuler™ DNA ladder	10 µL		
pPpKan 1,2	Backbones for ADH-SY ligation, cut (*Eco*RI & *Not*I) and purified	1 µL	4 000 bp	25 & 50 ng/µL
Std3	MassRuler™ DNA ladder	10 µL		
pPpKan 3	Backbone for ADH-C1 and ADH-C3 ligation, cut (*Eco*RI & *Not*I) and purified	1 µL	4 000 bp	30 ng/µL
ADH-C1	Insert for ligation, cut (*Eco*RI & *Not*I) and purified	1 µL	1 100 bp	30 ng/µL
ADH-C3	Insert for ligation, cut (*Eco*RI & *Not*I) and purified	1 µL	1 100 bp	30 ng/µL

The inserts were ligated into the pPpKan-backbone and the resulting plasmid was electrotransformed into *E. coli* TOP10F'cells. Transformants were selected for on LB/Kan^{100} plates and several colonies were streaked for plasmid isolation. After plasmid isolation, positive clones were identified by restriction cut, preferably using enzymes cutting in the vector backbone and the insert sequence (Table 12).

Table 12: Control cuts of ADH-FLAG expression plasmids

Construct	Restriction enzyme	Band quantity	Expected band sizes
pPpKan-ADH-C1	*Nde*I	2	1 200 bp, 3 800 bp
pPpKan-ADH-C3	*Nde*I	3	500 bp, 1 000 bp, 3 600 bp
pPpKan-ADH-SY	*Pst*I	2	2 800 bp, 2 000 bp

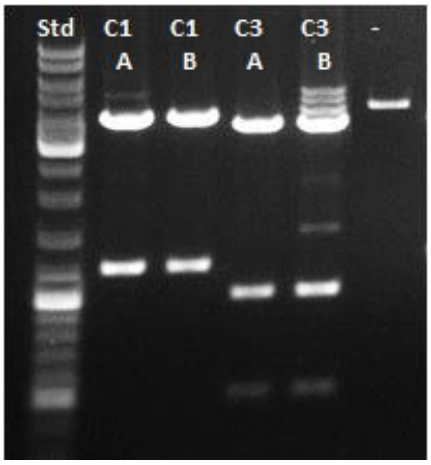

Figure 17: Control cuts of ADH-C1 and ADH-C3 expression plasmids

Table 13: Lane description of Figure 17

Lane	Description	Visible bands
Std	GeneRuler™ DNA ladder	
C1 A	pPpKan-ADH-C1	1 200 bp, 3 800 bp
C1 B	pPpKan-ADH-C1	1 200 bp, 3 800 bp
C3 A	pPpKan-ADH-C3	500 bp, 1 000 bp, 3 600 bp
C3 B	pPpKan-ADHC3	Contaminated
-	pPpKan	5 200 bp

Every tested plasmid containing ADH-C1 or ADH-C3 presented in Figure 17 is positive. In lane C1 A some uncut plasmid still was present, which explained the third band and the plasmid preparation in lane C3 B showed several unexpected bands. Therefore, this sample seemed to be contaminated and was not used for further experiments.

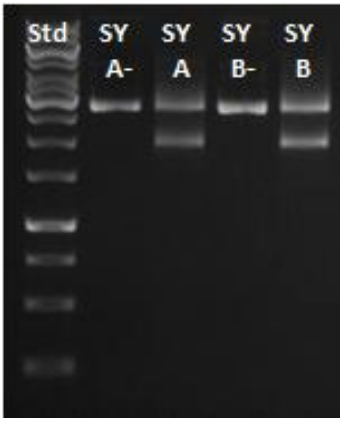

Table 14: Lane description of Figure 18

Lane	Description	Visible bands
Std	GeneRuler® 1kb DNA ladder	
SY A-	pPpKan-ADH-SY A	Uncut
SY A	pPpKan-ADH-SY A	3 000 bp, 2 000 bp
SY B-	pPpKan-ADH-SY B	Uncut
SY B	pPpKan-ADH-SY B	3 000 bp, 2 000 bp

Figure 18: Control cuts of ADH-SY expression plasmids

Analytical cut of pPpKan-ADH-SY plasmids resulted in every sample tested showing the two expected bands on the gel.

After verification of the different ADH expression plasmids with restriction enzyme control cuts, they were linearized with *Smi*I and integrated into *Pp*CBS7435 and *Pp*HPO/CPR-**P** via double crossover at the *Pichia pastoris AOX1* locus. Transformants were selected for on YPD/G418^{500} or YPD/G418^{400}/Zeo^{100} plates. Several transformants for each ADH in *Pp*CBS7435 and *Pp*HPO/CPR-**P** were chosen for Western blot analysis.

Western Blot analysis

SDS-PAGE, Western blot and subsequent immunodetection of the proteins were done according to the protocol described in Materials and Methods. Approximately 20 µg of TCA-precipitated proteins were loaded onto SDS-gels (NuPAGE®-Novex, 4-12% Bis-Tris). After Western blot, the membranes were stained in Ponceau S solution to control the efficiency of protein transfer. Detection of HPO protein as well as detection of all three ADHs was done with mouse anti-FLAG primary antibody (1:1 000 dilution) and detection of CPR protein with rabbit anti-myc primary antibody (1:1 000 dilution). Secondary antibodies used were goat anti-mouse IgG-HRP (1:5 000) and goat anti-rabbit IgG-HRP (1:20 000). Figure 19 and Figure 20 show several strains tested positive for each of the combinations.

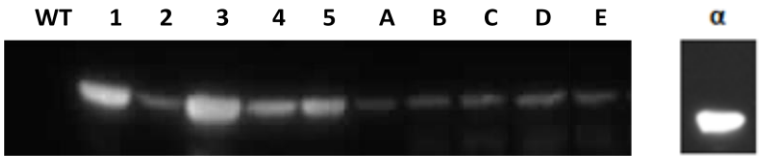

*Pp*CBS7435-strains containing ADH-C1, ADH-C3 and ADH-SY

Figure 19: Western blot analysis of ADH expression in *Pp*CBS7435

Table 15: Lane description of Figure 19

Lane	Description	Lane	Description	Lane	Description
1	WT-pPpKan-ADH-C1 transformant 1	A	WT-pPpKan-ADH-C3 transformant 1	α	WT-pPpKan-ADH-SY transformant
2	WT-pPpKan-ADH-C1 transformant 2	B	WT-pPpKan-ADH-C3 transformant 2	WT	*Pp*CBS7435
3	WT-pPpKan-ADH-C1 transformant 3	C	WT-pPpKan-ADH-C3 transformant 3		
4	WT-pPpKan-ADH-C1 transformant 4	D	WT-pPpKan-ADH-C3 transformant 4		
5	WT-pPpKan-ADH-C1 transformant 5	E	WT-pPpKan-ADH-C3 transformant 5		

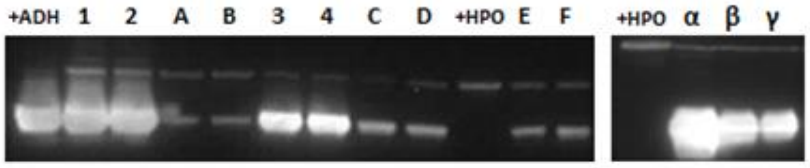

*Pp*HPO/CPR-**P**-strains containing ADH-C1, ADH-C3 and ADH-SY

Figure 20: Western blot analysis of ADH-expression in *Pp*HPO/CPR-P

Table 16: Lane description of Figure 20

Lane	Description	Lane	Description	Lane	Description
1	*Pp*HPO/CPR-**P**-pPpKan-ADH-C1 transformant 1	A	*Pp*HPO/CPR-**P** -pPpKan-ADH-C3 transformant 1	α	*Pp*HPO/CPR-**P**-pPpKan-ADH-SY transformant 1
2	*Pp*HPO/CPR-**P** -pPpKan-ADH-C1 transformant 2	B	*Pp*HPO/CPR-**P** -pPpKan-ADH-C3 transformant 2	β	*Pp*HPO/CPR-**P**-pPpKan-ADH-SY transformant 2
3	*Pp*HPO/CPR-**P** -pPpKan-ADH-C1 transformant 3	C	*Pp*HPO/CPR-**P** -pPpKan-ADH-C3 transformant 3	γ	*Pp*HPO/CPR-**P**-pPpKan-ADH-SY transformant 3
4	*Pp*HPO/CPR-**P** -pPpKan-ADH-C1 transformant 4	D	*Pp*HPO/CPR-**P** -pPpKan-ADH-C3 transformant 4		
		E	*Pp*HPO/CPR-**P** -pPpKan-ADH-C3 transformant 5	+HPO	*Pp*HPO/CPR-**P**
		F	*Pp*HPO/CPR-**P** -pPpKan-ADH-C3 transformant 6	+ADH	*Pp*CBS7435-pPpKan-ADH-C1

The Western blots showed very clearly that the alcohol dehydrogenases from *Sphingobium yanoikuyae* and *Pichia pastoris*, especially ADH-C1, are expressed to a high level. Figure 19 shows chemoluminescent detection of the different ADHs expressed in *Pp*CBS7435, ADH-C1 and ADH-C3 showed a signal at approximately 40 kDa and ADH-SY at 29 kDa. Figure 20 shows ADH expression in *Pp*HPO/CPR-**P**. As also HPO was FLAG-tagged, a light signal for HPO at ~58 kDa is detected in addition to the signal for the

different ADHs. ADHs are soluble proteins and, therefore, show a much brighter signal than the membrane bound protein HPO in anti-FLAG immunodetection. Furthermore, anti-myc detection of CPR in the *Pp*HPO/CPR-**P** strains was done (data not shown). Again, it did not work properly due to an old anti-myc antibody solution, as already stated above. Only very light bands were observed after acquiring the chemoluminescent signal for 1 h in the imager (G:BOX). *Pp*HPO/CPR-**P**-ADH strains expressing all three proteins (HPO, CPR, ADH) and showing a strong signal especially for HPO and the ADH on Western blots were chosen for further analysis with valencene resting cells and *cis*/*trans*-nootkatol assay. *Pp*CBS7435-ADH strains were used as comparison and reference strains if needed in Western blot analysis and the first experiments with the *cis*/*trans*-nootkatol assay. The following figures show the final results for *cis*/*trans*-nootkatol and valencene resting cells assays with strains coexpressing ADHs.

Cis/trans-nootkatol resting cells assay

The *cis/trans*-nootkatol resting cells assay was performed in the same manner as the valencene resting cells assays in Pyrex®-tubes, but using a equimolar mixture of *cis*- and *trans*-nootkatol as substrate. Conversion into nootkatone was monitored for 24 h. Aliquots were withdrawn at 0 h, 2 h, 12 h and 24 h, extracted with EtAc and quantified with GC-FID. The amount of substrate and product was calculated regarding mg/g CDW and mg/L cell culture. Quantifications were performed in triplicates. *Pp*CBS7435 and *Pp*HPO/CPR-**P** were used for comparison.

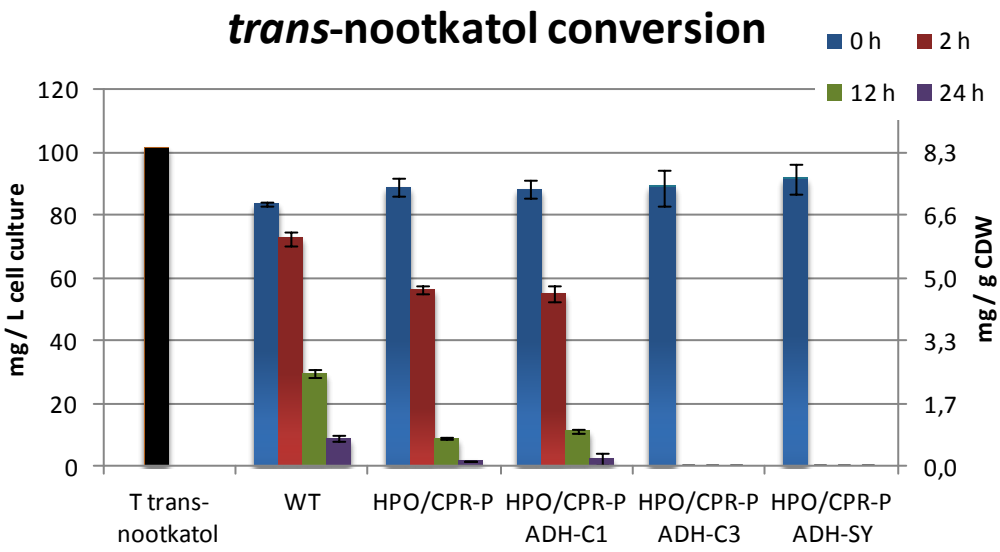

Figure 21: *Trans*-nootkatol recovered at indicated time points

Table 17: Legend of Figure 21

Lane	Description
T …	Amount of *trans- or cis*-nootkatol theoretically added at 0 h
WT	*Pp*CBS7435
HPO/CPR-P	*Pp*HPO/CPR-**P**
HPO/CPR-P ADH-C1	*Pp*HPO/CPR-**P**-pPpKan-ADH-C1
HPO/CPR-P ADH-C3	*Pp*HPO/CPR-**P**-pPpKan-ADH-C3
HPO/CPR-P ADH-SY	*Pp*HPO/CPR-**P**-pPpKan-ADH-SY

Figure 21 shows the depletion of the substrate *trans*-nootkatol during the assay. Several interesting facts can be observed. All tested strains, including *Pp*CBS7435 and *Pp*HPO/CPR-**P** that do not overexpress an ADH, are able to convert *trans*-nootkatol to nootkatone most certainly because of intrinsic ADHs in *Pichia pastoris*. Nevertheless, strains coexpressing ADH-C3 and ADH-SY outperform the other strains by converting *trans*-nootkatol much faster. Already after two h of conversion, *trans*-nootkatol was not detected anymore with GC-FID. ADH-C3 and ADH-SY seem to be perfect candidates to improve and speed up nootkatone production in valencene conversion assays. ADH-C1 did not significantly enhance *trans*-nootkatol conversion.

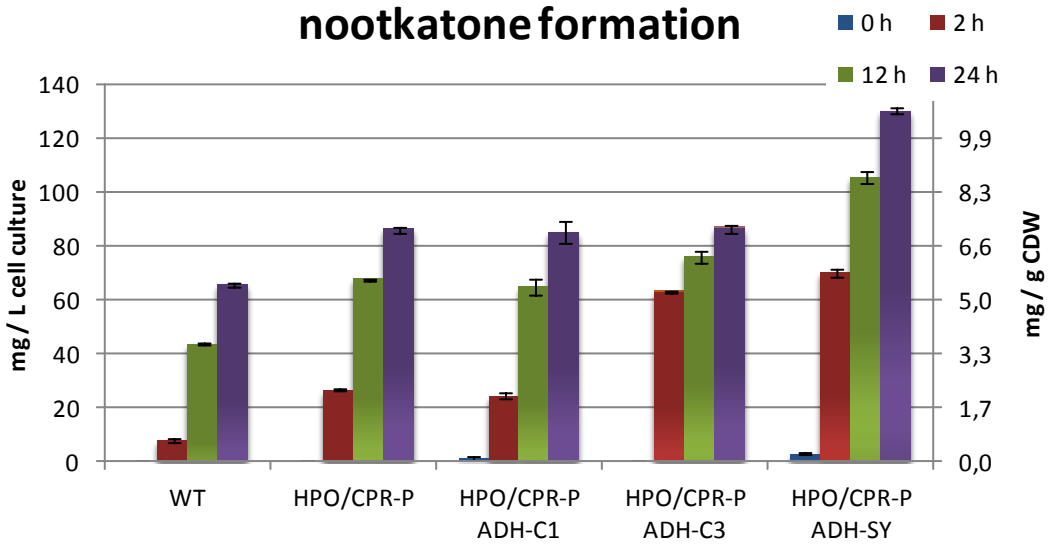

Figure 22: Nootkatone formation from *cis/trans*-nootkatol mixture

Description of the different lanes in Figure 22 can be looked up in Table 17. Figure 22 shows the increasing amounts of nootkatone built in *cis/trans*-nootkatol resting cells assay and proves that *trans*-

nootkatol is specifically converted to nootkatone by the intrinsic and overexpressed ADHs. Nootkatone yield increases directly proportional to the *trans*-nootkatol decrease in the assay.

The enantiomer of *trans*-nootkatol, *cis*-nootkatol, is obviously only converted by ADH-SY as can be seen in Figure 23.

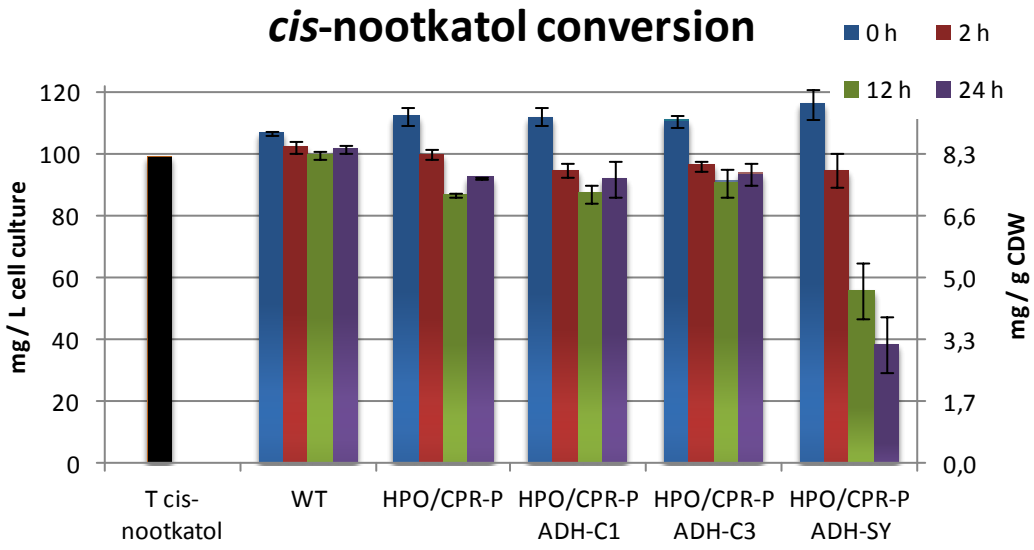

Figure 23: *Cis* –nootkatol recovered at indicated time points

Description of the different lanes in Figure 23 can be looked up in Table 17. ADH-SY comprised a higher substrate tolerance than the other ADHs tested and appeared to transform *cis*-nootkatol into nootkatone. ADH-C1 and ADH-C3 as well as further intrinsic *Pichia pastoris* ADHs did not to accept *cis*-nootkatol as substrate and the recovered amount stayed more or less constant during the assay. In Figure 23 the amounts of *cis*-nootkatol measured, especially at 0 h and 2 h exceeded the theoretically added amount of *cis*-nootkatol. This effect can be explained with the relatively low measurement accuracy at these time points, because only a very small amount of sample, i.e. 100 µL, was taken for extraction, which leaves a lot of space for inaccuracies. Another interesting result in Figure 23 is that *cis*-nootkatol remained constant in the assay during the conversion and was not lost due to evaporation. The presence of one alcohol function in the compound reduced its volatility extremely as compared to valencene.

ADH valencene resting cells assay

After confirming that coexpressing certain ADHs in *Pichia pastoris* fostered the conversion of *trans*-nootkatol, a valencene resting cells assay was done to test the effect on the whole conversion reaction. Resting cells assays were done according to the standard protocol described in Materials and Methods,

with valencene as substrate. Conversion of valencene to nootkatone was monitored for 24 h. Aliquots were withdrawn at 0 h, 2 h, 12 h and 24 h, extracted with EtAc and measured with GC-FID. The amount of substrate and product was calculated accordingly in mg/g CDW and mg/L cell culture. Measurements were performed in triplicates.

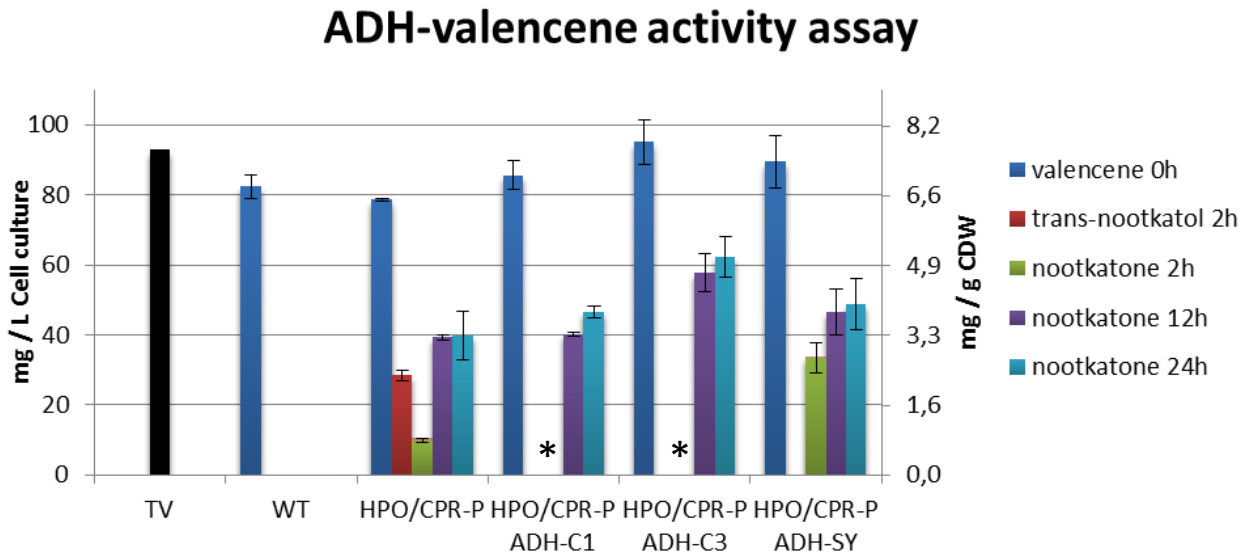

** For strains WT, HPO/CPR-**P**-ADH-C1 and HPO/CPR-**P**-ADH-C3, no 2 h sample was drawn.*

Figure 24: ADH valencene resting cells assay

Description of the different lanes in Figure 24 can be looked up in Table 17. Figure 24 shows that the coexpression of ADH-C3 and ADH-SY also had a positive effect to nootkatone formation if valencene was added as substrate. *Pichia* strains expressing ADH-C3 produced approximately 60% more nootkatone after 24 h of conversion compared with *Pp*HPO/CPR-**P** and the strain harboring ADH-SY produced still more than twice as much nootkatone after 2 h conversion as the reference strain without ADH coexpression.

Conclusion

The experiments on the coexpression of different ADHs in a HPO/CPR expressing strain clearly showed that the additional presence of ADH proteins had a positive effect on valencene conversion to nootkatone. ADH coexpression pushed the reaction towards the product, obviously by converting the intermediate product *trans*-nootkatol immediately to nootkatone when the former was built by the monooxygenase. As nootkatone featuring one additional carbonyl function in the compound was less volatile than valencene, the faster conversion of *trans*-nootkatol also reduces the losses due to valencene evaporation during the assay.

Project 2: Improved NADPH regeneration by coexpression of *Bs*GDH and *Pp*G6PDH

Outline

Cofactor regeneration and especially the regeneration of the nicotinamide cofactor NADPH is an important topic when speaking of class II cytochrome CYP450 mediated reactions. As we are working with membrane-attached CYP450 enzymes and simultaneous coexpression of an adequate P450-reductase which are always NADPH dependent, the development of an easy tool for enzymatic NADPH regeneration in eukaryotic systems like *Pichia pastoris* would be beneficial. While there has been a lot of research concerning NADH and NADPH regeneration for isolated coupled-enzyme and immobilized enzyme methods [28] and also several methods have been developed for *E. coli* whole cell regeneration [29], not a lot of research was going on concerning NAD(P)H regeneration in eukaryotic whole cell systems so far. With NADH regeneration, some approaches are in development, most notably in a work done in our house by the group of Prof. Anton Glieder [30]. They engineered the methanol utilization pathway in *Pichia pastoris* to increase the NADH pool in the cell. This was mainly done by overexpression of *Pichia pastoris* intrinsic proteins formate aldehyde dehydrogenase and formate dehydrogenase. As it comes to NADPH regeneration in *Pichia pastoris* whole cell systems only a limited number of possibilities to establish a regeneration system are feasible. After personal communication with our DSM research partner Monika Müller, it has been decided to try NADPH regeneration in *Pichia pastoris* by coexpression of the two NADP+ dependent enzymes glucose-1-dehydrogenase of *Bacillus subtilis* (*Bs*GDH) and glucose-6-phosphate-dehydrogenase of *Pichia pastoris* (*Pp*G6PDH).

Glucose 1-dehydrogenases (GDH)

Only abundant in prokaryotes, GDH catalyzes the oxidation of glucose to gluconolactone (Figure 25), under concomitant reduction of NAD^+ and $NADP^+$ [31].

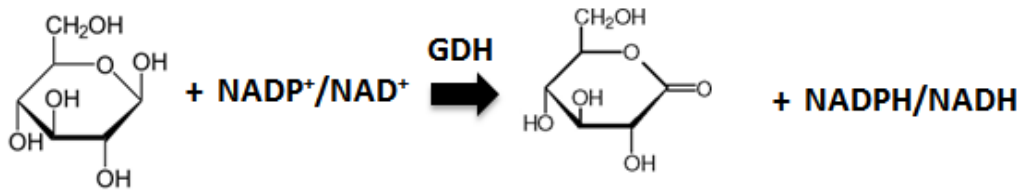

Figure 25: Nicotinamide cofactor regeneration by GDH

Bacillus subtilis GDH (*Bs*GDH) is widely used for cofactor regeneration in biotechnology in conjunction with cell free enzyme assays and whole cell systems in *E. coli* [32]. Concerning *Pichia pastoris*, only one example was found in literature of a group using the coexpression of a GDH from *Bacillus subtilis* for NADPH regeneration in a *Pichia pastoris* whole cell conversion, but not in combination with CYP450 mediated reactions [33]. Moreover, the group did not state whether the heterologous expression of this GDH did enhance product formation or did have any effect at all. The lack of publications using GDH in whole cell systems might be due to the fact that its substrate glucose gets phosphorylated glycolytically as soon as it enters the organism and therefore may not be available as substrate for the heterologous GDH anymore [34].

Glucose-6-phosphate dehydrogenase (G6PDH)

Two enzymes of the pentose phosphate pathway (PPP, glucose-6-phosphate dehydrogenase and 6-phosphogluconate dehydrogenase) are responsible for NADPH regeneration in nearly all living organisms [35]. Therefore, pushing the PPP seems to be a very reasonable approach to provide more NADPH inside the cell. One possibility to enhance the activity of PPP is the overexpression of intrinsic G6PDH in *Pichia pastoris (Pp*G6PDH*)*. G6PDH catalyzes the oxidation of glucose-6-phosphate to glucose-6-phosphatelactone and simultaneous NADPH regeneration. Glucose-6-phosphate is produced in the cell by intrinsic hexokinases from glucose which is added as cosubstrate.

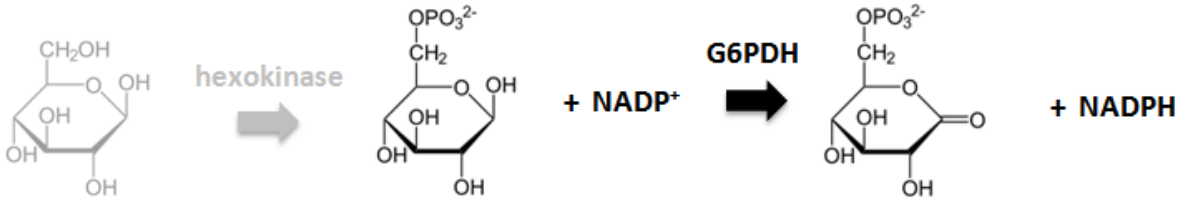

Figure 26: Nicotinamide cofactor regeneration by G6PDH

For *Pichia* strains expressing high amounts of CYP450 enzymes and reductases, a sufficient NADPH pool has to be guaranteed for optimal function. Thus, it would be essential to have an easy and effective NADPH regeneration system at hand. *Bs*GDH and *Pp*G6PDH expressing HPO/CPR strains were created and protein expression was assessed with Western blots. The effect of the coexpression was again determined with modified valencene resting cells assays. Table 18 summarizes the most important information about the tested proteins, *Bs*GDH and *Pp*G6PDH and gives their accession numbers in NCBI database.

Table 18: Enzymes used in NADPH regeneration experiment

Enzyme	Acc. Number	Nucleotides	Amino acids	Size	C-terminal tag
*Bs*GDH	NP_388275	786 bp	261 aa	28.1 kDa	6xHIS
*Pp*G6PDH	XP_002491203	1 515 bp	504 aa	57.7 kDa	6xHIS

Experimental

*Bs*GDH and *Pp*G6PDH expression constructs were created by cloning both genes into a plasmid bearing a Zeocin™ resistance (Figure 27 and 28). *Bs*GDH was additionally cloned into a plasmid bearing a KanMX6 (Kanamycin/Geneticin-G418 resistance) marker gene (Figure 27) to have a greater variety when testing the GDH influence on valencene conversion. It was not possible to clone the construct for *Pp*G6PDH into a pPpKan vector due to inadequate restriction sites present in the vector backbone and the gene. The gene sequence of *Pp*G6PDH contains several *Eco*RI restriction sites. Therefore, the alternative *Spe*I restriction site had to be used for cloning. The plasmid used for Kan/G418 resistance in the laboratory, pPpKan, does not possess this restriction site in its MCS and therefore cloning was possible.

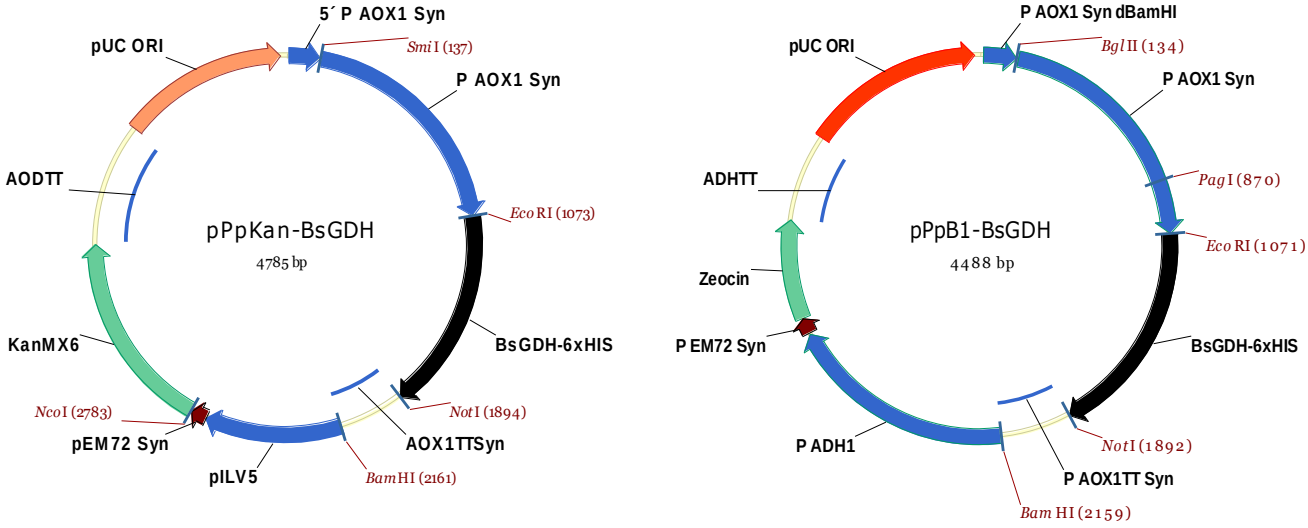

Figure 27: Plasmids for integration of *Bs*GDH-6xHIS into *P. pastoris* genome

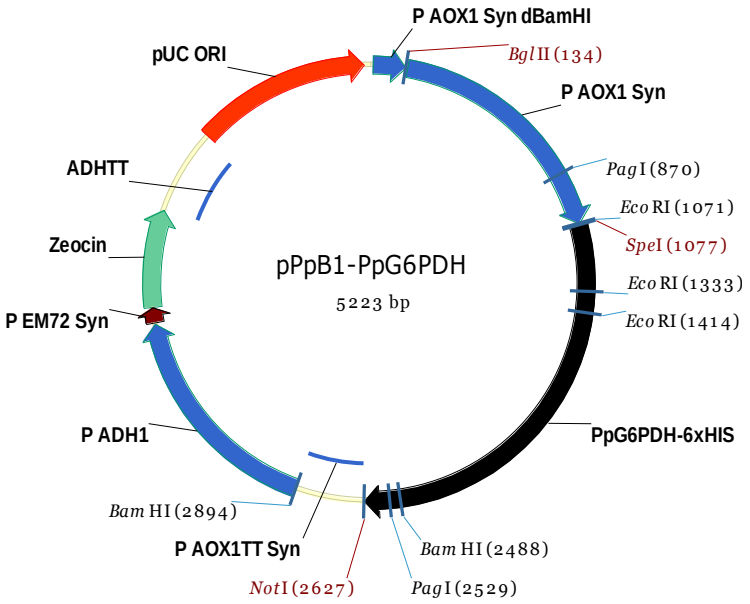

Figure 28: Plasmid for integration of *Pp*G6PDH into *P. pastoris* genome

The genes were amplified by cPCR from *Bacillus subtilis* (strain 168) and *Pichia pastoris* CBS7435 and C-terminally tagged by 6xHIS-tag.

PCR reaction mix, Phusion® High-Fidelity DNA Polymerase:

***Bs*GDH**		***Pp*G6PDH**	
3 µL	SN from *B. subtilis* colony	3 µL	SN from *P. pastoris* colony
3 µL	**Prim_fw**: BsGDH_fw	3 µL	**Prim_fw**: PpG6PDH_Spe_fw
3 µL	**Prim_rev**: BsGDHhis_rev	3 µL	**Prim_rev**: PpG6PDHhis_rev
10 µL	5x Phusion® HF Buffer	10 µL	5x Phusion® HF Buffer
5 µL	dNTPs (1 mM)	5 µL	dNTPs (1 mM)
0.5 µL	Phusion® DNA Polymerase	0.5 µL	Phusion® DNA Polymerase
25.5 µL	ddH_2O	25.5 µL	ddH_2O
50 µL	Total volume	50 µL	Total volume

PCR cycling conditions:

*Bs*GDH: 98°C/1 min-(98°C/10 s-70°C/30 s-72°C/30 s) x40 -72°C/7 min -4°C/∞

*Pp*G6PDH: 98°C/1 min-(98°C/10 s-68°C/30 s-72°C/50 s) x40 -72°C/7 min -4°C/∞

After PCR, the amplified product was cleaned up on a preparative agarose gel. The PCR products (inserts) were digested, *Bs*GDH with *EcoR*I and *Not*I, *Pp*G6PDH with *Spe*I and *Not*I and again cleaned up on a preparative agarose gel. The vector backbones were double digested according to the genes that were to be cloned into their MCS using *Eco*RI and *Not*I for *Bs*GDH and *Spe*I and *Not*I for *Pp*G6PDH cloning respectively. pPpKan backbone had already been prepared for the ADH experiments by preparative *Eco*RI and *Not*I cut, and could be used immediately (see Figure 16). The concentrations and the correct size of the other constructs were determined with an analytical agarose gel prior to ligation (Figure 29).

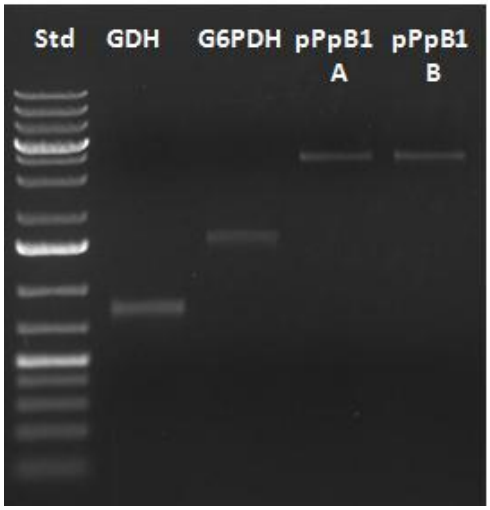

Figure 29: Analytical gel of *Bs*GDH and *Pp*G6PDH, as well as the vector backbone pPpB1

Table 19: Lane description of Figure 29

Lane	Description	Amount	Band	Concentrations
Std	GeneRuler™ 1kb Plus DNA ladder	5 µL		
GDH	*Bs*GDH insert for ligation, cut (*Eco*RI & *Not*I) and purified	1 µL	800 bp	5 ng/µL
G6PDH	*Pp*G6PDH insert for ligation, cut (*Spe*I & *Not*I) and purified	1 µL	1 500 bp	5 ng/µL
pPpB1 A & B	Vector backbones for *Bs*GDH and *Pp*G6PDH ligation, cut (*Eco*RI & *Not*I) and purified	1 µL	3 700 bp	5 ng/µL

The inserts were ligated into the vector backbones and the resulting plasmids were electrotransformed into *E. coli* TOP10F' cells. Transformants were selected for on LB/Zeo^{100} or LB/Kan^{100} plates and several colonies were streaked for plasmid isolation. After plasmid isolation, it was tried to identify positive clones by *Bam*HI restriction, but because of uncertain and unexpected band patters on the analytical gels (data not shown), correct cloning was confirmed by sequencing using primers pAOX1_fw and

TTpAOX1_rev. The comparison of the sequencing results to NCBI database entries confirmed correct plasmid sequences.

After verification of the different expression plasmids, pPpB1 plasmids were linearized with *Bgl*II, while pPpKan plasmids were cut with *Smi*I and integrated into *Pp*CBS7435 and *Pp*HPO/CPR-**P** (pPpKan-*Bs*GDH) as well as *Pp*HPO/CPR-**T** (pPpB1-*Bs*GDH and pPpB1-*Pp*G6PDH) via double crossover at the *AOX1* locus. Transformants were selected for on MD/Zeo^{100} or YPD/Zeo^{100}/G418^{400} plates. Several transformants for each combination were chosen for Western blot analysis.

Western blot analysis

SDS-PAGE, Western blot and subsequent immunodetection of the proteins were done according to the protocol described in Materials and Methods. Approximately 20 µg of TCA-precipitated proteins were loaded onto SDS-gels (NuPAGE®-Novex, 4-12% Bis-Tris). After Western blot, the membranes were stained in Ponceau S solution to control the efficiency of protein transfer. Detection of *Bs*GDH and *Pp*G6PDH was done with rabbit anti-6xHIS primary antibody (1:7 500 dilution). As secondary antibody a goat anti-rabbit IgG-HRP was used for chemoluminescent detection. The following figures show several strains tested positive for each of the above described combinations. *Bs*GDH-6xHIS and *Pp*G6PDH-6xHIS protein showed signals at ~30 kDa and ~60 kDa.

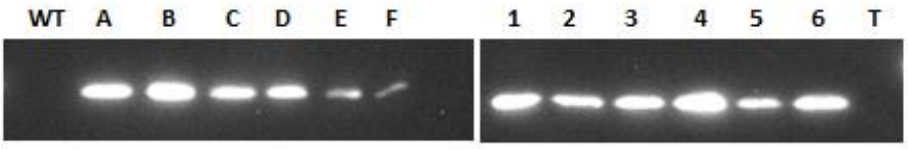

*Pp*CBS7435-*Bs*GDH strains and *Pp*HPO/CPR-**T**-*Bs*GDH strains

Figure 30: Western blot analysis of *Bs*GDH-6xHIS expression in *Pp*CBS7435 and *Pp*HPO/CPR-T**

Table 20: Lane description of Figure 30

Lane	Description	Lane	Description
WT	*Pp*CBS7435	1	*Pp*HPO/CPR-**T**-pPpB1-*Bs*GDH transformant 1
A	WT-pPpB1-*Bs*GDH transformant 1	2	*Pp*HPO/CPR-**T**-pPpB1-*Bs*GDH transformant 2
B	WT-pPpB1-*Bs*GDH transformant 2	3	*Pp*HPO/CPR-**T**-pPpB1-*Bs*GDH transformant 3
C	WT-pPpB1-*Bs*GDH transformant 3	4	*Pp*HPO/CPR-**T**-pPpB1-*Bs*GDH transformant 4
D	WT-pPpB1-*Bs*GDH transformant 4	5	*Pp*HPO/CPR-**T**-pPpB1-*Bs*GDH transformant 5
E	WT-pPpB1-*Bs*GDH transformant 5	6	*Pp*HPO/CPR-**T**-pPpB1-*Bs*GDH transformant 6
F	WT-pPpB1-*Bs*GDH transformant 6	T	*Pp*HPO/CPR-**T**

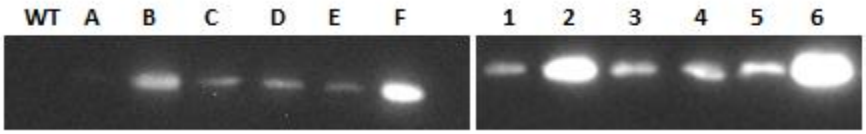

*Pp*CBS7435-*Bs*GDH strains and *Pp*HPO/CPR-**P**-*Bs*GDH strains

Figure 31: Western blot analysis of *Bs*GDH-6xHIS expression in *Pp*CBS7435 and *Pp*HPO/CPR-P**

Table 21: Lane description of Figure 31

Lane	Description	Lane	Description
WT	*Pp*CBS7435	1	*Pp*HPO/CPR-**P**-pPpKan-*Bs*GDH transformant 1
A	WT-pPpKan-*Bs*GDH transformant 1	2	*Pp*HPO/CPR-**P**-pPpKan-*Bs*GDH transformant 2
B	WT-pPpKan-*Bs*GDH transformant 2	3	*Pp*HPO/CPR-**P**-pPpKan-*Bs*GDH transformant 3
C	WT-pPpKan-*Bs*GDH transformant 3	4	*Pp*HPO/CPR-**P**-pPpKan-*Bs*GDH transformant 4
D	WT-pPpKan-*Bs*GDH transformant 4	5	*Pp*HPO/CPR-**P**-pPpKan-*Bs*GDH transformant 5
E	WT-pPpKan-*Bs*GDH transformant 5	6	*Pp*HPO/CPR-**P**-pPpKan-*Bs*GDH transformant 6
F	WT-pPpKan-*Bs*GDH transformant 6		

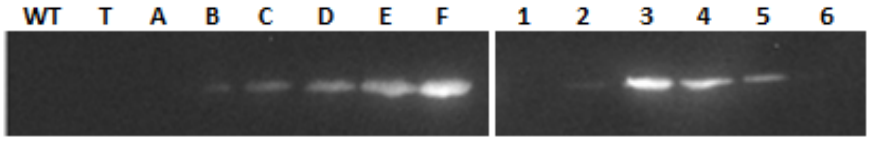

*Pp*CBS7435-*Pp*G6PDH strains and *Pp*HPO/CPR-**T**- *Pp*G6PDH strains

Figure 32: Western blot analysis of *Pp*G6PDH-6xHIS expression in *Pp*CBS7435 and *Pp*HPO/CPR-T**

Table 22: Lane description of Figure 32

Lane	Description	Lane	Description
WT	*Pp*CBS7435	1	*Pp*HPO/CPR-**T**-pPpB1-*Pp*G6PDH transformant 1
A	WT-pPpB1-*Pp*G6PDH transformant 1	2	*Pp*HPO/CPR-**T**-pPpB1-*Pp*G6PDH transformant 2
B	WT-pPpB1-*Pp*G6PDH transformant 2	3	*Pp*HPO/CPR-**T**-pPpB1-*Pp*G6PDH transformant 3
C	WT-pPpB1-*Pp*G6PDH transformant 3	4	*Pp*HPO/CPR-**T**-pPpB1-*Pp*G6PDH transformant 4
D	WT-pPpB1-*Pp*G6PDH transformant 4	5	*Pp*HPO/CPR-**T**-pPpB1-*Pp*G6PDH transformant 5
E	WT-pPpB1-*Pp*G6PDH transformant 5	6	*Pp*HPO/CPR-**T**-pPpB1-*Pp*G6PDH transformant 6
F	WT-pPpB1-*Pp*G6PDH transformant 6		
T	*Pp*HPO/CPR-**T**		

The Western blots showed that the proteins were expressed in the different strains. Interestingly *Bs*GDH in general showed better expression than *Pp*G6PDH. For the first studies on GDH/G6PDH activity and the influence of their coexpression on valencene conversion, one strain for each combination showing the brightest signal on Western blot was chosen (Table 23).

Table 23: Strains for GDH assay

Name	Strain	Western blot	Total protein concentration in homogenates
WT-GDH-Kan	*Pp*CBS7435-pPp-Kan-*Bs*GDH	Figure 31, F	14.78 mg/mL
WT-GDH-B1	*Pp*CBS7435-pPp-B1-*Bs*GDH	Figure 30, B	23.65 mg/mL
WT-G6PDH	*Pp*CBS7435-pPp-B1-*Pp*G6PDH	Figure 32, F	19.07 mg/mL
*Pp*HPO/CPR-**T**-GDH	*Pp*HPO/CPR-**T**-pPp-B1-*Bs*GDH	Figure 30, 4	18.94 mg/mL
*Pp*HPO/CPR-**T**-G6PDH	*Pp*HPO/CPR-**T**-pPp-B1-*Pp*G6PDH	Figure 32, 3	28.07 mg/mL
*Pp*HPO/CPR-**P**-GDH	*Pp*HPO/CPR-**P**-pPp-Kan-*Bs*GDH	Figure 31, 6	20.56 mg/mL

GDH assay

After confirming that *Bs*GDH and *Pp*G6PDH were expressed in *Pichia pastoris*, six strains were chosen (Table 23) and tested for functional protein expression with a simple in vitro microtiter plate GDH assay. The GDH assay is based on the different absorption of $NADP^+$ and NADPH at 340 nm.

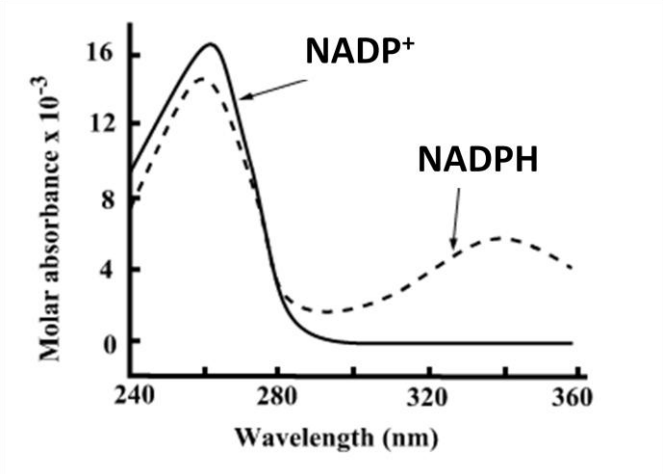

Figure 33: Comparison of the absorbance spectra of $NAPD^+$ and NADPH

$NADP^+$ has a single absorption maximum at approximately 260 nm, whereas NADPH absorbs as well at 340 nm. Therefore, an increasing absorption at 340 nm indicates an increasing abundance of NADPH.

Homogenates of the six chosen strains were prepared and used in 1:10 dilutions for the assay, which were performed in triplicates. Figures 34-36 show the change in absorption of different GDH/G6PDH expressing strains in comparison to their respective WTs at 340 nm. The values shown in the diagrams were normalized according to the protein concentrations of the homogenates (Table 23) and the initial absorbance values at 0 min.

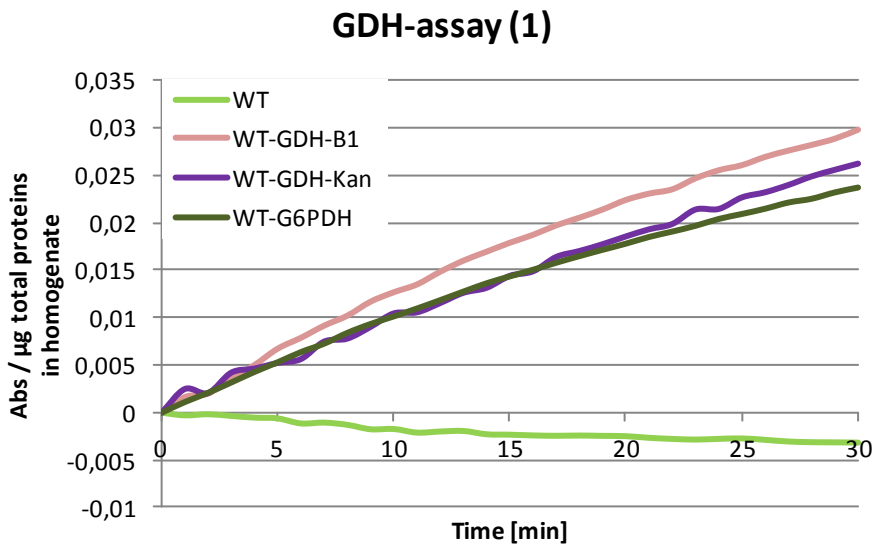

Figure 34: NAD(P)H regeneration analysis of *Pp*CBS7435 overexpressing GDH and G6PDH

Table 24: Legend of Figure 34

	Description
WT	*Pp*CBS7435
WT-GDH-B1	WT-pPpB1-*Bs*GDH
WT-GDH-Kan	WT-pPpKan-*Bs*GDH
WT-G6PDH	WT-pPpB1-*Pp*G6PDH

*Pp*CBS7435 strains expressing GDH or G6PDH show, in contrast to the WT, an increasing absorption in the measurement and therefore, an accumulation of NADPH, which indicates that GDH is expressed functionally and is able to generate NADPH in the cell.

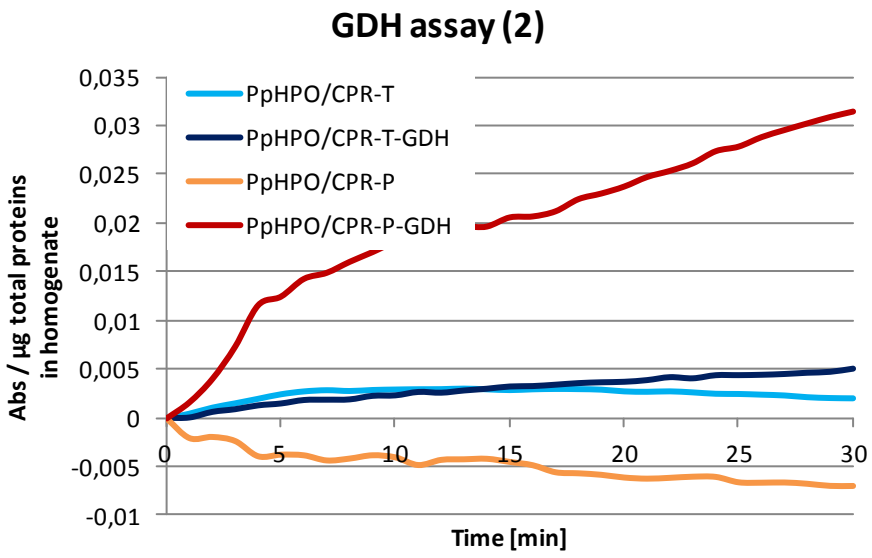

Figure 35: NAD(P)H regeneration analysis of *Pp*HPO/CPR strains overexpressing GDH

Table 25: Legend of Figure 35

	Description
*Pp*HPO/CPR-**T**	*Pp*HPO/CPR-**T**
*Pp*HPO/CPR-**T**-GDH	*Pp*HPO/CPR-**T**-pPpB1-*Bs*GDH
*Pp*HPO/CPR-**P**	*Pp*HPO/CPR-**P**
*Pp*HPO/CPR-**P**-GDH	*Pp*HPO/CPR-**T**-pPpKan-*Bs*GDH

Strain *Pp*HPO/CPR-**P**-GDH showed an increasing absorption in the course of the assay compared to its WT, while the absorption in *Pp*HPO/CPR-**T**-GDH stayed similar to its WT. There are two possible reasons for the different behavior of strain *Pp*HPO/CPR-**P**-GDH and *Pp*HPO/CPR-**T**-GDH; either the expression level/activity of GDH or the expression level/activity of CPR in the strains. In order to compare the expression levels of the proteins, a Western blot was performed (Figure 36 and Figure 37).

Western blot analysis

The expression levels of *Bs*GDH-6xHIS and *Pp*G6PDH-6xHIS were detected beside tagged HPO and CPR proteins. SDS-PAGE, Western blot and subsequent immunodetection of the proteins were done according to the protocol described in Materials and Methods. Approximately 20 µg of TCA-precipitated proteins were loaded on SDS-gels (NuPAGE®-Novex, 4-12% Bis-Tris). After Western blot, the membranes were stained in Ponceau S solution to control the efficiency of protein transfer. Detection of *Bs*GDH and *Pp*G6PDH was done with rabbit anti-6xHIS primary antibody (1:7 500 dilution). As secondary antibody a goat anti-rabbit IgG-HRP (1:20 000) was used. Detection of HPO and CPR was done using a 1:1 mixture of

rabbit anti-myc antibody (1:1 000 dilution) and mouse anti-FLAG antibody (1:1 000) to detect both proteins at once. Secondary antibodies used were goat anti-mouse IgG-HRP (1:5 000) and goat anti-rabbit IgG-HRP (1:20 000). The membranes were incubated o/n in the primary antibodies to get better results for CPR and HPO detection.

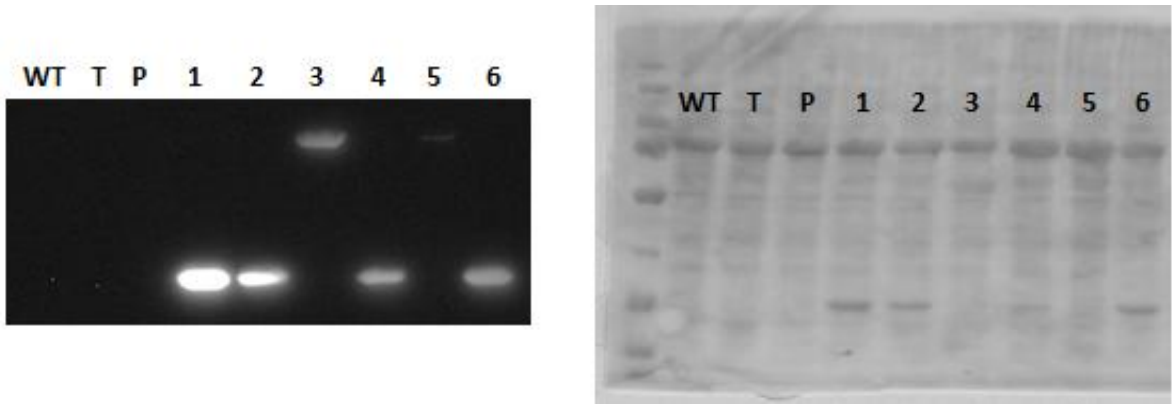

Figure 36: Western blot analysis detecting 6xHIS tagged GDH and G6PDH

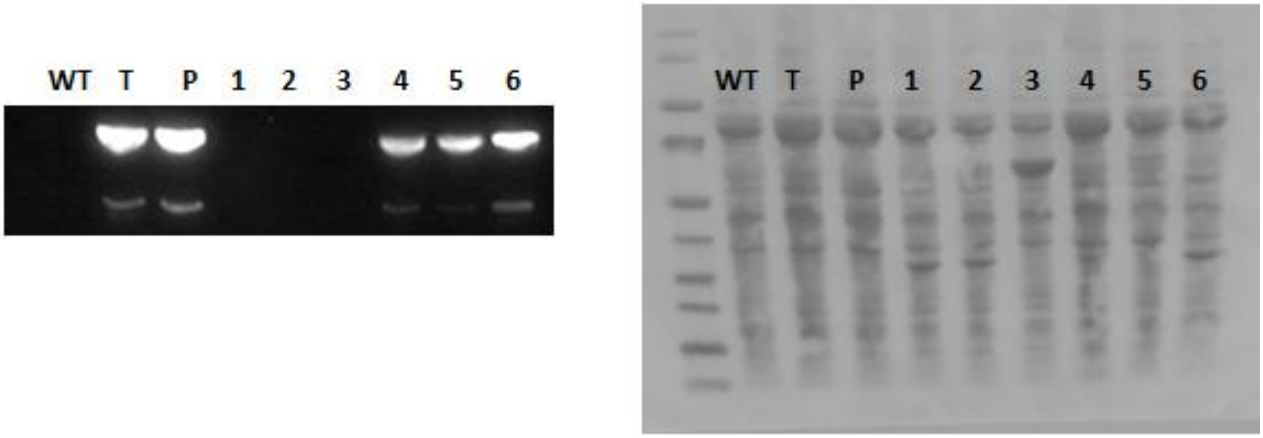

Figure 37: Western blot analysis of strains for GDH assay, HPO-FLAG and CPR-myc detection

Table 26: Lane description for Figure 36 and Figure 37

Lane	Description	Lane	Description
1	WT-pPpB1-*Bs*GDH	WT	*Pp*CBS7435
2	WT-pPpKan-*Bs*GDH	T	*Pp*HPO/CPR-**T**
3	WT-pPpB1-*Pp*G6PDH	P	*Pp*HPO/CPR-**P**
4	*Pp*HPO/CPR-**T**-*Bs*GDH		
5	*Pp*HPO/CPR-**T**-pPpB1-*Pp*G6PDH		
6	*Pp*HPO/CPR-**P**-*Bs*GDH		

When comparing the strains for expression level of GDH and CPR, both proteins were expressed to apparently similar amounts as the bands on Western blot show the same brightness. However, it might be that the *Pp*HPO/CPR-**T**-GDH transformant does not functionally express GDH and, therefore, does not show increasing absorbance in the GDH assay. A positive signal on Western blot does not automatically imply functional protein expression. Furthermore, it is possible that CPR expressed in *Pp*HPO/CPR-**T** is much more active than CPR expressed in *Pp*HPO/CPR-**P** strains and regenerated NADPH is immediately consumed. To exclude one of the scenarios, a CPR activity assay of the tested transformant would bring clarity, but was not done during this work. Testing further transformants of *Pp*HPO/CPR-**T**-GDH could solve the question, whether the results were ephemeral or occur in every *Pp*HPO/CPR-**T**-GDH/G6PDH strain.

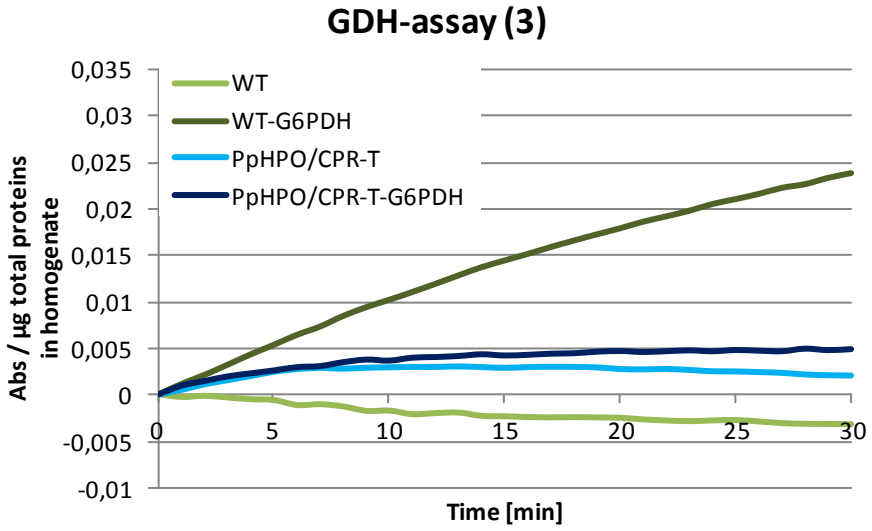

Figure 38: NAD(P)H regeneration analysis of *Pp*CBS7435 and *Pp*HPO/CPR-T overexpressing G6PDH

Table 27: Legend of Figure 38

	Description
WT	*Pp*CBS7435
WT-G6PDH	WT-pPpB1-*Pp*G6PDH
*Pp*HPO/CPR-**T**	WT-pPpHIS4-HPO-CPR
*Pp*HPO/CPR-**T**-G6PDH	*Pp*HPO/CPR-**T**-pPpB1-G6PDH

Figure 38 shows a picture very similar to Figure 35. The coexpression of G6PDH in the WT showed an increasing absorption over the time, similar to the results when GDH is coexpressed. However,

coexpression of G6PDH in *Pp*HPO/CPR-**T** did not show any effect and absorption was again similar to the WT.

In order to exclude that all effects shown in the figures above were due to unspecific NADP+ reduction, the assay was also performed using only NADP+ and without glucose as substrate (Figure 39).

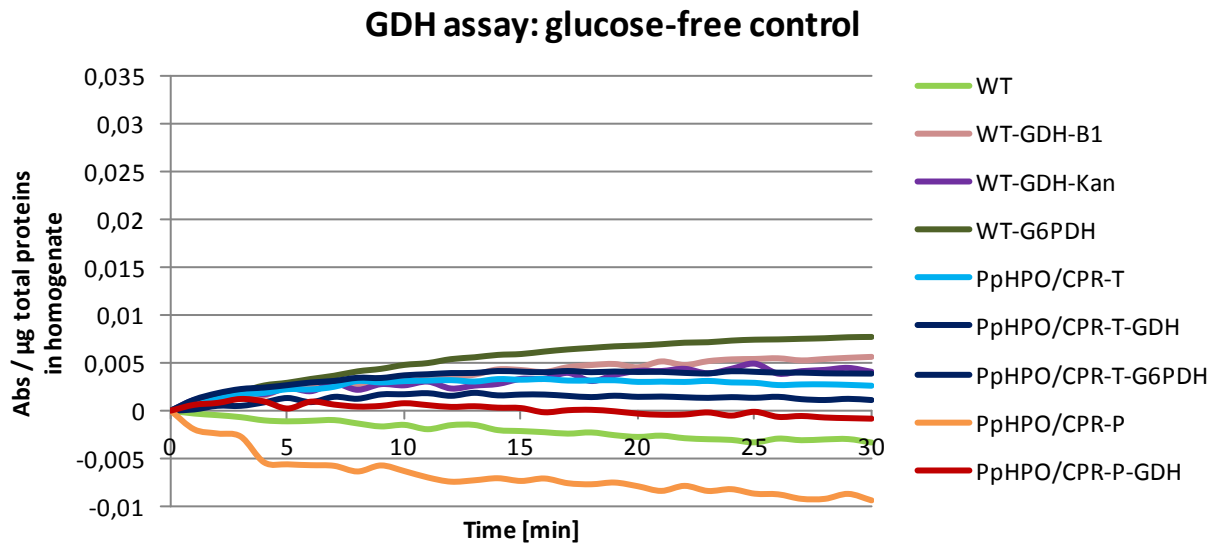

Figure 39: Control of unspecific $NADP^+$ reduction background

Figure 39 suggests that the enhanced absorption of GDH/G6PDH expressing strains was due to the addition of glucose. The lack of glucose in the assay kept absorption of all strains at a constant level and, therefore, the effects shown in the figures above were definitely due to the functional expression of GDH or G6PDH and not unspecific reduction of $NADP^+$ by other enzymes.

Influence of glucose on valencene conversion reactions

After confirming that GDH and G6PDH are, at least partially, functionally expressed in the different strains, the next step would be a valencene resting cells assay in order to check a possible influence of GDH and G6PDH coexpression on valencene conversion. The crucial point for this experiment was to find a good glucose concentration for the assay. Standard valencene resting cells assays have always been performed in 50 mM KP_i-buffer pH 7.4 and no cosubstrate had to be added to the reaction mixture.

After a series of experiments was done determining the influence of glucose in the resting cells assay, it has been shown that the addition of glucose to the assay decreased overall conversion rates of

valencene to nootkatone. Glucose in the resting cells assay was especially hindering the second reaction step, the alcohol oxidation to the ketone by decreasing the activity of the ADHs towards nootkatone. *Trans*-nootkatol got accumulated and the overall yield decreased. Figure 40 exemplifies this "glucose-effect" on valencene conversion by comparing resting cells assay done in 50 mM KP_i-buffer pH 7.4, 50 mM KP_i-buffer pH 7.4 + 2.5% glucose and BMGY medium. The assay was done according to the standard protocol with valencene as substrate, described in Materials and Methods. The "glucose effect" is shown for *Pp*HPO/CPR-**P** and *Pp*HPO/CPR-**P**-ADH-SY in 50 mM KP_i-buffer pH 7.4+ 2.5% glucose and for strain *Pp*HPO/CPR-**P** in BMGY medium, to determine a possible influence of glycerol onto the conversion reaction. Conversion of valencene to nootkatone was monitored for 24 h and aliquots were withdrawn at 0 h, 12 h and 24 h, extracted with EtAc and measured with GC-FID. The amount of substrate and product was calculated accordingly in mg/g CDW and mg/L cell culture. Measurements were performed in duplicates.

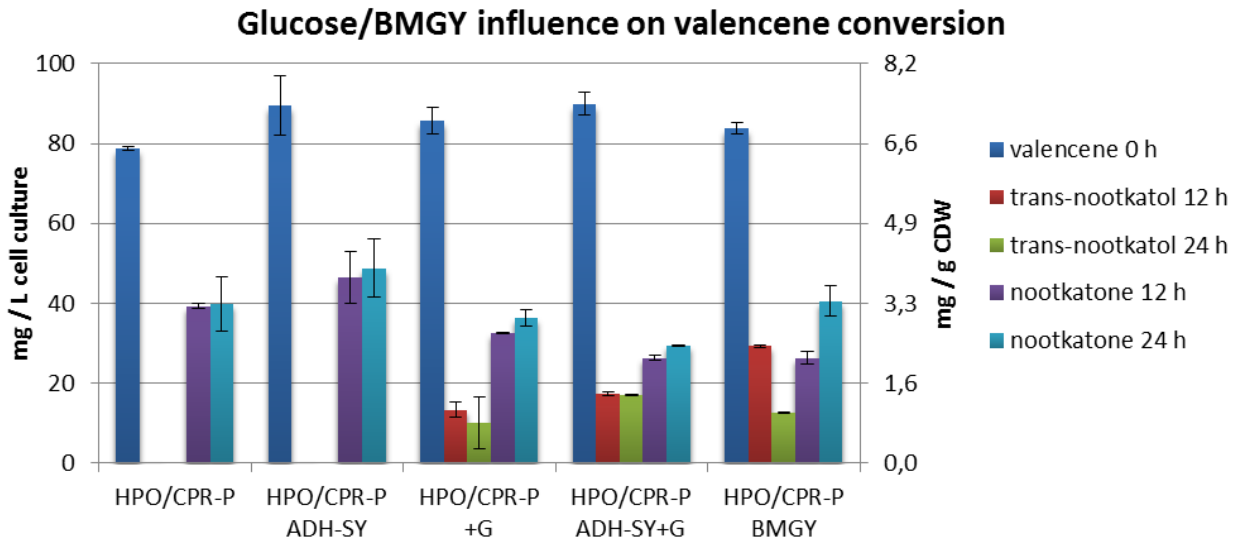

Figure 40: Valencene resting cells assay, influence of glucose on the conversion

Lane	Description
HPO/CPR-**P**	Strain *Pp*HPO/CPR-**P** in KP_i-buffer
HPO/CPR-**P** ADH-SY	*Pp*HPO/CPR-**P**-pPpKan-ADH-SY in KP_i -buffer
HPO/CPR-**P** +G	Strain *Pp*HPO/CPR-**P**, in Kpi-buffer + 2.5% glucose
HPO/CPR-**P** ADH-SY +G	*Pp*HPO/CPR-**P**-pPpKan-ADH-SY, in KP_i-buffer + 2.5% glucose
HPO/CPR-**P** BMGY	Strain *Pp*HPO/CPR-**P** in BMGY medium

Nootkatone production was decreased and *trans*-nootkatol accumulated in the resting cells assay when adding glucose to a final concentration of 2.5% (Figure 40). Especially the strain coexpressing ADH-SY showed a huge decrease in the productivity and only half of nootkatone after 12 and 24 h compared to standard resting cells assay. *Pp*HPO/CPR-**P** tested in BMGY medium showed an accumulation of *trans*-nootkatol after 12 and 24 h, and a decrease of nootkatone production after 12 h. On the other hand, the loss in nootkatone production caused by adding BMGY medium to the reaction was balanced after 24 h. BMGY only seemed to decelerate the conversion as the overall yield after 24 h stayed the same.

Valencene resting cells assay

Although the previous experiments showed a negative effect of glucose on the oxidation of *trans*-nootkatol to nootkatone, a valencene resting cells assay was performed. In order to find a reference point to which concentration of glucose as cosubstrate should be used as cosubstrate, a literature search for similar experiments in *Pichia* was carried out. The outcome was that only one paper has been published dealing with a GDH-regeneration system in a *Pichia pastoris* whole cell conversion [33]. In this work, the group suggests using a 1 M glucose/buffer solution with and without additional 0.1 mM $NADP^+$. This glucose concentration was expected to be too high for this reaction considering the results discussed above. Thus, the performance of GDH/G6PDH coexpressing strains and the respective WTs was also tested in BMDY-medium (1% glucose), and without adding any glucose to the assay for comparison. The assay was done according to the standard protocol with valencene as substrate and the conversion from valencene to nootkatone was monitored for 24 h. Aliquots were withdrawn at 0 h, 12 h and 24 h, extracted with EtAc and measured with GC-FID. The amount of substrate and product was calculated regarding mg/g CDW and mg/L cell culture. A single measurement was performed.

A superficial glance on the single data set showed that 1 M glucose, with or without $NADP^+$, is an excessively high concentration for this model reaction blocking most of ADH activity, especially in combination with strain *Pp*HPO/CPR-**T**. Thus, it was impossible to conclude on any effect regarding applicability of the NAD(P)H regeneration system (data not shown). Only the results of the assay performed in BMDY-medium (1%, ~55 mM glucose) can be used in order to compare GDH/G6PDH coexpressing strains and their respective WT's (Figure 41).

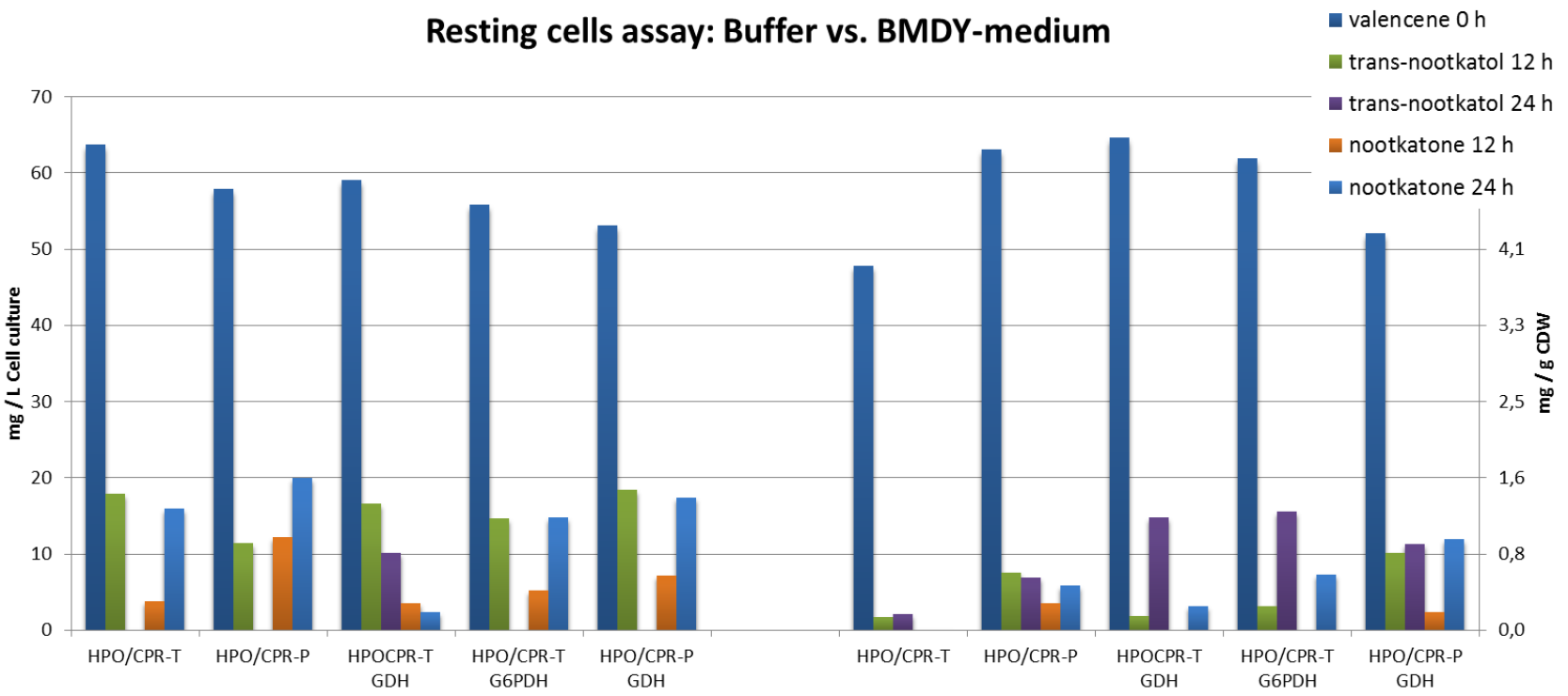

Figure 41: Valencene resting cells assay, effects of GDH and G6PDH coexpression

Figure 41 shows clearly that the levels of nootkatone reached in standard resting cells assay cannot be reached in assays containing glucose. Slightly contradicting to the results obtained by in vitro GDH assay with *Pp*HPO/CPR-**T** strains, this resting cells assay stipulates that the coexpression of GDH and G6PDH improves the performance of these strains in BMDY medium. The coexpression of GDH in strain *Pp*HPO/CPR-**P**-GDH improved its performance to a lower extent. The assay shown in general achieved rather low yields (Figure 41), also for standard resting cells assays, when compared with previous experiments. This might be due to the long storage times of the samples at -20°C, which is thought to decrease the amounts of terpenes analyzed with GC-FID.

Conclusion

It was possible to functionally coexpress GDH from *Bacillus subtilis* and G6PDH from *Pichia pastoris* in different *Pichia pastoris* strains, which was confirmed with Western blot analysis and GDH assay. However, the model reaction that was used for testing the usability of GDH or G6PDH in NADPH regeneration in a *Pichia pastoris* resting cells approach has several drawbacks. The major one was that the addition of glucose to the reaction buffer of the resting cells assay decreases the overall performance of the proteins involved in valencene to nootkatone conversion. Nevertheless, valencene resting cells assay showed that the coexpression of these two proteins had a beneficial effect when performing the assay in BMDY medium in comparison to the respective control strains.

III. Final discussion/Summary

When this Master's Thesis was started, already a lot of research had been done in this research area by Tamara Wriessnegger. She started HPO and CPR expression in *Pichia pastoris*, codon-optimized the genes, constructed several different expression plasmids and showed for the first time functional heterologous expression of both proteins. Furthermore, Tamara established several methods, assays and tools to monitor valencene conversion, measure protein performances and screen for best activity, which were adapted and used in this work.

Expression and verification of proteins in *Pichia pastoris*

The expression of various proteins, membrane bound (HPO, CPR) and soluble (ADHs, GDH, G6PDH), was driven from P_{AOX1} each time and, therefore, also integration of the coding sequences worked best and was always targeted for homologous recombination at the *AOX1* locus. The separation of growth phase and induction phase of *Pichia pastoris* fermentation using P_{AOX1} made fermentation and induction more reproducible and easier to control. *Pichia* transformants were not screened for Mut^S phenotype, which might show *AOX1* gene replacement and determine integration at *AOX1* locus. Transformants were always selected for histidine prototrophy or antibiotic resistance on adequate plates. As soon as a second gene was integrated, both selectable markers were tested in order to ensure integration of both genes. For most of the transformants, ectopic integration occurred which resulted in different expression levels of the proteins differing from strain to strain. This may also explain the difference of valencene conversion ability of strains *Pp*HPO/CPR-**T** and *Pp*HPO/CPR-**P**.

Protein expression was always verified with Western blot technique using different protein tags, the respective antibodies and chemoluminescent detection in an imager (G:BOX). Functionality of the expressed proteins was assessed using the valencene conversion reaction in resting cells assay and monitoring the nootkatone/*trans*-nootkatol production with GC-FID. The comparison of the expression levels of soluble proteins like ADH-C1 with the expression of HPO, which was possible because both proteins were FLAG-tagged (Figure 20), showed that the recombinant soluble proteins were expressed to much higher levels than membrane-attached enzymes in *Pichia pastoris*.

Expression of membrane-attached proteins HPO and CPR

For the first time a coexpression plasmid has been used in order to express both proteins at the same time and probably also in proximity to each other. Both proteins contain an N-terminal TMD and the

attachment of both proteins to the ER membrane is considered important for good substrate recognition and good interaction of both proteins. However, the limited space for membrane proteins in the membrane, the complex interaction between the subunits for good functionality and in general low expression levels of membrane-attached CYP450 enzymes make them difficult to express in high abundance. In order to be able to quantify the expression level of CYP450s the most general method is to record a CO-spectrum as the iron center forms a complex with CO absorbing at 450 nm. Although not mentioned in the results section of this work, CO-spectra of the different expression strains were recorded. It was found that the CYP450 enzymes were too little expressed to show a definite peak in the spectra. Expression of the proteins could be improved by generating multi-copy expression *Pichia pastoris* strains, which has been successfully done in house for other CYP450 enzymes. During this work no attempts have been made to create multi-copy strains as the tuning and manipulation of CYP450 mediated reactions and the conversion of hydrophobic substances was the predominant focus of research.

Valencene conversion

The conversion of valencene to nootkatone involves two proteins in our model reaction. The CYP450 HPO is not able to oxidize valencene to the final product nootkatone [18], but stops at the intermediate *trans*-nootkatol which is further oxidized by ADHs. Nevertheless, HPO showed a great regio- and stereospecificity towards valencene. Side product formation has not been observed in valencene resting cells assays chromatograms.

Valencene resting cells assay

One of the core experiments done various times during this thesis was the valencene resting cells assay, which enabled the direct comparison of engineered strains with their respective wild types to determine improvement or decrease of nootkatone production. Although improved for various aspects by Tamara in the past, the assay still comprises several drawbacks. The greatest disadvantage of the assay is the handling of the substrate valencene. Valencene is highly hydrophobic and completely immiscible with water. Therefore, special techniques had to be considered to keep the substrate loss during the reactions as low as possible. The method of choice when handling hydrophobic substrates in enzyme reactions is to use a two-phase system, organic solvent and water [36]. However, this technique has only reduced applicability with *Pichia pastoris* whole cell conversions, as substrate delivery to the cells is highly limited in two-phase systems and several solvents, especially water miscible ones, are toxic for the cells already in low concentrations [23]. In a tryout, a two-phase system using dodecane was applied

in some experiments but resulted in very low conversion rates as the substrate is completely soluble in dodecane and was apparently not delivered to the cell anymore because of the very unfavorable partition coefficient. As a compromise, the substrate valencene was dissolved in a DMSO/Triton® X-100 mixture. DMSO is an aprotic, water-miscible solvent able to dissolve polar and apolar substances. The detergent Triton® X-100 furthermore improved the dissolving behavior of valencene. In the assay, the final concentrations were only 2% DMSO and 0.02% Triton®-X-100 which was not considered toxic for the cells [23]. Using DMSO/Triton-X-100 in order to dissolve valencene for resting cells conversion resulted in less loss of the substrate. The loss of substrate was tested in buffer solution and buffer solution with resuspended *Pp*CBS7435 WT cells in order to evaluate whether substrate loss was only due to evaporation or also due to cell metabolism and/or side product formation. Figure 42 shows the loss of valencene during a 24 h assay. TV is the amount of valencene theoretically to the assay at 0 h.

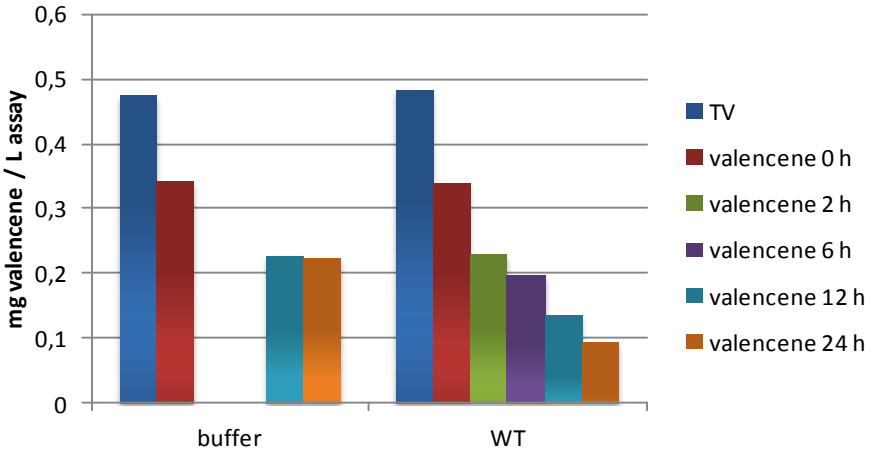

Figure 42: Loss of valencene during resting cells assay

Valencene loss in buffer and resting cells was similar at the beginning and comprised about 30% of total valencene used in the reaction, which therefore is lost for nootkatone production. In buffer, the loss stagnated at about 12 h and no further valencene loss was detected, whereas in WT the decrease continued to about 80% loss after 24 h of assay. This result might point to loss of valencene due to cell metabolism, but the chromatograms in Figure 43 which compare the samples drawn at 24 h for both systems showed no great differences in the peak pattern. Either valencene was metabolized by the cell to unknown products or the presence of the cells enhanced valencene evaporation or autoxidation.

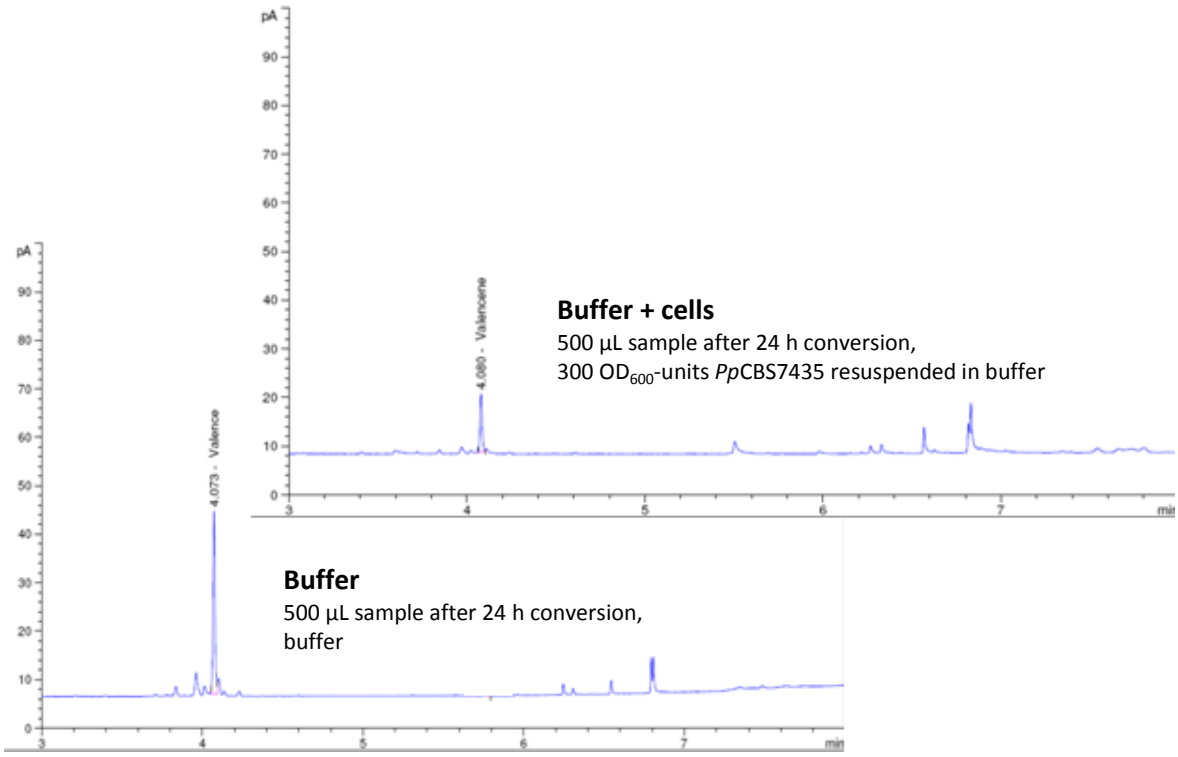

Figure 43: Chromatograms showing compounds retained in buffer vs. resting cells after 24 h

To conclude, at least 50% of the valencene added to the reaction is simply lost due to evaporation, which was one of the reasons to coexpress ADHs in **Project 1**. One expected outcome was that functional coexpression of different ADHs accelerated valencene conversion to nootkatone reducing valencene evaporation. Also, nootkatone is considerably less volatile due to its ketone functionalization and is more likely to stay dissolved in the assay.

ADH coexpression

The coexpression/overexpression of different ADHs successfully improved valencene conversion and overall nootkatone production in the resting cells assay. Intrinsic *Pichia pastoris* ADH-C3 showed the best results and is also likely to be mainly responsible for *trans*-nootkatol conversion in the tested WT strains. Different transformants of *Pp*HPO/CPR-**P**-ADH-C3 (WT-[pPpT4-HPO-CPR,pPpKan-ADH-C3] yielded in the highest amounts of nootkatone produced during the application of this assay, which was compared with published valencene conversion rates in order to classify the results.

Nootkatone production through the ages

The direct conversion of valencene to nootkatone by means of biocatalysis has been tried by several working groups in different approaches using different organisms, recombinant methods, variant CYP450 proteins in isolated enzyme techniques or even organic chemistry [2]. Table 28 summarizes the most recent and best results obtained and compares them to the best results we got for the strain *Pp*HPO/CPR-**P**-ADH-C3 (Figure 24). In order to compare, the yields were calculated in mol%, which is here defined by the per cent nootkatone (*trans*-nootkatol) made from initially added valencene. For data marked with an asterisk (*) the calculations were done by the authors of reference [2] and used for comparison, because the original source was not available. Furthermore the table shows, if available, the technique used, the time it took to prepare the reaction, conversion times and amounts of valencene added or nootkatone (*trans*-nootkatol) obtained. Only results generated using whole cells and for recombinant or isolated enzyme in biocatalytic conversion attempts are shown. Nootkatone formation by chemical synthesis or through in vivo valencene synthesis were not considered.

Table 28 features several different techniques to create nootkatone from valencene. A problem many groups faced with whole cell conversions, like in the listed cases **1-3**, is the formation of side products due to unspecific oxidizing enzymes in the organism or the metabolism of the cell. Therefore, in cases **7** and **11**, it has been tried to improve specificity of CYP450 enzymes by mutation. Using plant cells for conversion has brought good yields of nootkatone **(2)**, but their use is too complicated and time consuming for industrial applications. One approach used the heterologous expression of a valencene specific CYP450 from *Bacillus subtilis* in *E. coli* which yielded rather good results, especially for *trans*-nootkatol production **(10).** The problem in bacterial approaches is that overall complexity and instability of CYP450 enzymes, especially non-bacterial derived ones, and the need for cofactor regeneration makes bacterial approaches for most P450 enzymes too complicated and inefficient, which was proven by in house experiences gained from heterologous HPO expression in *E. coli* [37]. In **10** it has been announced to heterologously express an ADH in future work to further convert *trans*-nootkatol, i.e. as we did, but no data has been published yet. Also in other works, for instance with the mutein proteins in cases **7** and **11**, a high amount of *trans*-nootkatol is accumulated and the coexpression of an ADH would definitely improve conversion to nootkatone. Our approach of heterologous expression of HPO in *Pichia pastoris* together with *trans*-nootkatol specific ADH has obtained the best yield of nootkatone from valencene so far published. The techniques we use are reasonably efficient, easy and not very time consuming.

Table 28: Nootkatone production through the ages

#	*Organism* / Reaction mode	Reaction set up / time	Valencene used[a]	Nootkatone (*trans*-nootkatol) produced[a]	mol%	Reference, year
1	*Citrus paradisii* / whole plant cell conversion	Preparation of cultures: 9 months plant cell culture growth Conversion: 6 h	*nd*	1.1 mg/L (*nd*)	**19 (*nd*)**	[36], 1984
2	*Gynostemma pentaphyllum* / whole plant cell conversion	Preparation of culture: callus growth of the plant Conversion: 20 days	900 mg/L	597 mg/L (91.3 mg/L)	**62 (9)**	[38], 2005
3	*Chlorella fusca* var. *vacuolata* / whole algae cells conversion	Preparation of culture: 7 days algae culture growth Conversion: 18 days	400 mg/L	252 mg/L (0 mg/L)	**59 (0)**	[39], 2005
4	*Enterobacter* / whole bacterial cells conversion	*nd*	*nd*	*nd*	**11 (nd)**	[2], 1973*
5	*Rhodococcus* / whole bacterial cells conversion	*nd*	500 mg	2.5 mg (*nd*)	**0.5 (nd)**	[2], 1994*
6	*Pleurotus sapidus* / homogenized fresh mycelium, fedbatch	*nd*	10 000 mg/L	600 mg/L (*nd*)	**6 (*nd*)**	[2], 2008*
7	*Pseudomonas putida* mutein $CYP450_{cam}$ / isolated enzyme assay	*nd*	*nd*	*nd*	**9 (7)**	[40], 2005
8	*Chaetomium globosum* / whole fungi cells conversion	5 days preculture, 3 days inoculation,	460 mg/L	8 mg/L (1 mg/L)	**2 (<1)**	[41], 2005
9	*Pleurotus sapidus* / fungi lyophilisate	Preparation of culture, 9 days Conversion: 24 h	552 mg/L 2760 mg/L	225 mg/L (50 mg/L) 325 mg/L (90 mg/L)	**38 (8)** **11 (3)**	[42], 2009
10	*Bacillus subtilis* CYP109B1 / recombinant expression in *Escherichia coli* (two-phase system: isooctane/water)	Preparation of culture: 24 h Conversion: 8 h	408 mg/L	16 mg/L (318 mg/L)	**4 (72)**	[43], 2009
11	*Bacillus megaterium* mutein CYP102A1 / isolated enzyme assay	*nd*	*nd*	*nd*	**24 (12)** **12 (57)** **4 (74)**	[44], 2009
12	***Hyoscyamus muticus* HPO / recombinant expression in *Pichia pastoris* (coexpression of ADH-C3)**	**Preparation of cultures: 5 days** **Conversion: 24 h**	**473 mg/L**	**317 mg/L (0)**	**63 (0)**	**Myself, 2011**

nd: not determinable, not mentioned
[a]Amount calculated per L assay volume

NADPH regeneration

The practicability of an NADPH regeneration system was positively tested in vitro using cell homogenates and GDH assay. In order to test the system in vivo, i.e. in resting cells assay, the model reaction which is a two step conversion of valencene, was not suitable as the addition of glucose disturbed the conversion of *trans*-nootkatol to nootkatone.

Glucose addition

The intrinsic *Pichia pastoris* ADHs (C1 and C3) had initially not yet been annotated for *Pichia pastoris* strain *Pp*CBS7435 and therefore, the sequence and protein information for the genes were taken from the annotations made for *Pichia pastoris* strain GS115 in NCBI. The entries for the two ADHs suggest putative NAD(P) binding sites for both of the ADHs but also a broad substrate specificity. An $NADP^+$ dependency of the ADHs in order to be able to oxidize alcohols is unfavorable in testing the NADPH regeneration system in **Project 2**. In general terms, the addition of glucose to a resting cells assay already helps to regenerate NAD(P)H in the cells by providing the substrate for glycolysis and PPP [45]. If the oxidation of *trans*-nootkatol to nootkatone catalyzed by intrinsic *Pichia pastoris* ADHs is predominantly NADP+ dependent, which has not been determined experimentally yet, a greater NADPH pool provided by the addition of glucose to the resting cells medium would push the reaction equilibrium towards alcohol formation. The accumulation of *trans*-nootkatol after addition of glucose (Figure 40) kind of corroborated an NADP(H) dependency of the involved ADHs. The same behavior could be seen when testing an ADH-SY coexpressing strain, which is experimentally proven to be NADP+ dependent [27] and whose positive effects on valencene conversion were nearly totally lost when adding glucose to the resting cells assay.

Valencene uptake and microarrays

The experiments done in this thesis helped to better understand membrane attached enzyme expression in *Pichia pastoris* and the feasibility of high-level valencene conversion in this yeast. An unsolved problem nevertheless deals with substrate import/export of valencene and of hydrophobic substances in whole cell catalyzed *Pichia pastoris* conversion. It is supposed that after uptake to the cell, valencene is dissolved in the hydrophobic membrane areas of the cell making the use of membrane-attached CYP450 enzymes the system of choice. The enzymes are anchored in the membrane of the cell and, therefore, substrate delivery to membrane-attached enzyme is of course much easier than to soluble proteins in the cytosol. The mechanisms behind substrate uptake, substrate accumulation inside

the cell, product export and the system of transporter proteins involved has not been in the research focus yet. For other yeasts such as *Saccharomyces cerevisiae* the network of import into and export from the cell, i.e. the pleiotropic drug resistance network (PDR), has already been investigated intensively. In order to understand, and in the end improve substrate uptake in *Pichia pastoris*, the mechanisms behind have to be determined first.

The best way to explore the effects of obvious xenobiotics like valencene onto living cells is to check changes in the transcriptome of the cell by comparing two different conditions by microarrays. DNA microarrays can be used to monitor expression of all genes in an organism, simultaneously, at the RNA level and are the most common technology for transcriptome analysis [46]. For microorganisms like *Pichia pastoris,* this means that the whole genome information can be covered on one chip in order to globally determine changes in transcription levels when comparing two different samples under two different conditions. Today, major commercial sources like Affymetrix offer microarrays with high standards of quality and consistency to analyze changes in gene expression levels during protein expression or determine the influence of xenobiotics on gene transcription [47].

In combination with valencene addition and valencene conversion, the basic conditions for a microarray experiment dealing with the effects of valencene and nootkatone production as well as in situ valencene production in the cells have been established. The experiments will be done in November 2011 and are thought to bring deeper insights in *Pichia pastoris* multi drug resistance (MDR) network which would present starting points to enhance substrate uptake or product export.

Closing words/Prospect

After finishing the work in laboratory for this thesis, several loose ends still remained in some areas. As stated above, investigations on substrate uptake and the effect of very hydrophobic substances on the *Pichia pastoris* transcriptome will be carried out soon. The effects of NADPH regeneration together with a CYP450/CPR reaction, which does not comprise an unfavorable reaction step interfering with the readout, will be carried out as soon as Tamara Wriessnegger has established another CYP450 model reaction in our laboratory. As ADH coexpression demonstrably led to a better nootkatone production, their coexpression will further be involved in other valencene converting strains tested by Tamara and Anita Emmerstorfer in our lab.

IV. Materials and Methods

Chemicals, kits, media and buffers

Table 29: Chemicals and suppliers

Name	Supplier
Acetic acid	Roth GmbH, Germany
Agar Agar	Roth GmbH, Germany
Agarose LE	Biozyme, Germany
Ampicillin (Amp)	Sigma-Aldrich, Germany
Aqua bidest. (ddH_2O)	Fresenius Kabi GmbH, Austria
Bacto™ Agar	BD, USA
Bicine	Roth GmbH, Germany
Biotin	Roth GmbH, Germany
Bovine Serum Albumine (BSA)	Roth GmbH, Germany
***cis-, trans*-nootkatol**	DSM Pharma Chemicals, The Netherlands
D-glucose	Roth GmbH, Germany
Dimethyl sulfoxide (DMSO)	Roth GmbH, Germany
Dithiothreitol (DTT)	Roth GmbH, Germany
Ethidium bromide (EtBr)	Roth GmbH, Germany
Ethyl acetate (EtAc)	Roth GmbH, Germany
Ethylene glycol	Roth GmbH, Germany
Ethylenediamine tetraacetic acid (EDTA)	Roth GmbH, Germany
Geneticin (G418)	Roth GmbH, Germany
Glycerol	Roth GmbH, Germany
Glycin	Roth GmbH, Germany
Hydrochloric acid (HCl)	Roth GmbH, Germany
LB (Luria-Bertani) Lennox-medium	Roth GmbH, Germany
Loading Dye (6x)	Fermentas GmbH, Germany
Methanol (MeOH)	Roth GmbH, Germany
MOPS SDS Running buffer	Invitrogen, USA
Nootkatone	DSM Pharma Chemicals, The Netherlands
PageRuler™ Prestained Protein Ladder	Fermentas GmbH, Germany
Phenylmethylsulfonyl fluoride (PMSF)	Sigma-Aldrich, Germany
Ponceau S	Sigma-Aldrich, USA
Potassium chloride (KCl)	Roth GmbH, Germany

Potassium dihydrogen phosphate (KH_2PO_4)	Roth GmbH, Germany
Potassium hydrogen phosphate (K_2HPO_4)	Roth GmbH, Germany
Sodium chloride (NaCl)	Roth GmbH, Germany
Sodium hydroxide (NaOH)	Roth GmbH, Germany
Sorbitol	Roth GmbH, Germany
SuperSignal West Pico Chemoluminescent substrate for HRP	Pierce, USA
Trichloroacetic acid	Roth GmbH, Germany
Tris	Roth GmbH, Germany
Triton X-100	Sigma-Aldrich, Germany
Tryptone	Roth GmbH, Germany Bacto Laboratories Pty Ltd, Australia
Tween 20	Roth GmbH, Germany
Valencene	DSM Pharma Chemicals, The Netherlands
Whey powder	From local diary
Yeast extract	Roth GmbH, Germany Bacto Laboratories Pty Ltd, Australia
Yeast nitrogen base (YNB)	Difco®, BD
Zeocin™	Invitrogen, USA

Table 30: Buffers and solutions

Name	Composition
Ampicillin stock (1000x, 100 mg/ml)	1 g Ampicillin in 10 mL ddH_2O, filter sterilized and aliquoted to 1 mL
Biotin (500x)	10 mg biotin in 50 mL dH_2O and filter sterilized
Breaking buffer	50 mM sodium phosphate, pH 7.4, 1 mM PMSF in DMSO, 1 mM EDTA, 5% (v/v) glycerol
DTT (1 M)	1.54 g DTT in 10 mL dH_2O, filter sterilized
Geneticin, G418 stock (1000x, 100 mg/ml)	1 g G418 in 10 mL ddH_2O, filter sterilized and aliquoted to 1 mL
Glucose (10x)	200 g glucose in 1 L dH_2O and autoclaved
Glycerol (10x)	100 mL glycerol to 1 L with dH_2O
K_2HPO_4 (1 M)	136.09 g K_2HPO_4 in 1 L dH_2O, autoclaved
KH_2PO_4 (1 M)	174.18 g KH_2PO_4 in 1 L dH_2O, autoclaved
MOPS-running buffer (1x)	100 mL NuPage®-MOPS (10x) to 1 L with dH_2O
Ponceau S solution	0.1% (w/v) Poncau S in 5% (v/v) acetic acid solution
Potassium phosphate buffer (KP_i, 1M)	132 mL of 1 M K_2HPO_4 and 868 mL of 1 M KH_2PO_4, autoclaved, pH 6
TAE-buffer (1x)	40 mM Tris, 20 mM acetic acid, and 1 mM EDTA
TBS (10x)	30.3 g Tris, 87.6 g NaCl in 1 L dH_2O, pH adjusted with 1 M HCl to pH 7.5
TBST (1x)	100 mL TBS (10x) + 300 µl Tween-20, to 1 L with dH_2O

TBST-milk	5 g whey powder in 100 mL TBST (1x)
TCA (50%, w/v)	50 g TCA in 100 mL dH_2O
TE-buffer	10 mM Tris/HCl, 1 mM EDTA, pH 7.5
Transfer buffer (1x)	75 mL transfer buffer (20x), 150 mL MeOH and to 1.5 L with dH_2O
Transfer buffer (20x)	14.5 g Tris and 72 g glycin in 500 mL dH_2O
Tris-HCl buffer	Used in different molarities, pH adjusted with 1 M HCl
YNB (Yeast Nitrogen Base, 10x)	134 g YNB in 1 L dH_2O and filter sterilized
Zeocin stock (1000x, 100 mg/ml)	1 g Zeocin™ in 10 mL ddH_2O, filter sterilized and aliquoted to 1 mL

Table 31: Media and plates

Name	Composition
BEDS medium	10 mM bicine-NaOH, pH 8.3, 3% (v/v) ethylene glycol, 5% (v/v) DMSO, 1 M sorbitol
BMDY, 1 L	10 g yeast extract, 20 g peptone in 700 mL ddH_2O, autoclaved + 100 mL 1 M KP_i-buffer pH 6, 100 mL YNB (10x), 2 mL biotin (500x), 100 mL glucose (10x)
BMGY, 1 L	10 g yeast extract, 20 g peptone in 700 mL ddH_2O, autoclaved + 100 mL 1 M KP_i-buffer pH 6, 100 mL YNB (10x), 2 mL biotin (500x), 100 mL glycerol (10x)
BMMY10, 100 mL	1 g yeast extract, 2 g peptone in 70 mL ddH_2O, autoclaved + 10 mL 1 M KP_i-buffer pH 6, 10 mL YNB (10x), 0.2 mL biotin (500x), 10 mL glycerol (10x) + 5 mL MeOH
BMMY2, 1 L	10 g yeast extract, 20 g peptone in 700 mL ddH_2O, autoclaved + 100 mL 1 M KP_i-buffer pH 6, 100 mL YNB (10x), 2 mL biotin (500x), 100 mL glycerol (10x) + 10 mL MeOH
LB-medium, 1 L	10 g tryptone, 5 g yeast extract and 5 g NaCl in 1 L ddH_2O, autoclaved
LB-plates	LB medium + 20 g/L agar agar, autoclaved
MD-medium, 1 L	800 mL ddH_2O, autoclaved + 100 mL YNB (10x), 2 mL biotin (500x), 100 mL glucose (10x) to 1 L
MD-plates, 1 L	800 mL ddH_2O + 15 g agar agar, autoclaved + 100 mL YNB (10x), 2 mL biotin (500x), 100 mL glucose (10x) to 1L
SOC medium	20 g/L tryptone, 0.58 g/L NaCl, 5 g/L yeast extract, 2 g/L MgCl2, 0.16 g/L KCl, 2.46 g/L MgSO4, 3.46 g/L glucose
YPD-medium, 1 L	10 g/L yeast extract, 20 g/L peptone, 20 g/L glucose; glucose solution autoclaved separately
YPD-plates	YPD medium + 20 g/L agar agar, autoclaved
Addition of antibiotics: Antibiotics for media and plates that were added under sterile conditions in the laminar flow after cooling the medium to approximately 50°C. **Concentration of antibiotics in plates and media:** In the Results section the addition of antibiotics to media or plates is indicated by the number superscript behind the antibiotic in mg/L.	

Table 32: Employed kits

Name	Supplier
Gene Jet™ Plasmid Miniprep Kit	Fermentas GmbH, Germany
Maxima® Hot Start Green PCR Master Mix	Fermentas GmbH, Germany
SuperSignal West Pico Chemiluminescent Kit	Pierce, USA
Wizard® SV Gel and PCR Clean Up System	Promega Corporation, USA

Instruments and devices

Table 33: Instruments and devices

Task	Instrument/Device and supplier
Absorption measurement, OD_{600}	Spectramax Plus 384/Molecular Devices, Germany
Agarose gel electrophoresis	PowerPac™ Basic + Sub-Cell GT, Bio-Rad, USA
Centrifuge	Avanti™ Centrifuge J-20XP + JA-10 rotor, Beckman Coulter™, USA
Culture incubation	HT MultitronII, Infors AG, Switzerland HT, Infors AG
DNA-concentration	NanoDrop 2000c Spectrometer, PEQLAB Biotechnologie, Germany
Electro-transformation	MicroPulser™, Bio-Rad, USA Electroporation Cuvettes (2mm gap), Molecular BioProducts Inc
GC-FID	Hewlett Packard 6890 Series with a FID detector Agilent 19091J-141 (Capillary 10.0 m x 0.1 mm x 0.1 µm film), Agilent technologies, USA
Homogenization	MSK homogenizer, Braun, Germany
Imaging	Syngene G:Box, Great Britian
Incubator	Binder, Germany
Incubator (37°C, 30°C)	Binder, Germany
Laminar flow	UNIFLOW KR130 biowizard, UNIEQUIP, USA
Micro centrifuge	Centrifuge 5415R Eppendorf, Germany
OD_{600} measurement	BioPhotometer, Eppendorf, Germany Cuvettes (10x4x45mm), Sarstedt, Germany
PCR reactions	GeneAmp® PCR System 2700, Applied Biosystems, USA
Pipetting	Peqpette 20 µL, 200 µL, 1000 µL, Peqlab, Germany
SDS-PAGE + Western blot	NuPAGE® Novex 4-12% Bis-Tris Gels 1.0 mm, 17 well, Xcell SureLock Mini-Cell and PowerEaseR 500 Power Supply, all Invitrogen, USA Nitrocellulose membrane, Hybond-ECL™, Amersham Biosciences, USA
Tabletop centrifuge	Centrifuge 5810, Eppendorf, Germany
Thermomixer	Thermomixer comfort, Eppendorf, Germany
Valencene resting cells assay	Pyrex® tubes (10 mL), Sigma-Aldrich, USA
Vibrax	VXR basic, IKA®, Germany
Vortex	Vortex-Genie, Scientific Industries Inc, USA
Weighing	Lab scale: TE 1502S, sartorius, Germany Precision scale: Explorer, OHaus, Germany

Organisms, strains

Table 34: Strains and organisms

Organism	Strain	Genotype	Reference, source
Pichia pastoris	*Pp*CBS7435, WT	*Δku70Δhis4*	IMBT culture collection, #3518
Pichia pastoris	*TW 6+3t*	*Pp*CBS7435-[pPpHIS4-CPR]-[pPpT4-HPO]	Tamara Wriessnegger
Pichia pastoris	*TW 3F*	*Pp*CBS7435-[pPpT4-HPO]	Tamara Wriessnegger
Bacillus subtilis	Strain 168, CCM 2267	trpC2	IMBT culture collection, #310
Sphingobium yanoikuyae	B1, Gibson D.T. DSM 6900	-	IMBT culture collection, #5153
Escherichia coli	TOP10F'	F'{*lac*I^{q} Tn*10* (Tet^{R})} *mcr*A Δ(*mrr-hsd*RMS-*mcr*BC) Φ80 *lac*ZΔM 15 Δ*lac*X74 *rec*A1 *ara*D139 Δ(*ara-leu*)7697 *gal*U galK *rps*L *end*A1 *nup*G	Invitrogen, USA

Expression plasmids

All expression plasmids were taken from [10], vector maps and special properties are displayed in the Appendix.

Plasmid	Features
pPpT4	*Pichia pastoris* expression plasmid, Zeo^{R}, p*AOX1*
pPpKan	*Pichia pastoris* expression plasmid, Kan^{R}, G418^{R}, p*AOX1*
pPpHIS4	*Pichia pastoris* expression plasmid, *HIS4*, p*AOX1*
pPpB1	*Pichia pastoris* expression plasmid, Zeo^{R}, p*AOX1*

Enzymes and proteins

Table 35: Enzymes and other proteins

Protein	Supplier
FastAP™ alkaline phosphatase	Fermentas GmbH, Germany
FastDigest™ restriction enzymes	Fermentas GmbH, Germany
Goat anti-mouse IgG – HRP	Invitrogen, USA
Goat anti-rabbit IgG - HRP	Invitrogen, USA
Maxima® Hot Start Taq DNA Polymerase	Fermentas GmbH, Germany
Mouse anti-FLAG M2 monoclonal antibody	Sigma-Aldrich, USA
Phusion® DNA Polymerase	Finnzymes, Finnland
Rabbit anti-6xHIS polyclonal antibody	Rockland, USA
Rabbit anti-myc antibody	Sigma-Aldrich, USA
Restriction enzymes	Fermentas GmbH, Germany
T4 DNA Ligase	Fermentas GmbH, Germany

Table 36: Proteins coexpressed in *Pichia pastoris* CBS7435

Gene	description	Tag	
HPO	*Hyoscyamus muticus* premnaspirodiene oxygenase	FLAG-tag	Codon-optimized for *Pichia pastoris* by Tamara Wriessnegger
CPR	*Arabidopsis thaliana* cytochrome P450 reductase	myc-tag	Codon-optimized for *Pichia pastoris* by DSM
ADH-C1	*Pichia pastoris* alcohol dehydrogenase, chromosome 1	FLAG-tag	
ADH-C3	*Pichia pastoris* alcohol dehydrogenase, chromosome 3	FLAG-tag	
ADH-SY	*Sphingobium yanoikuyae*, alcohol dehydrogenase	FLAG-tag	
***Bs*GDH**	*Bacillus subtilis* glucose-1-dehydrogenase	6xHIS-tag	
***Pp*G6PDH**	*Pichia pastoris* glucose-6-phosphate dehydrogenase	6xHIS-tag	

Primers

Introduced restriction sites are displayed in **bold,** *Eco*RI (G^AATTC), *Not*I (GCGGCC^GC) and *Spe*I (A^CTAGT).

Table 37: Primers for gene amplification and gene tagging

Primer name	Sequence	Tm [°C]
FwADH-C1	5'-CCG**GAATTC**CGAAACGATGGCTTACCCAGACACTTTTG-3'	64
FwADH-C3	5'-CCG**GAATTC**CGAAACGATGACCACAGTTTTCGCTTAC-3'	61
RvADH-C1	5'-ATAGTTTA**GCGGCCG**CTTATTACTTATCGTCGTCATCCTTGTAATCTTCAAACTGTTTTCCGTAATTAGTAAG-3'	62
RvADH-C3	5'-ATAGTTTA**GCGGCCG**CTTATTACTTATCGTCGTCATCCTTGTAATCCCCCCTGACTTTACTTAGACTC-3'	60
Sy_ADH_fw	5'-CCG**GAATTC**CGAAACGATGACCACGCTTCCGACTGTTCTCATC-3'	74
SyADHflag_rev	5'-ATAGTTTA**GCGGCCG**CTTATTACTTATCGTCGTCATCCTTGTAATCGGCTTCCGGCCGATAGCG-3'	72
BsGDH_fw	5'-CCG**GAATTC**CGAAACGATGTATCCGGATTTAAAAGGAAAAGTCG-3'	68
BsGDHhis_rev	5'-ATAGTTTA**GCGGCCG**CTTATTAGTGGTGATGGTGATGATGACCGCGGCCTGCCTG3'	71
PpG6PDH_Spe_fw	5'-CCG**ACTAGT**CGAAACGATGACCGATACGAAAGCCG3'	65
PpG6PDHhis_rev	5'-ATAGTTTA**GCGGCCG**CTTATTAGTGGTGATGGTGATGATGCATCTTGTGCAGCACATCGG-3'	68

Table 38: Primers for strain verification and sequencing

Primer name	Sequence	Tm [°C]
FwPpHPO_TW2	5'-GGTCTGGCTGGTGGTTTTGA-3'	54
FwPpCPR_DSM3	5'-CTGCTGTCCCACCTCCTTTC-3'	53
Rv_Pp_HIS4	5'-GATCAGGAGCAAGCTCGTAC-3'	49
Sequencing		
pAOX1_fw	5'-GACTGGTTCCAATTGACAAGC-3'	64
TTpAOX1_rev	5'-GCAAATGGCATTCTGACATCC-3'	67

Kits and protocols

General methods

This section describes methods used in daily laboratory work. If any alterations have been applied to the below described standard method, they are mentioned separately in the Results section.

Gel electrophoresis

Gel electrophoresis was done using 1% agarose gels containing ethidium bromide (EtBr) in TAE-buffer. Analytical gels were run at 120-130 V for approximately 45 min, preparative gels at 90 V for approximately 80 min. The sizes and concentrations of DNA fragments were assessed by comparison to DNA standards.

***Plasmid isolation from* Escherichia coli**

For plasmid isolation from *E. coli* Fermentas GeneJET™ Plasmid Miniprep Kit was used. *E. coli* cell material from a quarter of an agar plate was collected for isolation with a toothpick. Final elution of the plasmid was done with 50 µL of ddH_2O.

DNA purification

For DNA purification after PCR, restriction cut or preparative agarose gel Promega Wizard® SV Gel and PCR Clean-Up System was used. Final elution of the purified DNA was done with 30 µL of ddH_2O.

Determination of DNA concentrations

DNA concentrations for sequencing, ligation set ups and preparative restriction cuts were determined with agarose gels or photometrically with NanoDrop. In order to estimate an approximate concentration of the DNA preparations with agarose gels, 1 µL of the eluted DNA preparation, 9 µL ddH_2O and 2 µL of Loading Dye (6x) were mixed and loaded onto an 1% agarose gels. The concentration was estimated according to the concentrations given by DNA Ladder standards. For photometrical determination with NanoDrop, 1 µL of the DNA preparation was used.

Polymerase Chain Reaction

Amplification of different genes from an organism

PCRs for insert generation were done with Phusion® DNA polymerase according to the recommended protocol of Finnzymes Phusion® High-Fidelity DNA Polymerase protocol. Primers, amounts of different reagents used and cycling conditions are stated at the experiment itself in the Results section. The template for PCR reactions was prepared by harvesting a small amount of a colony of the organism of origin with a pipette tip and resuspending the cell material in 25 µL ddH_2O. The resuspended cells were lysed at 95°C for 5 min in a thermomixer and afterwards chilled on ice for 5 min. The cell debris was separated by spinning in a table top centrifuge for 30 s at maximum speed. In general, 3 µL of the resulting supernatant (colony SN) was used for PCR reactions. A template-free negative control was performed with every PCR. After PCR, the whole volume, in general 50 µL, was loaded onto a preparative 1% agarose gel and the bands representing the amplified gene was cut out and cleaned up for further processing.

Colony PCR

Colony PCR was performed to determine integration of different genes into the genome of *Pichia pastoris* after transformation. Colony PCR was done using Maxima® Hot Start Green PCR Master Mix (2X) kit according to the recommended protocol. The template was prepared in the same manner as described above. After PCR, 5 µL of the PCR-mix was loaded onto an analytical 1% agarose gel.

DNA restriction

Control restriction cuts of plasmid DNA were done with Fermentas® restriction or Fermentas® FastDigest™ (FD) restriction enzymes. 1 µL of the DNA preparation was mixed with 1.5 µL of the adequate restriction buffer and the restriction enzymes. The preparation was filled up to 15 µL with ddH_2O. FastDigest™ reaction took place for 30 min at 37°C, while normal restriction cuts for 3-12 h at 37°C. After restriction the whole set up was put onto 1% agarose gels.

Preparative restriction cuts of plasmid DNA, PCR products, purified DNA preparations or linearizations of plasmid DNA for transformation were performed, if possible, using Fermentas® restriction enzymes. Before restriction, the DNA concentration was determined using NanoDrop or via gel electrophoresis. The amount of restriction enzymes used was adapted according to reaction volume, DNA concentration and reaction set up and varied between 1-3 µL. The reaction took place o/n at 37°C.

Generation of recombinant vectors

Preparations

Vector backbones were preparatively cut with adequate restriction enzymes, dephosphorylated and purified by gel electrophoresis and Promega Wizard® SV Gel and PCR Clean-Up System. Inserts were generated by PCR, restricted and cleaned up similarly. The concentrations of the fragments needed for ligation set up was determined by agarose gels or photometrically.

Dephosphorylation

Dephosphorylation of the vector backbone was done using Fermentas® FastAP alkaline phosphatase. 1 µL of the respective enzyme was pipetted directly into the preparative restriction set up and the reaction took place o/n at 37°C in the respective restriction enzyme buffer.

Ligation

The set up for the ligation was calculated with a ligation calculator [48] to 40 ng of the vector backbone used and a 3:1 insert to vector ratio was applied. The ligation was done for 1 h at RT mixing the required amounts of backbone vector and insert according to the calculation and adding 2 µL of 10x T4-ligation buffer. If necessary the reaction was filled up to 20 µL with ddH_2O. 1 µL of T4-ligase (10 U/µL) was added last. An insert-free negative control was done for every vector backbone to determine if the vector religated during ligation. After ligation, the ligase was deactivated for 10 min at 65°C and desalted for 30 min using 0.025 µm Millipore filter floating on ddH_2O before electrotransformation. Solutions were transferred to sterile Eppendorf tubes, immediately used for electrotransformation or stored at -22°C.

Electroporation of *E. coli* cells

The transformation of plasmids into electrocompetent *E. coli* TOP10F' cells followed a standard procedure. 50 µL of the electrocompetent cells were thawed on ice. After adding 1 µL of a plasmid preparation or 1-3 µL of a ligation reaction and transferring the mixture to chilled transformation cuvettes, the transformation mixtures were incubated on ice for 10 min before pulsing them in the electroporator. Immediately after the electro-pulse, 1 mL of SOC medium was added and the cells were regenerated at 37°C and 650 rpm for 1 h before plating 100 µL and the transformation-rest (TRAFO-rest) on selective media. TRAFO-rest was prepared by short centrifugation of the transformation mixture in a table top centrifuge, decanting the SN and resuspending the pellet in approximately 100 µL of medium left.

Plasmid isolation and control cuts

After successful transformation, which was determined by comparing the colony numbers of the plates with the corresponding negative controls, several transformants were streaked onto quarters of adequate plates and grown o/n at 37°C. The next day, a quarter of *E. coli* culture was abraded and the plasmids were isolated. In order to ensure that ligation was successful and the right plasmid was generated, restriction control cuts were made. After confirming correct cloning, the plasmids were stored at -20°C until further use.

Sequencing

If verification of cloned plasmids with restriction was not possible due to uncertain results of the control cuts or the lack of appropriate restriction enzymes, plasmids were sequenced by LGC genomics (https://shop.lgcgenomics.com/) using adequate sequencing primers and following the guidelines of the company.

Electrocompetent *E. coli* cells

30 mL of LB media were inoculated with the chosen *E. coli* strain and incubated over night at 37°C and 220 rpm (Infors Multitron II). The following day, the main culture of 400 mL of LB media was inoculated with 5 mL of the overnight culture and incubated at 37°C and 120 rpm until an OD between 0.7 and 0.9 was reached. After transferring the culture to chilled 500 mL centrifuge bottles, it was cooled on ice for 30 min before harvesting the cells at 2 000 x g and 4°C for 15 min (Beckman Coulter centrifuge, JA-10). The SN was discarded and the pellet was carefully resuspended in pre-chilled 500 mL ddH_2O. The suspension was centrifuged as before and the SN was discarded. Then, the cell pellet was resuspended in 35 mL of pre-chilled, sterile 10% glycerol and centrifuged at 4 000 x g and 4°C for 15 min. After discarding the supernatant, the pellet was resuspended in 1 mL ice-cold, sterile 10% glycerol before aliquoting the electrocompetent cells to 40 or 80 µL into sterile Eppendorf tubes. The cells were frozen in liquid N_2 and stored at -80°C until needed.

Pichia pastoris cultivation

Pichia pastoris colonies were cultivated in deep well plates (DWP), 250 or 300 mL and 1 L baffled shake flasks according to the requirements of the experiments the cells were used afterwards.

Micro-scale cultivation in DWPs

To screen for enzyme activity, to prepare strains for Western blot experiments or to generate glycerol stocks, *Pichia pastoris* transformants were grown in 96 DWPs. At least 3 wells were filled with media to

serve as a sterile control. Single *Pichia* colonies were inoculated into 250 µL BMGY medium and grown at 28°C, 320 rpm and 80% humidity (Infors Multitron II) for approximately 60 h to reach the stationary growth phase and depletion of glycerol. Then, 250 µL of BMMY2 (1% MeOH) were added resulting in a final concentration of 0.5% MeOH. At 12, 24 and 36 h after the start of induction, 50 µL of BMMY10 (5% MeOH) were added to compensate MeOH loss due to evaporation and consumption. The cultivation was stopped 12 h after the last MeOH addition, resulting in an overall induction period of 48 h.

Shake-flask cultivation

250 mL or 300 mL baffled shake-flasks were filled with 25 mL BMGY and inoculated with single colonies of *Pichia pastoris* strains. The cells were grown at 28°C and 110 rpm (Infors Multitron II) for approximately 60 h to reach the stationary growth phase and depletion of glycerol. Then, 25 mL of BMMY2 (1% MeOH) were added, resulting in a final concentration of 0.5% methanol. At 12, 24 and 36 h after the start of induction, 5 mL of BMMY10 (5% MeOH) were added to adjust MeOH loss due to evaporation and consumption. The cultivation was stopped 12 h after the last addition of MeOH, resulting in an overall induction period of 48 h.

When cells were grown in 1 L baffled shake flasks, 100 mL of BMGY were inoculated and induction was started with 100 mL of BMMY2. Additional induction steps were done with 20 mL of BMMY10 medium. The overall induction period was again 48 h.

Pichia pastoris - transformation

Generation of electrocompetent *P. pastoris* and transformation were based on the "Condensed protocol for competent cell preparation and transformation of *Pichia pastoris*" [49]. A single *Pichia pastoris* colony was inoculated in 5 mL YPD medium and grown o/n. 50 mL of YPD medium were inoculated to an OD_{600} of 0.01 with the ONC and grown o/n. Cells were harvested when reaching an OD_{600} of approximately 0.8, centrifuged in a micro centrifuge and the pellet was resuspended in 10 mL of freshly prepared BEDS/DTT medium, centrifuged again and resuspended in 0.5 mL BEDS medium. The cells were used immediately for transformation. Storing the cells at -20°C or -80°C significantly decreased their electrocompetence. For every transformation, the cells were freshly prepared.

For transformation, at least 800 ng of a linearized plasmid DNA was mixed with 80 µL of competent cells. Electroporation was carried out at 1500 V, 200 Ω and 25 µF. Immediately after the electro pulse, 0.5 mL YPD and 0.5 mL of 1 M sorbitol were added and the cells were regenerated for at least 1 h at 28°C and

moderate shaking. 100 µL, for MD^{-his} plates 50 µL, of the cell suspension and the TRAFO-rest were plated on selective media and incubated for 2-3 days at 30°C.

Protein analysis

SDS-PAGE

Sample preparation

Strains tested for protein expression by Western blot were grown and induced in DWPs.

Cell harvest and glass bead disruption

Cells of strains that were analyzed in more details were disrupted with glass beads. Therefore, the according cell culture from the DWP was transferred into an Eppendorf tube and centrifuged at 13 200 rpm and 4°C for 10 min. The SN was discarded and the cells were resuspended in 200 µL of ice-cold breaking buffer. Glass beads equivalent to the volume of 200 µL were added and the cells were disrupted in 8 alternating 30 s cooling/vortexing cycles. The mixture was centrifuged again at 5 000 rpm and 4°C for 5 min and the SN, i.e. cell free protein extract, was transferred into Eppendorf tubes or microtiter plates. The extracts were used immediately or stored at 4°C. To determine the concentrations of the cell lysates a Bio-Rad protein assay was done.

Determination of protein concentrations – Bio-Rad protein assay

Protein concentrations were determined according to the Bio-Rad protocol, which is based on the method of Bradford, for 96 well plates. To 10 µL of a sufficiently diluted protein sample, 200 µL of the 1:5 diluted Bio-Rad reagent were added. The plate was moderately shaken for 10 min at RT before measuring the absorption at 595 nm in a plate reader (Spectramax Plus 384). At least a triplicate measurement was performed. Bovine serum albumin (BSA) was used to generate a calibration curve in concentrations between 0 and 2 mg BSA/mL water.

TCA precipitation

In order to concentrate and purify the protein extracts, approximately 50 µg of proteins were precipitated with TCA. The amount equivalent to 50 µg of protein of the protein extract was added to 400 µL of ice-cold water. 100 µL of ice-cold TCA (50%, w/v) were added and the proteins were precipitated for at least 1 h on ice. The proteins were pelleted by centrifugation for 10 min at 4°C and 13 200 rpm in a table top centrifuge and washed with ddH_2O.

SDS-PAGE

SDS-PAGE was performed according to the manual of NuPage[R], Invitrogen. To 50 µg of pelleted and washed proteins, 5 µL of LDS sample buffer (4x), 2 µL of 1 M DTT and 13 µL of ddH_2O were added to a final volume of 20 µL. In order to finish sample preparation, the mixture was denatured at 70°C for 10 min. SDS-PAGE samples were used immediately or stored at -20°C. As standard, 5 µL of a protein ladder (Fermentas® PageRuler™ prestained protein ladder) were used. Approximately 20 µg of the protein sample was loaded onto the gel per lane. The gel was run at 110 mA/gel for 50 min.

Western blot

After SDS-PAGE, Western blot was performed according to the manual of NuPage[R], Invitrogen. Blotting pads, filter paper and nitrocellulose membrane were soaked in 700 mL 1x transfer buffer to remove air bubbles. The blotting sandwich was built as described in Figure 44 using soaked pads, gel(s) and filters. Air bubble formation was thoroughly avoided.

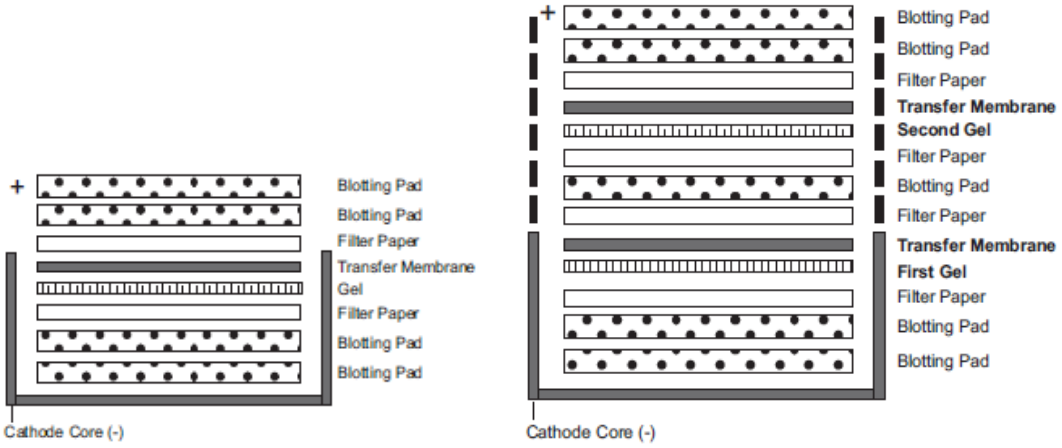

Figure 44: Left scheme: Blotting sandwich used for blotting one gel; Right scheme: Blotting sandwich used for blotting two gels (Manual NuPAGE®, Invitrogen)

The blotting sandwich was fixed with a Gel Tension Wedge in the XCell II unit and blotting was carried out according to the manual, exposing the sandwich to 250 mA, maximum voltage and maximum power for 1 h.

After blotting, membranes were stained with Ponceau S to detect transfer efficiency of proteins. After washing away excessive Ponceau S with ddH_2O, the membranes were blocked with 50 mL of TBST-milk at RT for 1 h o/n. Afterwards, TBST-milk was discarded and the membrane was incubated with the primary antibody by moderately shaking at RT. This step was followed by washing three times with TBST for 5 min each. Then, the membranes were treated with the secondary antibody at RT and moderately

shaking which was followed by three washing steps with TBST for 5 min each. Detection was carried out by covering the membranes with 4 mL of SuperSignal West Pico Chemoluminescent Substrate mixture. Chemoluminescence detection was done in a G:Box (Syngene) after 2-3 min incubation. Use of different antibodies, their dilution rates and incubation times are stated in the Results section.

Valencene resting cells assay

Preparations and starting the assay

Pichia pastoris strains were grown in 250 mL or 300 mL baffled shake flasks. After growth and induction with MeOH, the OD_{600} of every flask was measured and the amount of culture corresponding to 300 OD_{600}-units was calculated. If samples were needed for Western blot analysis, 1 mL of the culture was taken and pelleted by centrifuging for 2 min in a table top centrifuge at 13 200 rpm. The SN was discarded and SDS-PAGE samples were prepared according to the above protocol. The cells corresponding to 300 OD_{600}-units were put into sterile PYREX®-tubes. These were centrifuged for 3 min at 2 500 rpm and RT in the micro centrifuge and the SN was discarded completely. The pellet was resuspended in 1 mL of 50 mM KP_i-buffer pH 7.4. The assay was started by pipetting 30 µL of the prepared substrate solution into the PYREX®-tube. 100 µL of aliquots were withdrawn immediately after the start and were put into PYREX® tubes containing 2 mL EtAc for extraction (0 h sample). Aliquots were either immediately worked up (see below) or stored at -20°C. For the assay, the PYREX® tubes were incubated at 28°C and 215 rpm (Infors HT) and further aliquots were drawn at different time points specified for each assay.

Work up

PYREX® tubes containing the EtAc-cell suspension (frozen or fresh) were vibraxed, i.e. heavily agitated, for 30 min at 1 500 rpm (IKA Vibrax, VRX) and centrifuged for 5 min at 2 000 rpm and 4°C in a micro centrifuge. After centrifugation, some of the SN, i.e. EtAc phase, without cell pellet, was cautiously put into a GC-vial with inset and cramped. GC-vials were taken to GC-FID measurement immediately or stored at 4°C or -20°C.

The protocol listed above explains the standard procedure for valencene resting cells assay. This assay was modified for different measurements regarding amount of cells, use of substrate, addition of cosubstrates, volumes and extraction conditions. Whenever a modification was applied this is mentioned directly at the assay in the results section.

Preparation of substrate stock solutions

Valencene – substrate, 10 mL of 100 mM valencene

0.2919 g valencene reagent (Isobionics, 70% purity) were weighed on a precision scale into a 10 mL volumetric flask. Afterwards, valencene was dissolved in DMSO containing 1% Triton X-100 (v/v) and vigorously shaken. If not used immediately, parafilm was wrapped around and the substrate solution was stored at 4°C.

Nootkatol-substrate, 5 mL of 100 mM *cis/trans* nootkatol mixture

0.1132 g *cis*-nootkatol (Isobionics, 97% purity) and 0.1276 g *trans*-nootkatol (Isobionics, 86% purity) were weighed on a precision scale into a 5 mL volumetric flask. Nootkatol was dissolved in DMSO containing 1% Triton X-100 (v/v) and vigorously shaken. If not used immediately, parafilm was wrapped around and the substrate solution stored at 4°C.

GC-FID

GC measurements were performed in cooperation with Professor Erich Leitner and the Institute of Analytical Chemistry and Food Chemistry, Graz University of Technology. The methods were established for the efficient separation and analysis of the terpenes of interest by Erich Leitner.

GC-FID measurements were carried out using a HP-5 column (crosslinked 5% Ph-Me Siloxane; 10 m, 0.10 mm in diameter and 0.10 µm film thickness) on a Hewlett-Packard 6890 GC equipped with a flame ionisation detector (FID). Sample aliquots of 1 µL were injected in split mode at 250°C injector temperature and 320°C detector temperature with N_2 as carrier gas and with a flow rate set to 0.4 mL/min in constant flow mode. The oven temperature program was as follows: 100°C for 1 min, 20°C/min ramp to 250°C, and 45°C/min ramp to 280°C (0.5 min). Total run time was 8 min.

For analysis of the results, Instrument #1 Data Analysis, MSD Chemstation D.03.00552, Agilent Technologies, Agilent ChemStation B.0302, Agilent Technologies was used.

Quantification of terpenes with GC-FID

For the quantification of the substrate valencene and the products *cis/trans*-nootkatol and nootkatone, terpene standards were prepared at different dilutions and analyzed by GC-FID. For quantification, the peak areas were integrated and calibration curves were created by correlating to the areas with known concentrations. Based on this data, Erich Leitner programmed an automatic peak recognition and integration program that directly quantified the substances. A representative output file for GC-FID

measurement of a standard solution can be seen in Figure 45. The amount of substance measured is directly converted to ng/µL sample.

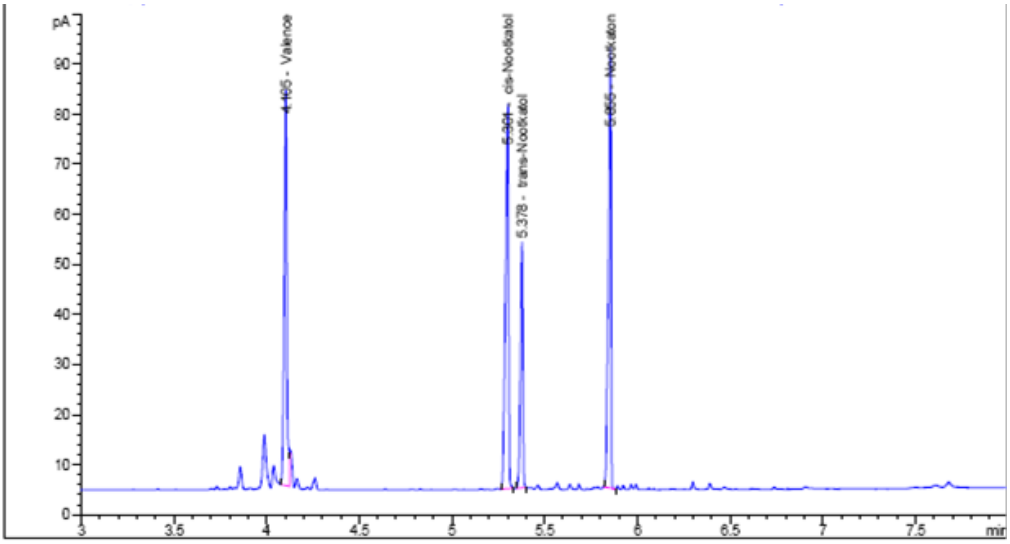


```
========================================================================
                    External Standard Report
========================================================================

Sorted By             :      Signal
Calib. Data Modified  :      23/03/2011 14:53:31
Multiplier:                   :      1.0000
Dilution:                     :      1.0000
Use Multiplier & Dilution Factor with ISTDs

Signal 1: FID1 B,

RetTime  Type     Area     Amt/Area    Amount   Grp   Name
 [min]          [pA*s]                [ng/ul]
-------|------|----------|----------|----------|--|------------------
  4.105 BV       79.71137    1.54817  123.40677    Valence
  5.301 BB       87.91110    1.71179  150.48525    cis-Nootkatol
  5.378 BB       45.57720    1.89973   86.58434    trans-Nootkatol
  5.855 BB       85.78452    1.12365   96.39159    Nootkaton

Totals :                             456.86795
```

Figure 45: Chromatogram and output sheet of a standard measured by GC-FID

Cell homogenate preparation, MSK cell disruption

Cell homogenates used for GDH assay or CO-spectra measurement was prepared by growing and inducing *Pichia pastoris* cultures in 1 L baffled shake flasks. The cells were harvested by centrifugation for 5 min at 5 000 rpm and 4°C (Beckman Coulter, JE-10), resuspended in 100 mL dH_2O and centrifuged again. Cell wet weight (CWW) was determined and per g CWW 1 mL of TE-buffer, pH 7.5 and 2 µL of 1 M PMSF dissolved in DMSO was added and the cells were resuspended. The cell suspension was transferred into cell disruption vessels and the same amount of glass beads was added. The cells were

disrupted in MSK homogenizer for 3 min with 5 s CO_2 cooling steps every 30 s. The disrupted cells and glass beads were centrifuged for 5 min at 4 000 rpm to remove cell debris in the micro centrifuge. The SN was aliquoted and stored at -20°C till use.

GDH activity assay

GDH assay was performed in UV star microtiter plates using the Spectramax Plus 384 plate reader. In each well, 100 µL of 1 M Tris/HCl-buffer, pH 7.4 and a 1:10 dilution of the cell homogenates were pipetted. The reaction was started by adding 50 µL of a glucose/$NADP^+$-mixture to a final concentration of 12.5 mM glucose and 1.25 mM $NADP^+$. Immediately after adding the glucose/$NADP^+$ mixture, measurement was started. The absorption was monitored for 30 min taking a reading every minute. Measurements were done at least in triplicates. In order to exclude unspecific $NADP^+$ absorption, an assay without adding glucose was done.

Correlation of OD_{600} of *Pichia pastoris* cells to their CDW

*Pp*CBS7435 was used in order to correlate *Pichia pastoris* CDW to OD_{600} measurements. Therefore, *Pp*CBS7435 was grown in 100 mL of BMDY medium for 60 h to reach stationary growth phase. Different amounts of samples corresponding to OD_{600} units from 1 to 500 were taken and transferred into weighed tubes. The cells were centrifuged at 3 200 x g for 10 min at RT in a table top centrifuge or a micro centrifuge. The SN was discarded and the resulting cell pellet was dried for two days at 60°C. A triplicate measurement was performed. The standard deviation was very small in the analysis and is therefore not displayed in Figure 46.

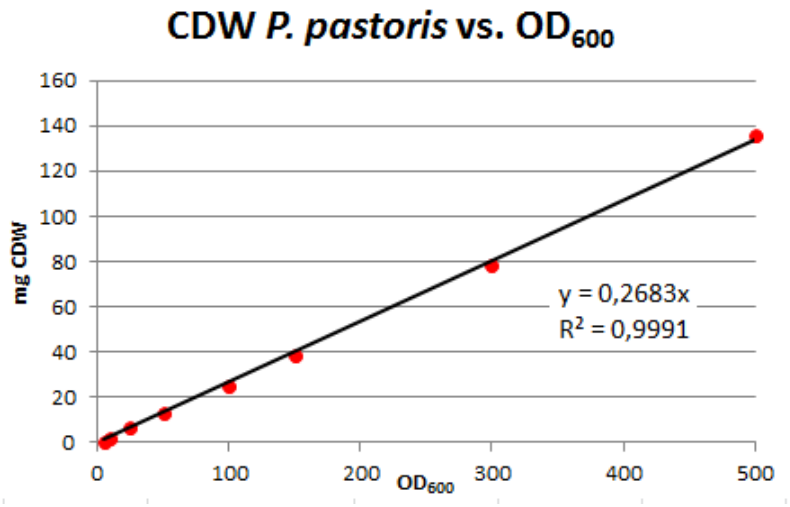

Figure 46: CDW of *Pichia pastoris* vs. OD_{600}

V. References

[1] J. Lin, R. L. Rouseff, S. Barros, and M. Naim, "Aroma composition changes in early season grapefruit juice produced from thermal concentration.," *Journal of agricultural and food chemistry*, vol. 50, no. 4, pp. 813-9, Feb. 2002.

[2] M. A. Fraatz, R. G. Berger, and H. Zorn, "Nootkatone--a biotechnological challenge.," *Applied microbiology and biotechnology*, vol. 83, no. 1, pp. 35-41, May. 2009.

[3] A. Ortuno et al., "Flavanone and Nootkatone Levels in Different Varieties of Grapefruit and Pummelo," *Journal of Agricultural and Food Chemistry*, vol. 43, no. 1, pp. 1-5, Jan. 1995.

[4] J. M. Cregg, I. Tolstorukov, A. Kusari, J. Sunga, K. Madden, and T. Chappell, "Expression in the yeast Pichia pastoris.," *Methods in enzymology*, vol. 463, pp. 169-89, Jan. 2009.

[5] G. P. Lin Cereghino et al., "New selectable marker/auxotrophic host strain combinations for molecular genetic manipulation of Pichia pastoris.," *Gene*, vol. 263, no. 1-2, pp. 159-69, Jan. 2001.

[6] H. R. Waterham, M. E. Digan, P. J. Koutz, S. V. Lair, and J. M. Cregg, "Isolation of the Pichia pastoris glyceraldehyde-3-phosphate dehydrogenase gene and regulation and use of its promoter.," *Gene*, vol. 186, no. 1, pp. 37-44, Feb. 1997.

[7] S. Macauley-Patrick, M. L. Fazenda, B. McNeil, and L. M. Harvey, "Heterologous protein production using the Pichia pastoris expression system.," *Yeast (Chichester, England)*, vol. 22, no. 4, pp. 249-70, Mar. 2005.

[8] C. P. Kurtzman, "Biotechnological strains of Komagataella (Pichia) pastoris are Komagataella phaffii as determined from multigene sequence analysis.," *Journal of industrial microbiology & biotechnology*, vol. 36, no. 11, pp. 1435-8, Nov. 2009.

[9] A. Küberl et al., "High-quality genome sequence of Pichia pastoris CBS7435.," *Journal of biotechnology*, vol. 154, no. 4, pp. 312-20, Jul. 2011.

[10] A. Glieder, *Pichia pool TU Graz - New Pichia pastoris strains and expression vectors*. 2009.

[11] Z. Dudásová, A. Dudás, and M. Chovanec, "Non-homologous end-joining factors of Saccharomyces cerevisiae.," *FEMS microbiology reviews*, vol. 28, no. 5, pp. 581-601, Nov. 2004.

[12] V. B. Urlacher and S. Eiben, "Cytochrome P450 monooxygenases: perspectives for synthetic application.," *Trends in biotechnology*, vol. 24, no. 7, pp. 324-30, Jul. 2006.

[13] D. R. Nelson, "Cytochrome P450 Nomenclature, 2004," *Methods in Molecular Biology*, vol. 320, pp. 1-10, 2004.

[14] G. A. Roberts, G. Grogan, A. Greter, S. L. Flitsch, and N. J. Turner, "Identification of a New Class of Cytochrome P450 from a Rhodococcus sp .," *Society*, vol. 184, no. 14, pp. 3898-3908, 2002.

[15] F. Hannemann, A. Bichet, K. M. Ewen, and R. Bernhardt, "Cytochrome P450 systems--biological variations of electron transport chains.," *Biochimica et biophysica acta*, vol. 1770, no. 3, pp. 330-44, Mar. 2007.

[16] T. Hamann, T. Laursen, and B. L. Møller, "Functional expression of N-terminally tagged membrane bound cytochrome P450.," *Protein expression and purification*, vol. 68, no. 1, pp. 18-21, Nov. 2009.

[17] "Personal communication with Tamara Wriessnegger."

[18] S. Takahashi et al., "Functional characterization of premnaspirodiene oxygenase, a cytochrome P450 catalyzing regio- and stereo-specific hydroxylations of diverse sesquiterpene substrates.," *The Journal of biological chemistry*, vol. 282, no. 43, pp. 31744-54, Oct. 2007.

[19] "http://drnelson.uthsc.edu/cytochromep450.html." .

[20] M. Mizutani and D. Ohta, "Two isoforms of NADPH:cytochrome P450 reductase in Arabidopsis thaliana. Gene structure, heterologous expression in insect cells, and differential regulation.," *Plant physiology*, vol. 116, no. 1, pp. 357-67, Jan. 1998.

[21] M. Karlsson, "Reconstitution of water channel function of an aquaporin overexpressed and purified from Pichia pastoris," *FEBS Letters*, vol. 537, no. 1-3, pp. 68-72, Feb. 2003.

[22] M. Dietrich et al., "Recombinant production of human microsomal cytochrome P450 2D6 in the methylotrophic yeast Pichia pastoris.," *Chembiochem: A European journal of chemical biology*, vol. 6, no. 11, pp. 2014-22, Nov. 2005.

[23] F. Ganske and U. T. Bornscheuer, "Growth of Escherichia coli, Pichia pastoris and Bacillus cereus in the presence of the ionic liquids [BMIM][BF4] and [BMIM][PF6] and Organic Solvents.," *Biotechnology letters*, vol. 28, no. 7, pp. 465-9, Apr. 2006.

[24] O. de Smidt, J. C. du Preez, and J. Albertyn, "The alcohol dehydrogenases of Saccharomyces cerevisiae: a comprehensive review.," *FEMS yeast research*, vol. 8, no. 7, pp. 967-78, Nov. 2008.

[25] "http://www.brenda-enzymes.org/Mol/reaction-popup.php4?id=49028&type=I&displayType=marvin." .

[26] I. Lavandera, A. Kern, B. Ferreira-Silva, A. Glieder, S. de Wildeman, and W. Kroutil, "Stereoselective bioreduction of bulky-bulky ketones by a novel ADH from Ralstonia sp.," *The Journal of organic chemistry*, vol. 73, no. 15, pp. 6003-5, Aug. 2008.

[27] I. Lavandera et al., "One-way biohydrogen transfer for oxidation of sec-alcohols.," *Organic letters*, vol. 10, no. 11, pp. 2155-8, Jun. 2008.

[28] W. a van der Donk and H. Zhao, "Recent developments in pyridine nucleotide regeneration," *Current Opinion in Biotechnology*, vol. 14, no. 4, pp. 421-426, Aug. 2003.

[29] R. Wichmann, "Cofactor Regeneration at the Lab Scale," *Biochemistry*, pp. 225 - 260, 2005.

[30] K. Schroer, K. Peter Luef, F. Stefan Hartner, A. Glieder, and B. Pscheidt, "Engineering the Pichia pastoris methanol oxidation pathway for improved NADH regeneration during whole-cell biotransformation.," *Metabolic engineering*, vol. 12, no. 1, pp. 8-17, Jan. 2010.

[31] E. Vázquez-Figueroa, J. Chaparro-Riggers, and A. S. Bommarius, "Development of a thermostable glucose dehydrogenase by a structure-guided consensus concept.," *Chembiochem: A European journal of chemical biology*, vol. 8, no. 18, pp. 2295-301, Dec. 2007.

[32] A. Weckbecker and W. Hummel, "Glucose Dehydrogenase for the Regeneration of NADPH and NADH," in *Microbial Enzymes and Biotransformations*, J. L. Barredo, Ed. Humana Press, 2005, pp. 225-238.

[33] H. Engelking, R. Pfaller, G. Wich, and D. Weuster-Botz, "Stereoselective reduction of ethyl 4-chloro acetoacetate with recombinant Pichia pastoris," *Tetrahedron: Asymmetry*, vol. 15, no. 22, pp. 3591-3593, Nov. 2004.

[34] D. Zehentgruber, "Biotransformationen mit Cytochrom P450 Monooxygenasen," 2009.

[35] N. J. Kruger and A. von Schaewen, "The oxidative pentose phosphate pathway: structure and organisation," *Current Opinion in Plant Biology*, vol. 6, no. 3, pp. 236-246, Jun. 2003.

[36] F. Drawert, R. G. Berger, and R. Godelmann, "Regioselective biotransformation of valencene in cell suspension cultures of Citrus sp.," *Plant Cell Reports*, vol. 3, no. 1, pp. 37-40, Feb. 1984.

[37] A. Emmerstorfer, "Membrane Protein Expression in E. coli, Master's Thesis," Graz University of Technology, 2010.

[38] H. Sakamaki et al., "Biotransformation of valencene by cultured cells of Gynostemma pentaphyllum," *Journal of Molecular Catalysis B: Enzymatic*, vol. 32, no. 3, pp. 103-106, Jan. 2005.

[39] M. Furusawa, T. Hashimoto, Y. Noma, and Y. Asakawa, "Highly efficient production of nootkatone, the grapefruit aroma from valencene, by biotransformation.," *Chemical & pharmaceutical bulletin*, vol. 53, no. 11, pp. 1513-4, Nov. 2005.

[40] R. J. Sowden, S. Yasmin, N. H. Rees, S. G. Bell, and L.-lok Wong, "Biotransformation of the sesquiterpene (+)-valencene by cytochrome P450cam and P450BM-3.," *Organic & biomolecular chemistry*, vol. 3, no. 1, pp. 57-64, Jan. 2005.

[41] R. Kaspera, U. Krings, T. Nanzad, and R. G. Berger, "Bioconversion of (+)-valencene in submerged cultures of the ascomycete Chaetomium globosum.," *Applied microbiology and biotechnology*, vol. 67, no. 4, pp. 477-83, Jun. 2005.

[42] M. A. Fraatz et al., "A novel oxygenase from Pleurotus sapidus transforms valencene to nootkatone," *Journal of Molecular Catalysis B: Enzymatic*, vol. 61, no. 3-4, pp. 202-207, Dec. 2009.

[43] M. Girhard, K. Machida, M. Itoh, R. D. Schmid, A. Arisawa, and V. B. Urlacher, "Regioselective biooxidation of (+)-valencene by recombinant E. coli expressing CYP109B1 from Bacillus subtilis in a two-liquid-phase system.," *Microbial cell factories*, vol. 8, no. 4, p. 36, Jan. 2009.

[44] A. Seifert et al., "Rational design of a minimal and highly enriched CYP102A1 mutant library with improved regio-, stereo- and chemoselectivity.," *Chembiochem : a European journal of chemical biology*, vol. 10, no. 5, pp. 853-61, Mar. 2009.

[45] H.-S. Bea, Y.-M. Seo, M.-H. Cha, B.-G. Kim, and H. Yun, "Kinetic resolution of α-methylbenzylamine by recombinant Pichia pastoris expressing ω-transaminase," *Biotechnology and Bioprocess Engineering*, vol. 15, no. 3, pp. 429-434, Jul. 2010.

[46] J. C. D. Hinton, I. Hautefort, S. Eriksson, A. Thompson, and M. Rhen, "Benefits and pitfalls of using microarrays to monitor bacterial gene expression during infection.," *Current opinion in microbiology*, vol. 7, no. 3, pp. 277-82, Jun. 2004.

[47] R. T. Kerns and M. F. Miles, "Microarray analysis of ethanol-induced changes in gene expression.," *Methods in molecular biology (Clifton, N.J.)*, vol. 447, pp. 395-410, Jan. 2008.

[48] "http://www.insilico.uni-duesseldorf.de/Lig_Input.html." .

[49] J. Lin-Cereghino, W. Wong, S. Xiong, and W. Giang, "Condensed protocol for competent cell preparation and transformation of the methylotrophic yeast Pichia pastoris," *Science*, vol. 38, no. 1, pp. 44-48, 2005.

VI. Appendix

Protein and gene sequences

In the following the gene sequences of the different genes cloned into the vectors are shown, including different **restriction enzyme sequences, Kozak sequences** and **protein tags** including **stop codons** marked in different colors.

HPO-FLAG, *Hyoscyamus muticus*

Gene sequence:

GAATTCCGAAACGCAT**ATG**CAATTCTTCAGCTTGGTTAGTATCTTCTTGTTTCTGTCTTTTTTGTTTTTGTTAAGAAAGTGGAAAAATTCCAACA
GCCAGAGTAAAAAGTTGCCTCCAGGTCCATGGAAGTTGCCATTACTGGGTAGCATGCTTCACATGGTTGGTGGATTGCCACATCATGTTCTTA
GAGATTTGGCTAAGAAGTATGGACCATTGATGCATTTGCAATTGGGTGAAGTTTCTGCTGTTGTTGTTACTTCTCCTGATATGGCCAAGGAAG
TCCTGAAGACTCATGATATTGCGTTCGCGTCTAGACCTAAGTTGTTAGCACCAGAGATTGTCTGTTATAATAGATCCGACATTGCGTTTTGCCC
TTACGGTGATTATTGGAGACAAATGCGAAAGATTTGTGTATTGGAAGTGTTGAGTGCAAAAAATGTTAGATCCTTCTCTTCTATTAGACGCGA
TGAAGTGTTGCGACTTGTTAACTTTGTACGATCTTCCACGAGTGAGCCGGTTAATTTTACTGAAAGGCTCTTTTTATTCACCAGTTCGATGACAT
GTAGATCCGCTTTTGGGAAGGTATTTAAAGAGCAAGAAACATTTATCCAGCTGATCAAGGAAGTAATCGGTCTGGCTGGTGGTTTTGATGTA
GCTGACATCTTCCCATCTCTCAAATTCCTACATGTCCTGACTGGTATGGAGGGTAAAATTATGAAAGCTCACCATAAGGTCGATGCTATTGTTG
AGGATGTAATCAACGAGCATAAGAAAAATTTGGCCATGGGCAAGACTAACGGTGCTTTAGGCGGTGAGGATCTGATTGATGTTTTGTTAAGA
TTGATGAACGATGGAGGCTTGCAATTTCCTATCACGAACGACAATATCAAGGCTATTATCTTTGACATGTTTGCTGCTGGCACCGAGACTTCTT
CTAGCACCTTGGTCTGGGCTATGGTACAAATGATGAGAAACCCAACTATCCTTGCAAAGGCTCAAGCTGAAGTCAGAGAAGCCTTCAAGGGT
AAGGAAACTTTCGATGAAAACGATGTAGAAGAGTTGAAGTATTTGAAACTTGTAATTAAGGAAACTCTGAGACTCCATCCACCAGTTCCATTG
TTGGTACCAAGAGAATGTAGAGAAGAAACCGAAATCAACGGCTATACTATTCCAGTCAAAACGAAGGTAATGGTTAACGTTTGGGCCCTGGG
AAGAGATCCGAAGTATTGGGACGACGCTGATAATTTCAAACCAGAGAGATTTGAGCAGTGTTCCGTAGACTTTATCGGTAATAACTTTGAATA
CTTGCCATTTGGTGGTGGAAGAAGAATCTGTCCAGGCATCTCTTTTGGTCTGGCTAACGTTTACTTGCCATTGGCTCAATTGCTGTACCATTTT
GATTGGAAGCTACCTACTGGAATGGAACCAAAGGACTTGGATTTGACCGAATTGGTTGGAATCACTATTGCCAGAAAAAGTGATTTGATGTT
GGTTGCGACTCCTTACCAACCTTCCCGAGAG**GATTACAAGGATGACGACGATAAG**TAATAACTGCAGCGGCCGC

Properties:

- Accession number, native gene: EF569601
- Optimized by Tamara Wriessnegger for *Pichia pastoris* expression
- Length: 1 565 bp (between restriction sites: 1 558 bp)
- *Eco*RI (5'-G^AATTC-3') and *Not*I (5'-GC^GGCCGC-3') restriction sites
- FLAG-tagged: 5'- GATTACAAGGATGACGACGATAAG -3'
- Kozak sequence: 5'-CGAAACG-3'

Protein sequence:

MQFFSLVSIFLFLSFLFLLRKWKNSNSQSKKLPPGPWKLPLLGSMLHMVGGLPHHVLRDLAKKYGPLMHLQLGEVSAVVVTSPDMAKEVLK
THDIAFASRPKLLAPEIVCYNRSDIAFCPYGDYWRQMRKICVLEVLSAKNVRSFSSIRRDEVLRLVNFVRSSTSEPVNFTERLFLFTSSMTCRSA
FGKVFKEQETFIQLIKEVIGLAGGFDVADIFPSLKFLHVLTGMEGKIMKAHHKVDAIVEDVINEHKKNLAMGKTNGALGGEDLIDVLLRLMN
DGGLQFPITNDNIKAIIFDMFAAGTETSSSTLVWAMVQMMRNPTILAKAQAEVREAFKGKETFDENDVEELKYLKLVIKETLRLHPPVPLLV
PRECREETEINGYTIPVKTKVMVNVWALGRDPKYWDDADNFKPERFEQCSVDFIGNNFEYLPFGGGRRICPGISFGLANVYLPLAQLLYHFD
WKLPTGMEPKDLDLTELVGVTAARKSDLMLVATPYQPSRE**DYKDDDDK****

Properties:

- Accession number: ABS00393
- Size: 502 aa (510 aa), 56.8 kDa (including tag: 57.8 kDa)
- FLAG-tagged: N-DYKDDDDK-C

CPR-myc, *Arabidopsis thaliana*

Gene sequence:

GAATTCCGAAACGCAT**ATG**ACTTCTGCTTTGTACGCTTCTGATTTGTTCAAGCAATTGAAGTCCATCATGGGTACTGATTCTTTGTCTGACGAT
GTTGTTTTGGTTATCGCTACCACTTCTTTGGCTTTGGTTGCTGGTTTCGTTGTCTTATTGTGGAAGAAGACCACCGCTGATCGTTCTGGTGAATT
GAAGCCATTGATGATCCCAAAGTCTTTGATGGCCAAGGACGAAGATGACGACTTGGACTTGGGTTCTGGTAAGACCAGGGTCTCCATCTTCTT
CGGTACTCAAACTGGTACTGCTGAAGGTTTCGCCAAGGCTTTGTCTGAAGAAATCAAGGCCCGTTATGAAAAGGCTGCTGTCAAGGTCATTG
ACTTGGATGACTACGCTGCTGATGATGACCAATACGAAGAAAAGTTGAAGAAGGAAACTTTGGCCTTCTTCTGTGTTGCCACCTACGGTGATG
GTGAACCAACTGACAACGCTGCCAGATTCTACAAATGGTTCACCGAAGAAAACGAAAGAGATATCAAGTTGCAACAATTGGCTTACGGTGTC
TTTGCTTTAGGTAACAGACAATACGAACACTTCAACAAGATCGGTATTGTCTTGGACGAAGAATTGTGTAAGAAGGGTGCCAAGAGATTGAT
TGAAGTTGGTTTGGGTGACGATGACCAATCCATTGAAGATGACTTCAACGCCTGGAAGGAATCTTTATGGTCTGAATTGGACAAATTGTTGAA
GGACGAAGACGACAAATCCGTTGCCACTCCATACACTGCTGTCATTCCAGAATACAGAGTTGTCACCCACGACCCAAGATTCACCACTCAAAA
GTCCATGGAATCCAACGTTGCTAACGGTAACACCACCATCGATATCCACCACCCATGTCGTGTCGATGTTGCCGTTCAAAAGGAATTGCACAC
TCACGAATCTGACCGTTCTTGTATTCATTTGGAATTTGACATCTCCAGAACCGGTATCACTTACGAAACCGGTGACCACGTTGGTGTTTACGCT
GAAAACCATGTCGAAATCGTCGAAGAAGCTGGTAAGTTGTTGGGTCACTCTTTGGACTTGGTTTTCTCCATCCACGCTGACAAGGAAGACGGT
TCTCCATTGGAATCTGCTGTCCCACCTCCTTTCCCAGGTCCATGTACCTTAGGTACTGGTTTAGCTAGATACGCTGATCTATTAAACCCTCCAAG
AAAGTCTGCTTTGGTTGCTTTGGCTGCTTACGCCACTGAACCATCTGAAGCTGAAAAGTTGAAGCATTTGACTTCTCCAGATGGTAAGGACGA
ATACTCTCAATGGATTGTTGCTTCTCAAAGATCCTTGTTGGAAGTTATGGCTGCTTTCCCATCTGCCAAGCCACCATTAGGTGTCTTCTTCGCTG
CCATTGCTCCAAGATTACAACCAAGATACTACTCCATCTCCTCTTCTCCAAGATTGGCTCCATCCAGAGTTCACGTTACTTCTGCTTTGGTCTAC
GGTCCAACTCCAACTGGTAGAATCCACAAGGGTGTTTGTTCCACTTGGATGAAGAACGCTGTTCCAGCTGAAAAGTCCCACGAATGTTCTGGT
GCCCCAATCTTTATCAGAGCTTCCAACTTCAAATTGCCATCCAACCCATCTACCCCAATTGTCATGGTTGGTCCAGGTACCGGTTTGGCTCCATT
CAGAGGTTTCTTGCAAGAAAGAATGGCTTTGAAGGAAGATGGTGAAGAATTGGGTTCCTCTCTATTATTCTTCGGTTGTAGAAACAGACAAAT
GGACTTCATTTACGAAGACGAATTGAACAACTTTGTCGACCAAGGTGTCATCTCTGAATTGATCATGGCCTTCTCTCGTGAAGGTGCTCAAAA
GGAATACGTTCAACACAAGATGATGGAAAAGGCTGCTCAAGTCTGGGACTTGATCAAGGAAGAAGGTTACTTGTACGTTTGTGGTGATGCTA
AGGGTATGGCCAGAGATGTCCACAGAACTTTGCACACCATTGTCCAAGAACAAGAAGGTGTTTCCTCTTCTGAAGCTGAAGCCATTGTCAAGA
AATTGCAAACCGAAGGTAGATACTTGAGAGATGTCTGG**GAACAAAAATTGATTTCTGAAGAGGATTTG**TAATAACTCGAGCGGCCGCAA
GCTTTAAAGGAGGGTTTATTAATGATAAGGATCC

Properties:

- Accession number, native gene: NM_118585
- Optimized by DSM for *Pichia pastoris* expression
- Length: 2 157 bp (between restriction sites: 2 105 bp)
- *Eco*RI (5'-G^AATTC-3') and *Not*I (5'-GC^GGCCGC-3') restriction sites
- Kozak sequence: 5'-CGAAACGCAT-3'
- Myc-tagged: 5'-GAACAAAAATTGATTTCTGAAGAGGATTTG-3'

Protein sequence:

MTSALYASDLFKQLKSIMGTDSLSDDVVLVIATTSLALVAGFVVLLWKKTTADRSGELKPLMIPKSLMAKDEDDDLDLGSGKTRVSIFFGTQT
GTAEGFAKALSEEIKARYEKAAVKVIDLDDYAADDDQYEEKLKKETLAFFCVATYGDGEPTDNAARFYKWFTEENERDIKLQQLAYGVFALG
NRQYEHFNKIGIVLDEELCKKGAKRLIEVGLGDDDQSIEDDFNAWKESLWSELDKLLKDEDDKSVATPYTAVIPEYRVVTHDPRFTTQKSME
SNVANGNTTIDIHHPCRVDVAVQKELHTHESDRSCIHLEFDISRTGITYETGDHVGVYAENHVEIVEEAGKLLGHSLDLVFSIHADKEDGSPLE
SAVPPPFPGPCTLGTGLARYADLLNPPRKSALVALAAYATEPSEAEKLKHLTSPDGKDEYSQWIVASQRSLLEVMAAFPSAKPPLGVFFAAIA
PRLQPRYYSISSSPRLAPSRVHVTSALVYGPTPTGRIHKGVCSTWMKNAVPAEKSHECSGAPIFIRASNFKLPSNPSTPIVMVGPGTGLAPFR
GFLQERMALKEDGEELGSSLLFFGCRNRQMDFIYEDELNNFVDQGVISELIMAFSREGAQKEYVQHKMMEKAAQVWDLIKEEGYLYVCGD
AKGMARDVHRTLHTIVQEQEGVSSSEAEAIVKKLQTEGRYLRDVW**EQKLISEEDL****

Properties:

- Accession number: NP_194183
- Size: 502 aa (512 aa), 76,8 kDa (including tag: 77,8 kDa)
- Myc-tagged: N-EQKLISEEDL-C

ADH-C1-FLAG, *Pichia pastoris*

Gene sequence:

GAATTCCGAAACG**ATG**GCTTACCCAGACACTTTTGAAGGATTTGCAGTTCACGACCCAAGTAAGTGGTCCGAAGTAAAGAAA
ATTCAATTTACTCCTAGACCTTTCCAGGAAGATGATGTTGACATCAAGATCGAAGCATGTGGTATATGCTCCAGTGATATTCAC
ACCATTTCCGGAGGGTGGGGTCAGCCAAAGCTTCCCTCCATTGTTGGTCATGAGATTGTTGGAACTGTAGTTAGAGTTGGTTC
AAAGGTCGACAATATCAAGGTTGGAGACACTGTCGGTATGGGAGCAATGTGTTGGGCTGATTTGACGTGTGATGTCTGCAAG
TCCAAAAACGAAAACTACTGTCCTAACTGGATTGATACATATGATGACGCTTATCCCGATGGGTCAAGAACCTATGGTGGTTAC
TCCAACTATGCTCGTTGCAACAAAGAGTTTGCATTCAAGATTCCAAAAGGATTATCCGTAGAAGGAGTTGCTCCAATGTTGTGC
GCTGGTATCACCACTTATTCTCCTTTAAAGAGAAACAATATTGGACCAGGCAAGAAGGTGGGTGTTGTTGGTATCGGTGGTTT
GGGGCATTTTGCTCTTCAATTCGCCAAGGCTCTTGGAGCTGAAGTCTACGCAATTTCCAGGAATGACAAGAAGAAAGCAGACG
CTCTTAAATTGGGAGCTGATTACTTCATTGAAACTGAGAAGGAAGGTTGGAACTTACCATACAAGTATAAGTTCGACTTAATCA
TTAGTACAGCCAATTCCAGCCAGAACTTTGACCTTGATGCCTATGTATCCACACTTAATATTGGGGCAAAGTTTGTATCTGTCGG
ACTTCCAGAGGACAAGATGGAAATGAATGCTGGATCTTTCATCAAGAACGGCTGCTATTTCGGTTCTTCTCATTTGGGTAACCG
TGAAGAAATGAAAGAGATGCTTGAGTTAGCTGCTGAAAAGGGTATTGAAGCTTGGTATGAGCCAATTTCAATCTCTCAGGAG
GGTATTAAAAACGGACTGGAGAAGTTGCACCGCAACGATGTCAAATACCGTTTCACCCTTACTAATTACGGAAAACAGTTTGA
ATAG**GATTACAAGGATGACGACGATAAG**TAATAAGCGGCCGC

Properties:

- Accession number: XM_002489969
- Intrinsic *Pichia pastoris* gene
- Length: 1 125 bp (between restriction sites: 1 118 bp)
- *Eco*RI (5'-G^AATTC-3') and *Not*I (5'-GC^GGCCGC-3')restriction sites
- FLAG-tagged: 5'-GATTACAAGGATGACGACGATAAG-3'
- Kozak sequence: 5'-CGAAACG-3'

Protein sequence:

MAYPDTFEGFAVHDPSKWSEVKKIQFTPRPFQEDDVDIKIEACGICSSDIHTISGGWGQPKLPSIVGHEIVGTVVRVGSKVDNIKVGD
TVGMGAMCWADLTCDVCKSKNENYCPNWIDTYDDAYPDGSRTYGGYSNYARCNKEFAFKIPKGLSVEGVAPMLCAGITTYSPLKR
NNIGPGKKVGVVGIGGLGHFALQFAKALGAEVYAISRNDKKKADALKLGADYFIETEKEGWNLPYKYKFDLIISTANSSQNFDLDAYV
STLNIGAKFVSVGLPEDKMEMNAGSFIKNGCYFGSSHLGNREEMKEMLELAAEKGIEAWYEPISISQEGIKNGLEKLHRNDVKYRFTL
TNYGKQFE**DYKDDDDK****

Properties:

- Accession number: XP_002490014
- Size: 357 aa (365 aa), 39.4 kDa (including tag: 40.4 kDa)
- FLAG-tagged: N-DYKDDDDK-C

ADH-C3-FLAG, *Pichia pastoris*

Gene sequence:

GAATTCCGAAACG**ATG**ACCACAGTTTTCGCTTACGCAGCTCCCTCTGCCAGTGGTGAGCTAGGACCCTTTTCATATGAGCCTAG
AAATCTCAGAAATGACGATGTGGAAATAAAGATTCTGTATTGCGGAGTTTGTCACACAGACCTGCACAAGTGCCGGAATCACT
GGGGAGGTTCACAGTACCCACTTGTTCCAGGACACGAAATCGTGGGGAAGGTAGCCCGAGTCGGGACATCGGTGACCAAATA
CAAGCTGGGAGATGTTGCGGCGGTGGGATGTCTTGTGGATTCATGTGGGAACTGCCGATCGTGTAAAGACGGACTGGAGAAC
TATTGTGAGAACGCGCCAACTCTGACTTATGACGCTGATGACCGCAAAGATGGCAAGCGTCTTTATGGAGGATATTCTGAGTC
GATTACCGTCAGAGAAAGTTTTGTGTTGCGAGTGCCCAGCGGGTTGGACGTGAAGTCTGCGGCACCACTTCTTTGCGCTGGAA
TCACTATGTGGTCGCCGTTGCGGAATTGGAAAGTGAACAGCAAGTCCAAGGTTGCAGTGGCCGGGCTTGGAGGATTGGGCCA
TATGGGTATCAAGCTTGCTAAAGGCCTGGGGGCACACGTTACACTACTTTCTCGTTCGCCAGGAAAGGCCACAGACGGGCGAC
GACTGGGGGCAGACGATGTGCTAATTACCACAGACGAAGCAGCGGTCGCACGGGCAAGCAACCGGTTCGACATCATACTCGA
TACAGTACCGTACGACCACGACGTGAACCCGTACCTGAGCCTACTTCGACGAGACGGGAATCTCGTTCTGCTTGGGTTAATTG
GCAACATCCAGGCGACGCCACTGAACACTGGGCCAATGCTATCTGCGCGGCGCTCGGTATCAGGCTCAGGAATTGGAGGGAT
ACAAGAGACGCAAGAGCTGCTTGACTTCTGTGCGGCCAAAAAGATTTTGCCGGACGTTGAAATGATTGCGATCCAAGAGATCA
ACGATGCATACGAGCGGCTTATCAAAGGGGATGTGAAGTATAGGTTTGTGATTGACATTGAGAGTCTAAGTAAAGTCAGGGG
GTAG**GATTACAAGGATGACGACGATAAG**TAATAAGCGGCCGC

Properties:

- Accession number: XM_002492172
- Intrinsic *Pichia pastoris* gene
- Length: 1 116 bp (between restriction sites: 1 109 bp)
- *Eco*RI (5'-G^AATTC-3') and *Not*I (5'-GC^GGCCGC-3')restriction sites
- FLAG-tagged: 5'-GATTACAAGGATGACGACGATAAG-3'
- Kozak sequence: 5'-CGAAACG-3'

Protein sequence:

MTTVFAYAAPSASGELGPFSYEPRNLRNDDVEIKILYCGVCHTDLHKCRNHWGGSQYPLVPGHEIVGKVARVGTSVTKYKLGDVAA
VGCLVDSCGNCRSCKDGLENYCENAPTLTYDADDRKDGKRLYGGYSESITVRESFVLRVPSGLDVKSAAPLLCAGITMWSPLRNWK
VNSKSKVAVAGLGGLGHMGIKLAKGLGAHVTLLSRSPGKATDGRRLGADDVLITTDEAAVARASNRFDIILDTVPYDHDVNPYLSLLR
RDGNLVLLGLIGNIQATPLNTGPMLSARRSVSGSGIGGIQETQELLDFCAAKKILPDVEMIAIQEINDAYERLIKGDVKYRFVIDIESLSK
VRG**DYKDDDDK****

Properties:

- Accession number: XP_002492217
- Size: 355 aa (362 aa), 38.2 kDa (including tag: 39.2 kDa)
- FLAG-tagged: N-DYKDDDDK-C

ADH-SY-FLAG, *Sphingobium yanoikuyae*

Gene sequence:

GAATTCCGAAACG**ATG**ACCACGCTTCCGACTGTTCTCATCACCGGCGCCTCCTCCGGTATCGGCGCCACCTACGCCGAGCGCTT
CGCCCGCCGCGGCCACGACCTCGTGCTGGTTGCACGCGACAAGGTGCGCCTCGATGCGTTGGCCGCGCGCCTGCGTGACGAA
AGCGGTGTGGCCGTCGAAGCGCTGCAGGCCGACCTGACCCGGCCTGCGGATCTGGCCGCGGTCGAGATTCGTCTGCGCGAG
GACGCTCGCATAGGCATCCTGATCAACAACGCCGGGATGGCTCAGTCGGGCGGCTTCGTGCAGCAGACCGCTGAGGGCATCG
AACGCCTGATCACGCTCAACACCACGGCGCTCACGCGGCTCGCAGCCGCGGTCGCTCCGCGCTTCGTGCAGTCGGGTACCGGC
GCAATCGTCAACATCGGCTCGGTGGTGGGTTTCGCGCCCGAGTTCGGCATGTCGATTTACGGCGCCACCAAGGCGTTTGTGCT
GTTCCTGTCGCAGGGATTGAACCTCGAGTTGTCGCCCAGCGGCATCTACGTCCAGGCGGTGCTTCCGGCAGCGACCCGCACGG
AGATCTGGGGGCGCGCCGGCATCGACGTCAATACGCTTCCCGAGGTGATGGAAGTCGACGAACTGGTTGATGCGGCACTGGT
CGGCTTCGATCGCCGCGAACTCGTGACTATCCCGCCGCTGCACGTGGCGGCGCGCTGGGACGCATTGGATGGCGCGCGTCAA
GGGCTCATGTCGGACATTCGACAAGCCCAGGCGGCCGACCGCTATCGGCCGGAAGCCTGA**GATTACAAGGATGACGACGAT
AAG**TAATAA**GCGGCCGC**

Properties:

- Accession number: EU427523.1
- Length: 840 bp (between restriction sites: 833 bp)
- *Eco*RI (5'-G^AATTC-3') and *Not*I (5'-GC^GGCCGC-3')restriction sites
- FLAG-tagged: 5'-GATTACAAGGATGACGACGATAAG-3'
- Kozak sequence: 5'-CGAAACG-3'

Protein sequence:

MTTLPTVLITGASSGIGATYAERFARRGHDLVLVARDKVRLDALAARLRDESGVAVEALQADLTRPADLAAVEIRLREDARIGILINNA
GMAQSGGFVQQTAEGIERLITLNTTALTRLAAAVAPRFVQSGTGAIVNIGSVVGFAPEFGMSIYGATKAFVLFLSQGLNLELSPSGIYV
QAVLPAATRTEIWGRAGIDVNTLPEVMEVDELVDAALVGFDRRELVTIPPLHVAARWDALDGARQGLMSDIRQAQAADRYRPEA
DYKDDDDK**

Properties:

- Accession number: ACB78183.1
- Size: 262 aa (270 aa), 27.9 kDa (including tag: 28.9 kDa)
- FLAG-tagged: N-DYKDDDDK-C

*Bs*GDH-6xHIS, *Bacillus subtilis*

Gene sequence:

GAATTCCGAAACG**ATG**TATCCGGATTTAAAAGGAAAAGTCGTCGCTATTACAGGAGCTGCTTCAGGGCTCGGAAAGGCGATG
GCCATTCGCTTCGGCAAGGAGCAGGCAAAAGTGGTTATCAACTATTATAGTAATAAACAAGATCCGAACGAGGTAAAAGAAG
AGGTCATCAAGGCGGGCGGTGAAGCTGTTGTCGTCCAAGGAGATGTCACGAAAGAGGAAGATGTAAAAAATATCGTGCAAA
CGGCAATTAAGGAGTTCGGCACACTCGATATTATGATTAATAATGCCGGTCTTGAAAATCCTGTGCCATCTCACGAAATGCCGC
TCAAGGATTGGGATAAAGTCATCGGCACGAACTTAACGGGTGCCTTTTTAGGAAGCCGTGAAGCGATTAAATATTTCGTAGAA
AACGATATCAAGGGAAATGTCATTAACATGTCCAGTGTGCACGAAGTGATTCCTTGGCCGTTATTTGTCCACTATGCGGCAAGT
AAAGGCGGGATAAAGCTGATGACAGAAACATTAGCGTTGGAATACGCGCCGAAGGGCATTCGCGTCAATAATATTGGGCCAG
GTGCGATCAACACGCCAATCAATGCTGAAAAATTCGCTGACCCTAAACAGAAAGCTGATGTAGAAAGCATGATTCCAATGGGA
TATATCGGCGAACCGGAGGAGATCGCCGCAGTAGCAGCCTGGCTTGCTTCGAAGGAAGCCAGCTACGTCACAGGCATCACGT
TATTCGCGGACGGCGGTATGACACAATATCCTTCATTCCAGGCAGGCCGCGGT**CATCATCACCATCACCAC**TAATAAGCGGCC
GC

Properties:

- Accession number: not available; Genome Accession number: AL009126.3
- Length: 828 bp (between restriction sites: 821 bp)
- *Eco*RI (5'-G^AATTC-3') and *Not*I (5'-GC^GGCCGC-3') restriction sites
- 6xHIS-tagged: 5'-CATCATCACCATCACCAC-3'
- Kozak sequence: 5'-CGAAACG-3'

Protein sequence:

MYPDLKGKVVAITGAASGLGKAMAIRFGKEQAKVVINYYSNKQDPNEVKEEVIKAGGEAVVVQGDVTKEEDVKNIVQTAIKEFGTL
DIMINNAGLENPVPSHEMPLKDWDKVIGTNLTGAFLGSREAIKYFVENDIKGNVINMSSVHEVIPWPLFVHYAASKGGIKLMTETLA
LEYAPKGIRVNNIGPGAINTPINAEKFADPKQKADVESMIPMGYIGEPEEIAAVAAWLASKEASYVTGITLFADGGMTQYPSFQAGR
G**HHHHHH****

Properties:

- Accession number: NP_388275
- Size: 261 aa (267 aa), 28.1 kDa (including tag: 29.9 kDa)
- 6xHIS-tagged: N-HHHHHH-C

*Pp*G6PDH-6xHIS, *Pichia pastoris*

Gene sequence:

GAATTCCGAAACG**ATG**ATGACCGATACGAAAGCCGTAGAATTTGTGGGCCACACAGCCATTGTAGTCTTTGGAGCTTCAGGG
GACCTGGCTAAGAAGAAGACTTTCCCTGCCCTCTTCGGACTTTACCGTGAGGGATACCTGTCCAACAAGGTGAAGATTATTGG
CTATGCTAGATCAAAGCTGGATGACAAGGAGTTCAAGGATAGAATTGTGGGCTATTTCAAGACAAAGAACAAGGGCGACGAG
GACAAAGTTCAAGAATTCTTAAAGTTGTGCTCATATATTTCAGCTCCTTATGACAAACCAGATGGGTATGAAAAGTTGAATGAA
ACTATTAACGAATTCGAAAAGGAAAACAACGTCGAACAGTCTCACAGGTTGTTCTACTTAGCTTTGCCCCCTTCTGTTTTCATAC
CTGTTGCTACGGAGGTCAAGAAGTATGTTCATCCAGGTTCTAAAGGGATTGCTCGGATTATCGTGGAAAAACCTTTCGGGCAC
GACTTGCAGTCAGCAGAAGAGCTTTTGAATGCTTTGAAGCCGATCTGGAAAGAAGAGGAATTGTTTAGAATCGACCACTATCT
AGGTAAGGAGATGGTTAAGAATTTGTTGGCCTTCCGTTTTGGAAACGCATTCATCAATGCTTCTTGGGACAACAGACATATCAG
CTGTATCCAAATCTCGTTCAAGGAGCCTTTTGGAACAGAAGGTCGTGGTGGCTATTTTGACTCAATTGGTATAATAAGAGACGT
CATTCAGAACCACTTGCTTCAAGTGTTAACCCTCTTAACCATGGAGAGACCCGTCTCTAATGACCCTGAGGCTGTTAGAGATGA
AAAGGTTCGCATTCTGAAGTCAATTTCTGAGCTAGATTTGAACGACGTTTTGGTGGGTCAATACGGCAAATCTGAGGATGGAA
AGAAGCCAGCTTATGTGGATGATGAAACTGTTAAGCCAGGTTCTAAATGTGTCACATTTGCAGCCATTGGCTTGCACATCAACA
CAGAAAGGTGGGAAGGTGTCCCAATCATTTTAAGAGCTGGTAAGGCTTTGAACGAAGGTAAAGTTGAGATTAGAGTGCAATA
CAAACAGTCTACTGGATTTCTCAATGATATTCAGCGAAATGAATTGGTCATCCGTGTGCAGCCTAACGAAGCCATGTACATGAA
ACTGAACTCCAAAGTCCCAGGTGTTTCCCAAAAGACTACTGTCACTGAGCTAGACCTCACTTACAAAGACCGTTACGAAAACTT
TTACATTCCAGAGGCATATGAATCACTTATCAGAGATGCTATGAAGGGAGATCACTCTAATTTTGTCAGAGATGACGAGTTGAT
ACAAAGTTGGAAGATTTTCACTCCTTTACTGTATCACTTGGAGGGCCCTGATGCACCGGCTCCAGAAATCTATCCCTACGGATC
CAGAGGTCCAGCTTCATTGACCAAATTCTTGCAAGATCATGATTACTTCTTTGAATCACGCGACAATTACCAATGGCCAGTGAC
AAGACCCGATGTGCTGCACAAGATG**CATCATCACCATCACCAC**TAATAAGCGGCCGC

Properties:

- Accession number: XM_002491158
- Length: 840 bp (between restriction sites: 833 bp)
- *Spe*I (5'-A^CTAGT-3') and *Not*I (5'-GC^GGCCGC-3') restriction sites
- 6xHIS-tagged: 5'-CATCATCACCATCACCAC-3'
- Kozak sequence: 5'-CGAAACG-3'

Protein sequence:

MTDTKAVEFVGHTAIVVFGASGDLAKKKTFPALFGLYREGYLSNKVKIIGYARSKLDDKEFKDRIVGYFKTKNKGDEDKVQEFLKLCSYI
SAPYDKPDGYEKLNETINEFEKENNVEQSHRLFYLALPPSVFIPVATEVKKYVHPGSKGIARIIVEKPFGHDLQSAEELLNALKPIWKEEE
LFRIDHYLGKEMVKNLLAFRFGNAFINASWDNRHISCIQISFKEPFGTEGRGGYFDSIGIIRDVIQNHLLQVLTLLTMERPVSNDPEAV
RDEKVRILKSISELDLNDVLVGQYGKSEDGKKPAYVDDETVKPGSKCVTFAAIGLHINTERWEGVPIILRAGKALNEGKVEIRVQYKQS
TGFLNDIQRNELVIRVQPNEAMYMKLNSKVPGVSQKTTVTELDLTYKDRYENFYIPEAYESLIRDAMKGDHSNFVRDDELIQSWKIFT
PLLYHLEGPDAPAPEIYPYGSRGPASLTKFLQDHDYFFESRDNYQWPVTRPDVLHKM**HHHHHH****

Properties:

- Accession number: XP_002491203
- Size: 504 aa (510 aa), 57.7 kDa (including tag: 58.5 kDa)
- 6xHIS-tagged: N-HHHHHH-C

Pichia pastoris expression plasmids

pPpT4

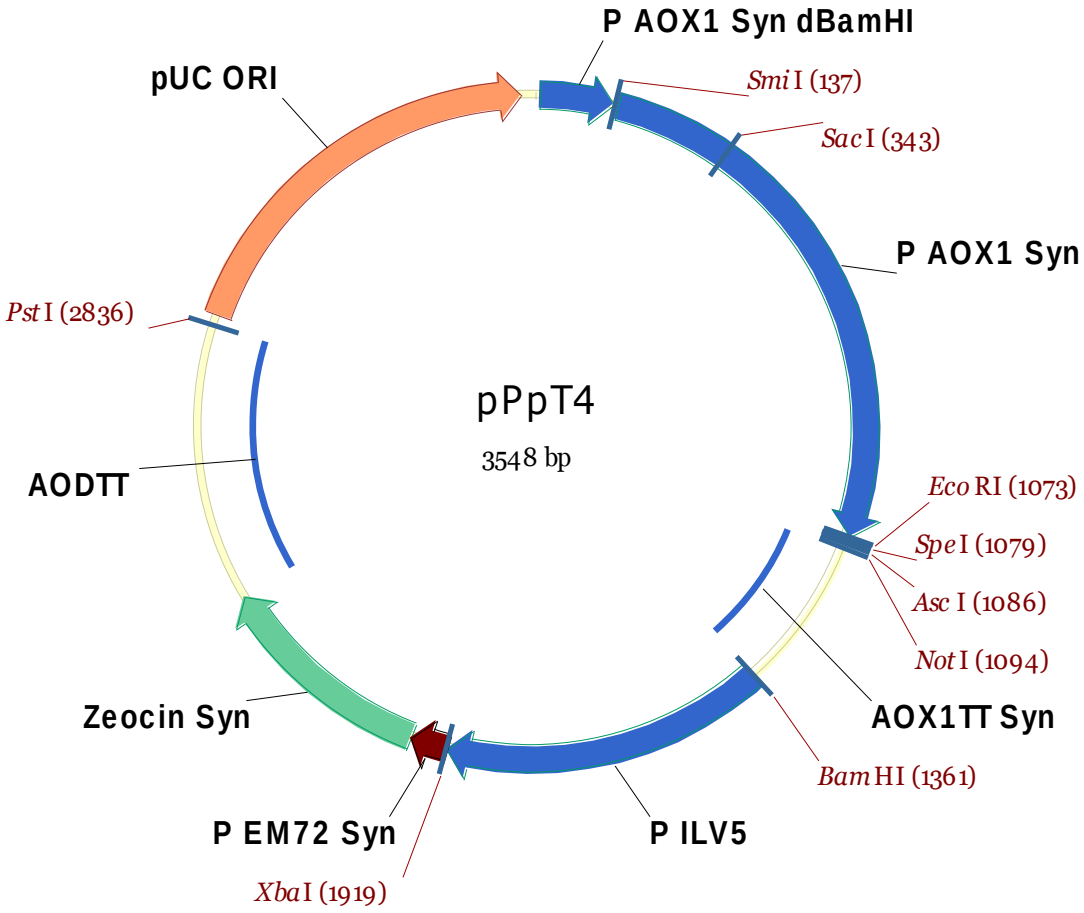

Special considerations:

- Zeocin™ selection in *Escherichia coli* and *Pichia pastoris*
- For intracellular expression of gene of interest
- MCS: *Eco*RI, *Spe*I, *Asc*I, *Not*I
- For integration at *AOX1* locus, linearization with *Bgl*II (recommended) or *Sac*I
- For integration at *AOX1TT*, linearization with *Bam*HI
- Little background observed
- Completely sequenced

pPpKan_SynPDI

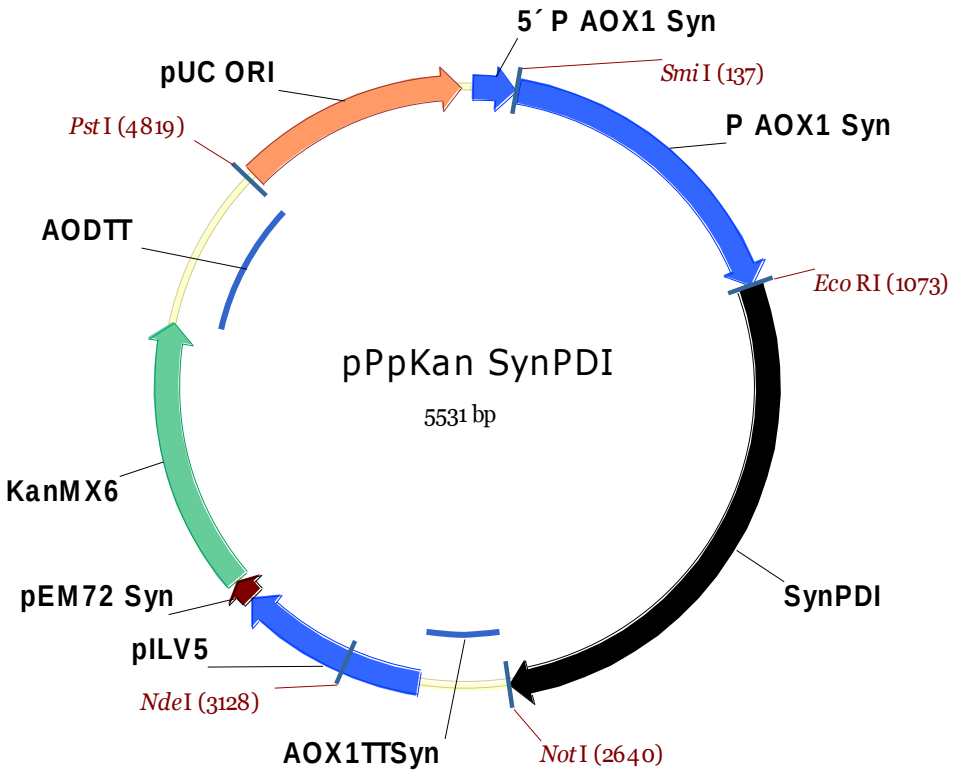

For expression vector pPpKan, only this plasmid, already containing the protein Syn*PDI* was available. Therefore, in order to generate pPpKan backbones, Syn*PDI* had to be preparatively cut out with *Eco*RI and *Not*I and the gene of interest was ligated into this backbone. This limited the possibilities of cloning into this vector to fragments featuring *Eco*RI and *Not*I restriction sites.

Special considerations:

- Kan selection in *Escherichia coli*, G418 selection in *Pichia pastoris*
- For integration at *AOX1* locus, linearization with *Smi*I (recommended) or *Sac*I
- For integration at *AOX1TT*, linearization with *Bam*HI
- Syn*PDI* (Synthetic PDI) ligated into plasmid via *Eco*RI and *Not*I
- Completely sequenced

pPpB1

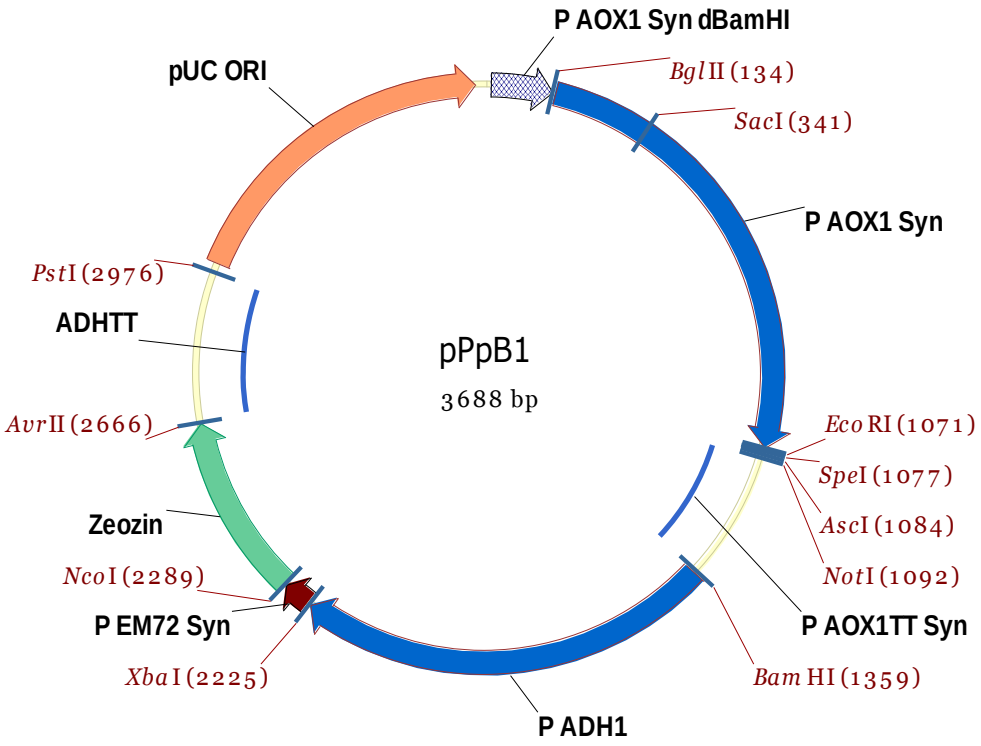

Special considerations:

- Zeocin™ selection in *Escherichia coli* and *Pichia pastoris*
- For intracellular expression of gene of interest
- For integration at *AOX1* locus, linearization with *Bgl*II (recommended)
- For integration at *AOX1TT*, linearization with *Bam*HI
- Recommended Regeneration: 500 µL of 1 M sorbitol +1%EtOH, after 1 h addition of 500 µL YPD
- Completely sequenced

pPpHIS4

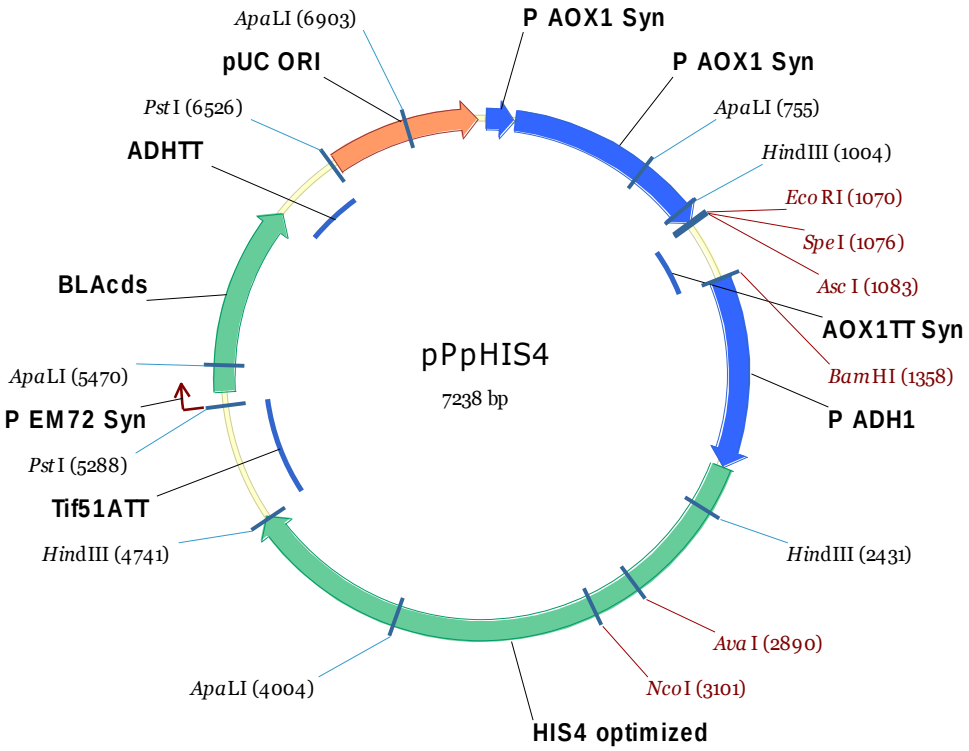

Special considerations:

- Ampicillin selection in *E. coli,* auxotrophic selection in *Pichia pastoris*
- For intracellular expression of gene of interest
- MCS: *Eco*RI, *Spe*I, *Asc*I, *Not*I
- For integration at *AOX1* locus, linearization with *Bgl*II (recommended) or *Sac*I
- For integration at *AOX1TT*, linearization with *Bam*HI
- Growth rate seems to be dependent on copy number. Single (low) copy transformants grow slower than the wild type strain and resemble background after 2-3 d of cultivation on minimal media without supplementation
- Completely sequenced

DNA and protein ladders

All standards used were bought from Fermentas®, Germany.

GeneRuler™ 1 kb Plus DNA Ladder
O'GeneRuler™ 1 kb Plus DNA Ladder, ready-to-use

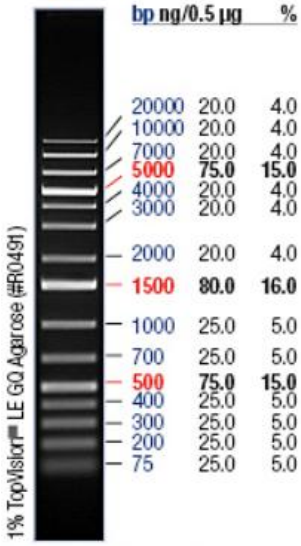

bp	ng/0.5 µg	%
20000	20.0	4.0
10000	20.0	4.0
7000	20.0	4.0
5000	**75.0**	**15.0**
4000	20.0	4.0
3000	20.0	4.0
2000	20.0	4.0
1500	**80.0**	**16.0**
1000	25.0	5.0
700	25.0	5.0
500	**75.0**	**15.0**
400	25.0	5.0
300	25.0	5.0
200	25.0	5.0
75	25.0	5.0

0.5 µg/lane, 8 cm length gel,
1X TAE, 7 V/cm, 45 min

GeneRuler™ 1 kb DNA Ladder
O'GeneRuler™ 1 kb DNA Ladder, ready-to-use

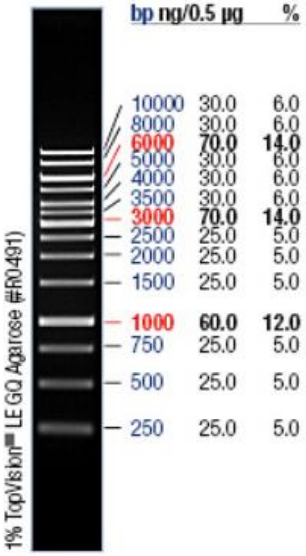

bp	ng/0.5 µg	%
10000	30.0	6.0
8000	30.0	6.0
6000	**70.0**	**14.0**
5000	30.0	6.0
4000	30.0	6.0
3500	30.0	6.0
3000	**70.0**	**14.0**
2500	25.0	5.0
2000	25.0	5.0
1500	25.0	5.0
1000	**60.0**	**12.0**
750	25.0	5.0
500	25.0	5.0
250	25.0	5.0

0.5 µg/lane, 8 cm length gel,
1X TAE, 7 V/cm, 45 min

GeneRuler™ DNA Ladder Mix
O'GeneRuler™ DNA Ladder Mix, ready-to-use

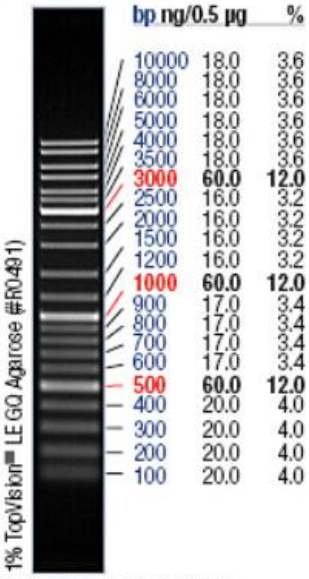

bp	ng/0.5 µg	%
10000	18.0	3.6
8000	18.0	3.6
6000	18.0	3.6
5000	18.0	3.6
4000	18.0	3.6
3500	18.0	3.6
3000	**60.0**	**12.0**
2500	16.0	3.2
2000	16.0	3.2
1500	16.0	3.2
1200	16.0	3.2
1000	**60.0**	**12.0**
900	17.0	3.4
800	17.0	3.4
700	17.0	3.4
600	17.0	3.4
500	**60.0**	**12.0**
400	20.0	4.0
300	20.0	4.0
200	20.0	4.0
100	20.0	4.0

0.5 µg/lane, 8 cm length gel,
1X TAE, 7 V/cm, 45 min

MassRuler™ DNA Ladder, Mix, ready-to-use

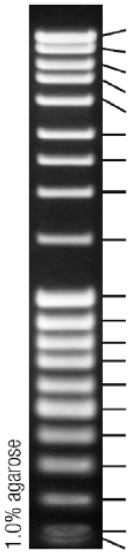

bp	ng/20µl	ng/15µl	ng/10µl	ng/5µl
10000	**200**	**150**	**100**	**50**
8000	160	120	80	40
6000	120	90	60	30
5000	100	75	50	25
4000	80	60	40	20
3000	60	45	30	15
2500	52	39	26	13
2000	40	30	20	10
1500	32	24	16	8
1031	**200**	**150**	**100**	**50**
900	180	135	90	45
800	160	120	80	40
700	140	105	70	35
600	120	90	60	30
500	**200**	**150**	**100**	**50**
400	80	60	40	20
300	60	45	30	15
200	40	30	20	10
100	20	15	10	5
80	16	12	8	4

20µl/lane,
8cm length gel,
1X TAE, 7V/cm, 45min

Protein standard: PageRuler™ prestained protein ladder